DOE/CS/23337-2

ENERGY CONSERVATION

SEASONAL PERFORMANCE OF AIR CONDITIONERS—AN ANALYSIS OF THE DOE TEST PROCEDURES: THE THERMOSTAT AND MEASUREMENT ERRORS

Report No. 2

By
Glenn Lamb
David R. Tree

January 1981

Work Performed Under Contract No. AC02-80CS23337

Ray W. Herrick Laboratories
Purdue University
West Lafayette, Indiana

U. S. DEPARTMENT OF ENERGY

Division of Industrial Energy Conservation

DISCLAIMER

DISCLAIMER

Available from the National Technical Information Service, U. S. Department of Commerce, Springfield, Virginia 22161.

Price: Printed Copy A09
Microfiche A01

DOE/CS/23337-2
Distribution Category UC-95d

IMPROVEMENT ON METHODS OF DETERMINING SEASONAL PERFORMANCE CHARACTERISTICS OF UNITARY AIR CONDITIONERS AND HEAT PUMPS

Research Contract #0141-54-12885

SEASONAL PERFORMANCE OF AIR CONDITIONERS - AN ANALYSIS OF THE DOE TEST PROCEDURES: THE THERMOSTAT AND MEASUREMENT ERRORS

Sponsored by

Department of Energy
Washington, D.C.

Report No. 2 HL 81-1

DOE Contract No.

DE/23337

Submitted by:

Glenn Lamb, Graduate Research Assistant
David R. Tree, Principal Investigator

Approved by:

Raymond Cohen, Director
Ray W. Herrick Laboratories

January 1981

TABLE OF CONTENTS

LIST OF TABLES

LIST OF FIGURES

NOMENCLATURE

A	Cross-sectional area of the duct ($ft.^2$)
A_s	Surface area ($ft.^2$)
C	Empirical constant used in Eq. 3D-5
C_d	Coefficient of degradation due to cyclic operation
c_p	Specific heat of air (Btu/lbm-^oF)
D	Diameter (ft. or in.)
D1	Distance from coil to downstream thermocouple (ft.)
D2	Distance from coil to upstream damper (ft.)
D3	Distance from downstream damper to thermocouple (ft.)
E	Thermostat switch, on or off
F	View factor for radiant exchange
h	Convective heat transfer coefficient (Btu/hr-ft^2-^oF)
K	Steady state gain (^oF/hr. or ^oF)
k	Thermal conductivity (Btu/hr.-ft.-^oF)
L	Losses from conditioned space (^oF/hr.)
L	Length or thickness (ft. or in.)
M	Number of area elements
m	Mass
N	Empirical constant used in Eq. 3D-5
Q	Capacity (Btu)
QACTUAL	Actual capacity of a unit (Btu)

QCOIL	Added capacity due to the mass of the coil
QIDEAL	Capacity under ideal conditions (Btu)
QMEAS	Measured capacity (Btu)
$\dot{q}$	Heat transfer rate (Btu/hr.)
SD	Switch differential (^{o}F)
T	Temperature or temperature rise (^{o}F)
TIME	Time (min. or sec.)
TSET	Thermostat set point (^{o}F)
T81	Measurement scheme using 81 temperatures
T9	Measurement scheme using 9 temperatures
T9A	Measurement scheme using 9 averaged temperatures
ΔT	Temperature difference across the evaporator coil (^{o}F)
t	Time (min. or sec.)
U	Overall heat transfer coefficient (Btu/hr.-ft.^{2}-^{o}F)
V	Velocity (ft/sec) or volumetric flow rate (ft^{3}/min)
V81	Measurement scheme using 81 velocities
V9	Measurement scheme using 9 velocities
V9A	Measurement scheme using 9 averaged velocities
v	Specific volume of air (ft^{3}/lbm of air-water mixture)
W_n	Humidity ratio (lbm water/lbm dry air)
X	Output of a heating/cooling plant (^{o}F/hr.)

GREEK SYMBOLS

ε	Emissivity of a surface
Γ	Integral over time of ΔT (^{o}F-sec.)
ν	Kinematic viscosity of air ($ft.^{2}/sec$)
ρ	Density ($lbm/ft.^{3}$)
σ	Stefan-Boltzmann constant ($Btu/hr.-ft.^{2}-^{o}R^{4}$)
τ	Time constant (min. or sec.)

SUBSCRIPTS

A	Test A
a	Anticipator
air	Air
ave	Average
B	Test B
C	Test C
c	Coil
cyc	Cyclic
D	Test D
dry	Dry coil
e	Bimetal element
h	Heat exchanger
i	Inside
in	Incoming
meas	Measured
o	Outside
o	Initial condition
on	On or on-time
out	Outgoing
p	Heating/cooling plant
r	Room
ss	Steady state

t	Thermocouple
w	Duct wall

ABSTRACT

Lamb, Glenn Doyle, M.S., Purdue University, December 1980. Seasonal Performance of Air Conditioners - An Analysis of the DOE Test Procedures: The Thermostat and Measurement Errors. Major Professor: David R. Tree.

Two aspects of the DOE test procedures are analyzed. First, the role of the thermostat in controlling the cycling of conditioning equipment is investigated. The test procedures call for a cycling scheme of 6 minutes on - 24 minutes off for Test D. To justify this cycling scheme as being representative of cycling in the field, it is assumed that the thermostat is the major factor in controlling the cycle rate. This assumption is examined by studying a closed-loop feedback model consisting of a thermostat, a heating/cooling plant and a conditioned space. Important parameters of this model are individually studied to determine their influence on the system. It is found that the switch differential and the anticipator gain are the major parameters in controlling the cycle rate. This confirms the thermostat's dominant role in the cycling of a system.

The second aspect of the test procedures concerns transient errors or differences in the measurement of cyclic capacity. In particular, errors due to thermocouple

response, thermocouple grid placement, dampers and nonuniform velocity and temperature distributions are considered. Problems in these four areas are mathematically modeled and the basic assumptions are stated. Results from these models help to clarify the problem areas and give an indication of the magnitude of the errors involved. It is found that major disagreement in measured capacity can arise in these four areas and can be mainly attributed to test set-up differences even though such differences are allowable in the test procedures. An understanding of such differences will aid in minimizing many problems in the measurement of cyclic capacity.

CHAPTER I - INTRODUCTION

Section A - Background

As the decade of the '80's dawns, energy remains a very important issue. Many of the difficulties and inconveniences caused by energy shortages and rising costs that were experienced during the '70's are continuing into the '80's. This emphasizes again the need to understand the implications of our energy usage and resolve the problems related to it. This, however, will not be easy because at the heart of the energy issue is the dilemma between the need for energy and the need to conserve energy.

With the impetus of the 1973 oil embargo, the '70's saw numerous changes attempting to stop, or at least slow down, increasing energy consumption and its even more increasing cost. New energy programs, policies, ideas and attitudes flourished, attacking waste, improving efficiency, providing alternatives and promoting conservation. One such venture was the enactment of the Energy Policy and Conservation Act in 1974 by the United States government, "an energy conservation program for consumer products " (Federal Register [1979]).* An important aspect of this

*Reference located alphabetically in List of References

law is the requirement that certain specified consumer products be labeled with a seasonal energy usage number which would allow a buyer to estimate the cost of operating that product on a seasonal basis. It was hoped that the buyer would purchase the more energy-efficient products which would eventually clear the marketplace of the less efficient models. Thus, a significant energy savings could be realized by the use of highly efficient consumer products (Thomas [1980]).

Central air conditioners and heat pumps are among those consumer products to be labeled. To this end, the United States Department of Energy (DOE) with technical assistance from the National Bureau of Standards (NBS) had to develop standard test procedures to obtain a number for the label, the Seasonal Energy Efficiency Ratio (SEER), which would be both informative to the consumer and not overly burdensome for the air conditioning industry to obtain. The options were many as were the trade-offs and under the constraints imposed on them, particularly time, NBS produced the present set of test procedures. (See Thomas [1980] for a detailed discussion of these options.)

The test procedures basically call for the running of four tests which in part comply with the American Society of Heating, Refrigeration and Air Conditioning Engineers (ASHRAE) Standard 37-78 [1978] and the Air Conditioning and Refrigeration Institute (ARI) Standard 210-79 [1979]. Three of the tests, tests A, B and C, are conducted under

steady state conditions and the fourth test, test D, is a cyclic test. These tests, along with their basic operating conditions, are listed in Table 1A-1. The results of these tests are used to ultimately calculate the SEER. See the Federal Register [1979] for this calculation. The option is also given to eliminate tests C and D and substitute instead an assigned value of 0.25 for the degradation coefficient (C_D) and then calculate the SEER. The degradation coefficient characterizes the transient response of the unit and is defined in the Federal Register [1979].

However, testing has not gone smoothly. While the air conditioning industry has performed steady state tests for years, the new requirements of test C and D, namely low humidity (a dry coil test) and transient measurements, have caused many difficulties and raised many questions (Thomas [1980]). It should be emphasized that the industry as a whole has made a sincere effort to abide by the test procedures. They have spent a considerable amount of time and money trying to understand and comply with them. Nevertheless, at a DOE test procedure workshop held July 15-16, 1980 at Purdue University, it was made very clear that problems still exist (DOE Workshops [1980]).

The Air Conditioning and Refrigeration Institute (ARI) responded to these problems by sponsoring a study of the test procedures. This study was conducted by the Ray W. Herrick Laboratories and a report was published in March, 1979 (See Thomas, Tree and Goldschmidt

Table 1A-1 Summary of Requirements for DOE Test Procedures

	Indoor Dry-Bulb Temperature	Indoor Wet-Bulb Temperature	Outdoor Dry-Bulb Temperature	Outdoor Wet-Bulb Temperature (1)	Mode of Operation
Test A	80°F (26.7°C)	67°F (19.4°C)	95°F (35°C)	75°F (23.9°C)	steady-state
Test B	80°F (26.7°C)	67°F (19.4°C)	82°F (27.8°C)	65°F (18.3°C)	steady-state
Test C	80°F (26.7°C)	See Note (2)	82°F (27.8°C)	-------	steady-state
Test D	80°F (26.7°C)	See Note (2)	82°F (27.8°C)	-------	Cyclic 6 min. on-time 24 min. off-time

1— Applies only to those units which reject condensate to the outdoor coil.

2— Shall at no time exceed that value of the wet-bulb temperature which results in the production of condensate by the indoor coil at the dry-bulb temperatures existing for the air entering the indoor portion of the unit.

[1979]. DOE has also attempted to be responsive to these problems by funding a continued study of the test procedures which is presently being completed by the Ray W. Herrick Laboratories. The ARI report along with the Master's thesis of Steven Thomas [1980] forms the basis for the present study. It is recommended that these two documents be carefully reviewed by all who are concerned with the test procedures.

Section B - Purpose of the Present Work

The purpose of this work is to complete a portion of the above DOE study. This work will address two important aspects of the test procedures. First, the role of the thermostat in controlling the cycling of conditioning equipment will be analytically investigated. While the cycling of equipment in test D is done manually, the prescribed duty cycle of six minutes on - twenty-four minutes off is the result of thermostat dynamics as described by the NEMA Standards [1972]. To justify this cycling scheme as being representative of cycling in the field, NBS has assumed that the thermostat is the major factor in controlling the cycle rate of a conditioning system. This assumption will be examined by studying a closed-loop feedback model consisting of a thermostat, a heating/cooling plant and a conditioned space. The important parameters of this system will be individually studied to determine their influence on the system. In this way, the role of the thermostat will be better understood.

The second half of this work will study transient errors or differences in the measurement of cyclic capacity. In particular, errors due to thermocouple response, thermocouple grid placement, dampers and nonuniform velocity and temperature distributions will be considered. Errors in these four areas are closely associated with the test set-up. Since many aspects of the test set-up are not clearly defined in the governing standards (ASHRAE 37-78 and ARI 210-79) or the DOE test procedures and vary from company to company, the comment has been made that test set-ups are being tested rather than air conditioning units (DOE Workshops [1980]). This work will attempt to resolve this problem, and aid in obtaining a correct and reproducible measurement of the cyclic capacity of a unit.

Section C - Literature Sampling

There is ample literature concerning the thermostat. In some cases, it is considered simply as a black box, on/off switch. Other references consider it in more detail, studying some of its component parts. The emphasis of this work is on the role of the thermostat in a system and the influence of its parameters on that system. Therefore, only those references that deal with this subject will be discussed.

Several models exist in the literature which include the thermostat as one element of a conditioning system. Nelson [1974] proposed a rather detailed model which is

shown in Figure 1C-1. The purpose of this model was to simulate a residential heating system on an analog computer. He found that the performance of the heating equipment was influenced by the thermostat design. In particular, the cycle rate could be changed by adjusting the anticipator current. He also justified an exponential approximation to the heating plant response. Nelson [1974] and Nelson and Magnussen [1974] further stated that the effect of furnishings (thermal mass) in a room was to cut the temperature swing as much as half when compared to an empty room. This had the effect of changing the cycle rate.

Using this same model, Anderson and Tobias [1974] found that the switch differential (SD) and the anticipator temperature rise (K_a) affected the cycle rate. They also stated that for SD>.25°F (.14°C) the cycle rate is nearly independent of the heating plant response time.

Gable and Koenig [1977] included the thermostat in their computer simulation of a heating system to study certain energy-saving ideas. They concluded that the cycle rate depended on the anticipator, the time constant of the bimetal element, the switch differential and the percent on-time. For a set point of 70°F (21°C) they found K_a=4.37°F (2.43°C), τ_e=7 min., SD=1.5°F (.83°C) and 6 cph at 50% on time. They modeled the anticipator simply as a steady state gain device.

The National Electrical Manufacturers Association (NEMA) Standards [1972] provided definitions of thermostat

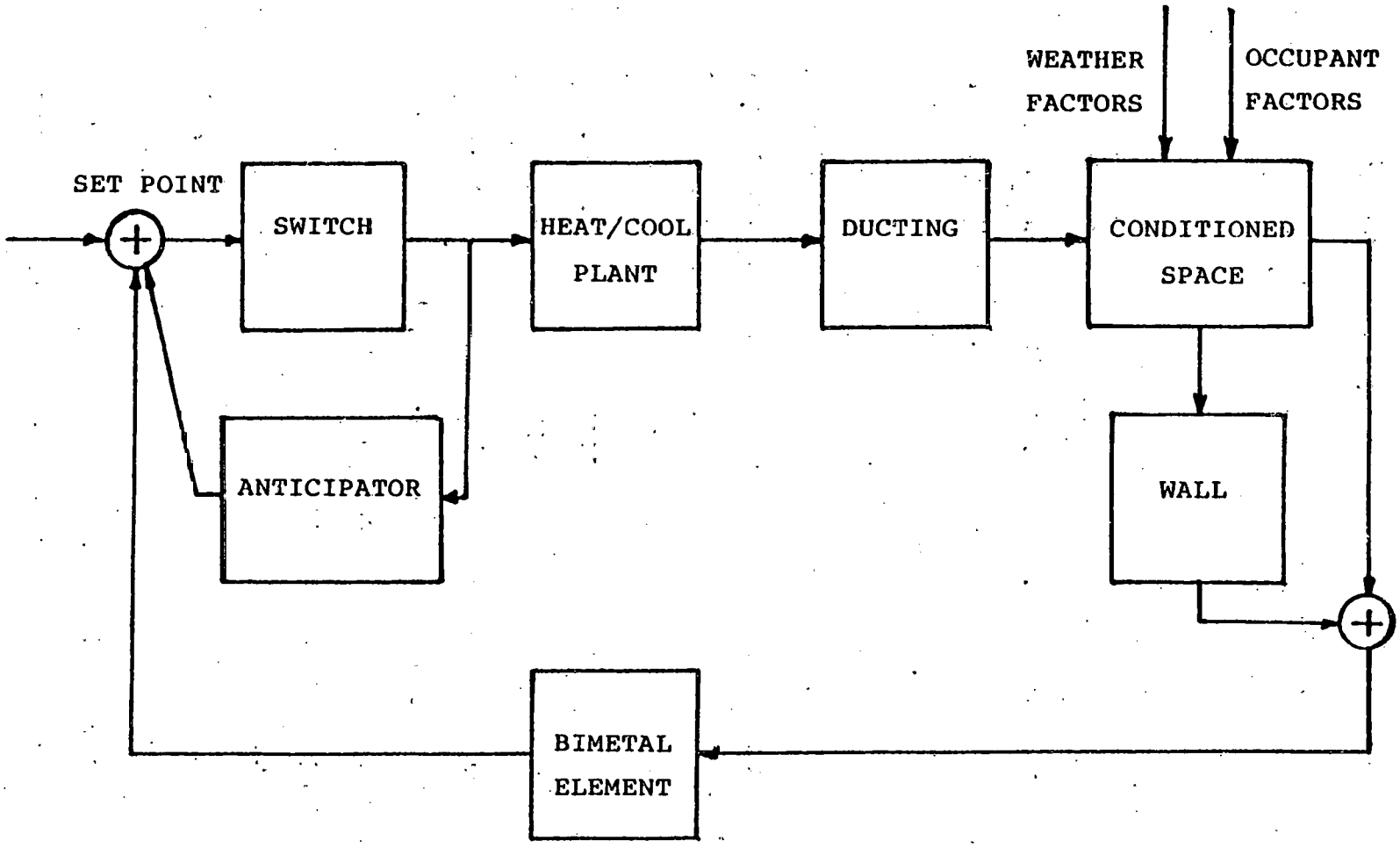

Figure 1C-1 Thermostat Model of Nelson

terms and testing conditions that could be used to study the dynamic performance of a thermostat. These tests included a switch differential test and a cycle rate test which were used to standardize thermostat design. Both Didion [1978] and McBride [1979] used the NEMA Standards to determine component values for their models.

Didion [1978] examined in some detail the component parts of the thermostat, such as the bimetal element and the anticipator heater. His computer simulation compared various types of thermostats and concluded that the anticipating thermostats generally provided better comfort due to their higher cycling rate than that provided by the unanticipating thermostats. He attributed the higher cycle rate to the anticipator and the switch differential. His model will be studied further in Chapter II.

Experimenting on low voltage thermostats in a test room, Cape and Tull [1969] measured SD to be .8-2.0°F (.4-1.1°C). They found that the type of heating system had little effect on cycling. They also provided a good discussion on the role of the anticipator and how it increased cycling to decrease temperature swings.

McBride [1979] provided a very comprehensive study of the thermostat which was supported by extensive field and laboratory work as well as anlaytical investigation. His model is shown in Figure 1C-2. He also examined the component parts of the thermostat both analytically and with several tests, including the NEMA Standards tests. His

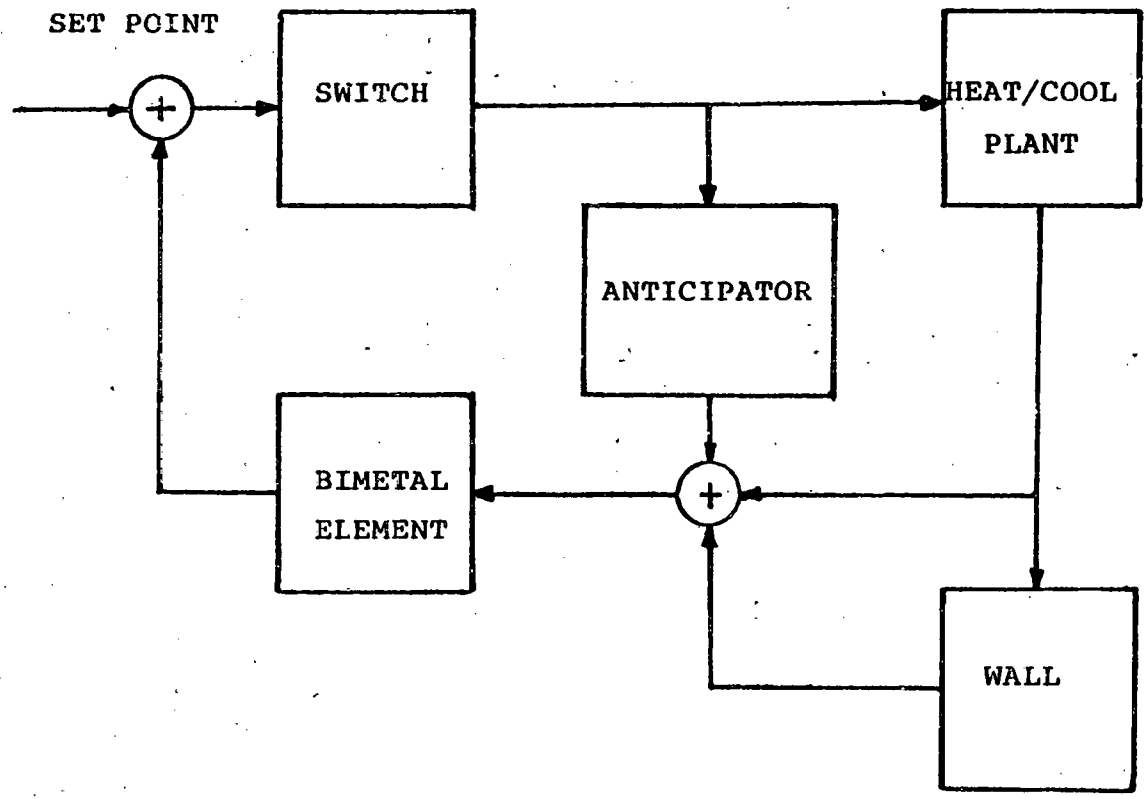

Figure 1C-2 Thermostat Model of McBride

numerical results concerning the switch differential, the bimetal element, etc. will be discussed in Chapter II. McBride had several conclusions which concerned the thermostat. He found that the bimetal element could be approximately modeled as a first order system, and that the anticipator could be described simply as a steady state gain device. He found that changing air velocities and temperature ramp rates had little effect on cycling. Finally, he concluded that the anticipator was the dominant factor in cycling the equipment.

Two more references are of interest in understanding the thermostat. Both Murphy [1977] and Hart [1978] prepared percent on-time versus on-time plots of experimental data taken from an air conditioner and a heat pump (heating mode), respectively. Both plots showed on-time tending to a finite value as percent on-time tended to zero, indicating that the thermostat was controlling the cycling. Similar results will be found analytically in Chapter II.

Chapter III of this work will look at transient measurement errors associated with four areas: thermocouple response, thermocouple grid placement, dampers and nonuniform velocity and temperature distributions at the measuring locations. There is some literature on transient measurements that pertains to these four areas. There is a wealth of literature concerning steady state measurement errors. Only selected steady state literature in these areas will be included in this sampling.

When using thermocouples for transient temperature measurements, there are at least two concerns: accuracy and time response. Didion [1980-B] pointed out that the making and handling of thermocouples could cause inaccuracies. He mentioned that soft solder should be used for the junctions, instead of silver solder or spot welding. Cold working of the thermocouple wires could also cause inaccuracies and should be avoided. He noted that using a series arrangement where temperature difference is measured, instead of individual temperatures, would minimize these inaccuracies because they would tend to cancel each other.

Anderson and McGill [1980] stated that a fluctuating thermocouple reference junction temperature and noise contribute to thermocouple inaccuracy as high as 1-2°F. They have found the reference junction oven to be more reliable than the ice bath or the electronic ice bath. They also suggested appropriate room and equipment grounding, thermocouple wire lengths limited to 50 ft. (15 m), and wire shielding to minimize the effects of noise.

Johnson et. al. [1957] made thermocouple measurements in a changing temperature field. They stated that if the thermocouple is placed facing upstream and then bent back downstream, conduction errors could be neglected because there would be essentially no gradient from the leads to the junction to distort the measurement. They also claimed that radiation effects are small for conditions similar to those used in the DOE test procedures.

Thomas [1980] and Murphy and Goldschmidt [1978] showed that the time response of the thermocouple caused the measured capacity to lag the actual capacity but that for a time constant of 2.5 seconds, the effect was less than 1%. Moffat [1957] provided a good discussion on thermocouple response. He briefly developed the thermocouple theory and described the effect of mass, velocity and wire diameter on the time response of the thermocouple. He noted, for example, that time response is shortened by using thinner wire or increasing the velocity. Moffat also mentioned five common sources of measurement deviation. First, he cited conduction. To avoid error, he suggested stripping the wire about five diameters back to the insulation. Second, he mentioned the size of the weld or solder bead. This should be kept as small as possible to reduce the thermal mass. Third, he commented on junction shape. He suggested that the wires from the junction form an open loop. Fourth, radiation was mentioned. Fifth, he cited orientation in the air stream. These last two effects were considered small when temperatures and velocities are low such as in air conditioning or heat pump applications.

Errors due to grid placement are mainly caused by thermal mass effects, mass transfer and heat transfer through the duct walls. In their final report on the DOE test procedures, Kelly and Parken [1978] warned that consideration must be given to these effects. Colborne [1957], in studying the performance of intermittently-fired

oil furnaces, also noted that these effects needed to be included when considering the cyclic performance of the furnace.

Murphy and Goldschmidt [1978] provided an excellent analysis of grid placement and thermocouple response applicable to the test procedures. Using a computer simulation, they studied the effects of thermal mass, heat transfer and insulation on the cyclic capacity measurement made at several locations. They found that these effects caused the measured capacity to decrease as it was measured further downstream. When comparing the cyclic capacity measured at the blower exit (near the coil) to the capacity measured 20 ft. (6m) downstream, they found a 9% difference. It is recommended that this reference be consulted for more insight into the problem of grid placement.

Certain steady state results are useful because they provide an upper bound on the effects of heat transfer. Kuelhert [1980] did testing on thermal storage units and found that forced warm air which passed through a 6 ft. (1.8m) section of sheet metal ducting had its temperature change 2-3^{o}F (1.1-1.7^{o}C). This indicated that heat transfer was taking place. McPherson et. al. [1951] proposed a simpler method of finding the efficiency of a furnace which included measuring duct losses. They found 2-3% losses in capacity due to heat transfer through the ducting. Hise and Holman [1977] stated that an uninsulated duct in an unheated crawl space might lose 1.5 Btu/ft^{2}-hr-^{o}F

(8.5 $W/m^{2o}C$) and that 1 in. (2.54 cm) of insulation would reduce this loss by a factor of three. All of the above results came from heating plants. But they indicate that heat transfer does affect capacity measurements. This fact, then, should also be considered when testing air conditioners.

The dampers have the effect of trapping cold air around the evaporator coil. Thomas [1980] claimed that this slug of cold air would have a small effect on the measurement of capacity. Murphy and Goldschmidt [1979] discussed refrigerant dynamics as they related to start-up conditions. They indicated that such dynamics are difficult to predict and made transient temperature measurements uncertain. They discussed the off-time effects of the refrigerant flow. They found that their evaporator coil filled with hot refrigerant from the condenser at shut down which warmed the surrounding air. They [1978] also studied off-time effects of the test set-up by computer simulation. They found that measurable cooling occurred during the off-time and that heat transfer during the off-time affected the start-up conditions of the subsequent test. The results of both of these references are applicable to the role of dampers in the test installation.

Nonuniform velocity and temperature distributions can cause uncertainty in temperature measurements. Kelly and Parken [1978] cautioned that these nonuniformities could cause measurement problems and encouraged the use of good

air mixers. In fact, Kuelhert [1980] could not get acceptable results until he placed several air mixers in the duct. Only then was he able to record representative temperatures in order to compute capacity.

Many excellent texts are available which discuss transient measurement problems in general. Several of these have been consulted and have provided insight into the problems investigated in this work. They are recommended for their general information and bibliographic listings. See Doebelin [1975], Beckwith and Buck [1961], Holman [1966] and McAdams [1954].

CHAPTER II - THE THERMOSTAT

Section A - Introduction to the Thermostat Model

Residential energy consumption has been, and continues to be, the subject of much study as the need for energy efficiency and conservation increases. In trying to understand and predict such energy consumption, it has been recognized that the thermostat has an important role (McBride [1979]). Since conditioning the air, both heating and cooling, is a large consumer of energy, it seems logical that the role of the thermostat be included when considering the seasonal performance of the conditioning equipment.

Accordingly, test D of the DOE test procedures calls for a duty cycle of six minutes on - twenty-four minutes off which is based on thermostat dynamics. For most central air conditioners and heat pumps, the thermostat is adjusted so that the equipment cycles at about 3 cycles per hour (cph) at 50% on-time. (3 cph is chosen mainly for equipment life and, to a lesser degree, for comfort considerations.) Since most thermostats conform to the NEMA Standards [1972], they should maintain a definite cycling pattern given 3 cph at 50% on-time. This cycling pattern is discussed in the NEMA Standards and can be

roughly approximated by a parabola as shown in Figure 2A-1. This curve will hereafter be called the NEMA curve (Thomas [1980]). The six minutes of on-time is based on the observation that many air conditioners and heat pumps appear to have reached steady state conditions by six minutes (Thomas [1980], Murphy and Goldschmidt [1978]). 24 minutes of off-time makes a total of 30 minutes of cycle time, or 2 cph, and makes a duty cycle consisting of 20% on-time. From the NEMA curve, 20% on-time corresponds to about 2 cph. This indicates that the transient test is governed by a duty cycle that is representative of ideal thermostat cycling even though the test procedures do not actually use a thermostat for cycling.

The assumption made in the test procedures, as reflected by the choice of the duty cycle, is that the thermostat is the major factor in controlling the cycling of a system. Much work has been done in this regard, notably the work of McBride [1979]. The purpose of this work is to further investigate this assumption. This will be done by examining a simple mathematical model of a conditioning system which includes the thermostat. The parameters of this system will be analytically studied to determine their influence on the cyclic behavior of the system.

Section B - The Thermostat Model

Several models of the conditioning system exist. They vary in complexity and purpose but usually include the

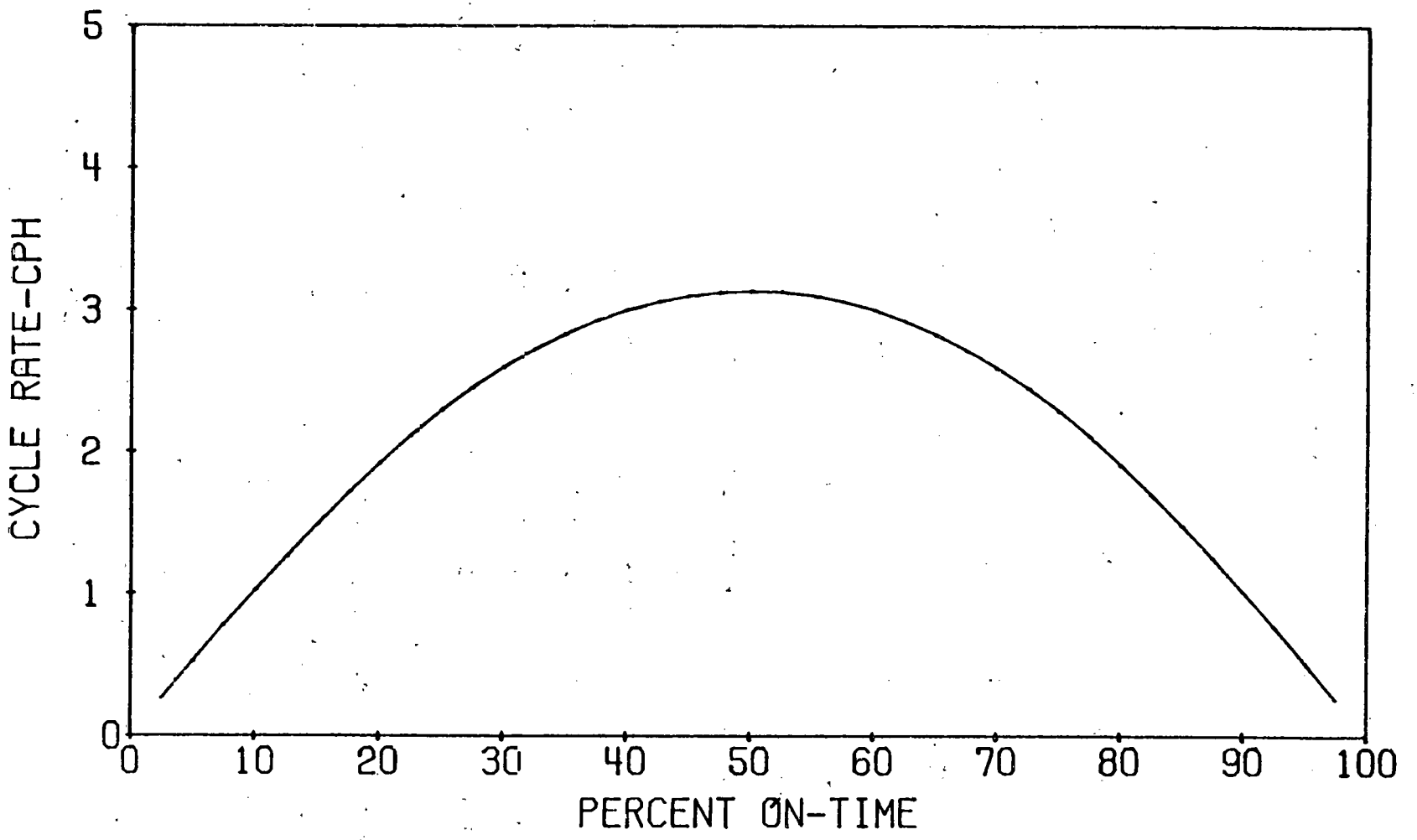

Figure 2A-1 Thermostat Performance Based on NEMA Standards (NEMA Curve)

thermostat, the heating/cooling plant and the conditioned space. See Nelson [1974] and McBride [1979] for two of these models. Didion [1978] has also proposed a model and it is shown in block form in Figure 2B-1. This closed-loop feedback model is not as detailed as those of Nelson and McBride, but it does include the three basic groups of a conditioning system: the controller, the heating/cooling plant and the conditioned space. This model will be used to study the role of the thermostat in the conditioning system. The inclusion of the "Losses" in the model is intended to account for those effects which act contrary to the effects of the heating or cooling plant. For example, in the cooling mode, these losses would represent heat gains from leakage, heat transfer from the outside, etc. It will be assumed in this work that the effects of mass transfer (leakage), heat transfer and thermal storage (the walls and the furnishings) are adequately modeled by the space losses. However, there is some indication that furnishings do have an influence on cycling beyond that which is modeled as the space losses. See Goldschmidt and Murphy [1979] and Nelson [1974].

Before proceeding to the analysis, one more comment is necessary. Only the heating plant will be considered. To study the effects of the cooling plant on the system, the only model change necessary is to reverse the role of the anticipator. In the heating mode, the anticipator is activated during the on-time. In the cooling mode, the

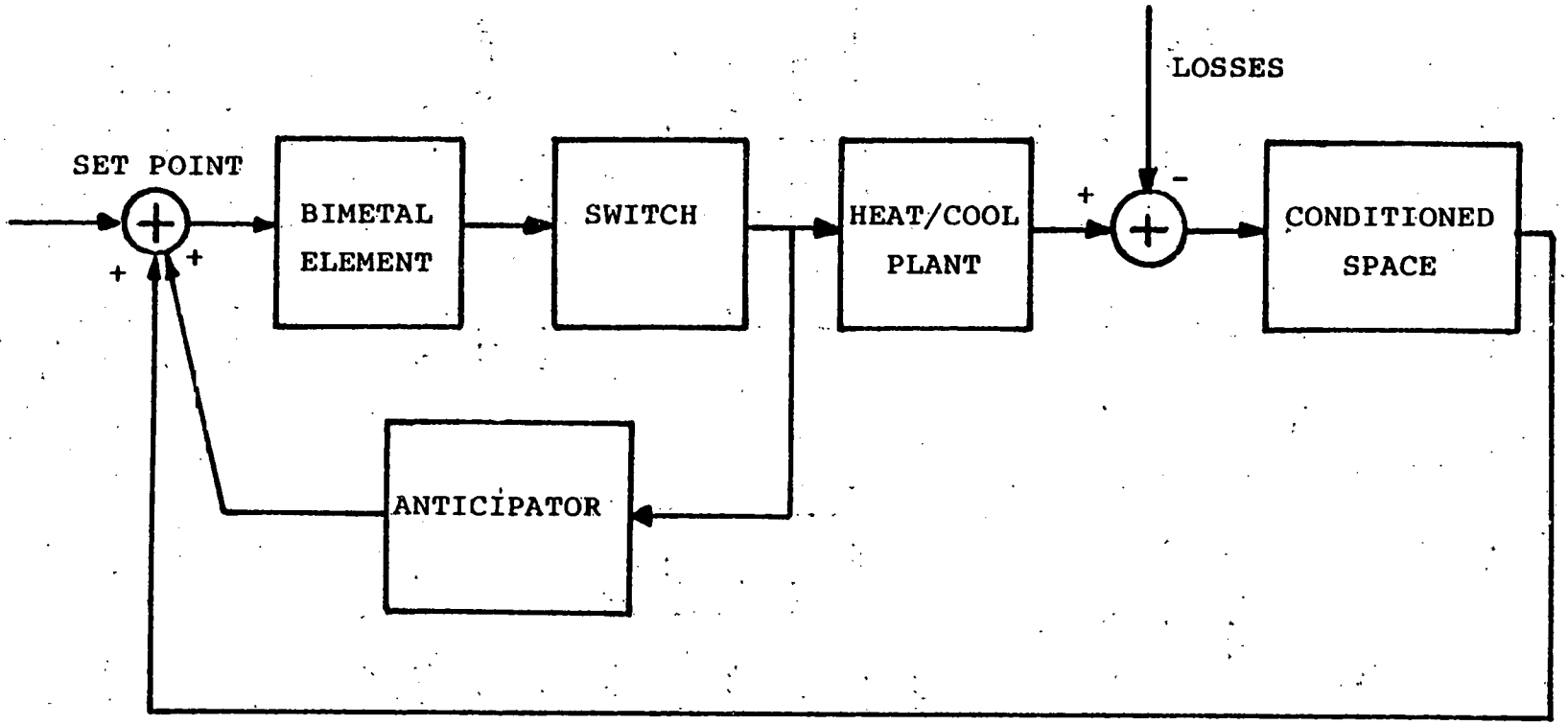

Figure 2B-1 Thermostat Model of Didion

anticipator is activated during the off-time. However, the results that will be obtained (the influence of the system parameters on the cycle rate) will apply to both the heating and cooling modes.

The three main groups of this model can be further detailed. The controller group consists of the bimetal element, the switch and the anticipator. The bimetal element and the anticipator are modeled as first order systems while the switch is simply an on-off function. The heating plant is activated by the switch and is also modeled to respond as a first order system. The conditioned space is modeled as a simple linear system. See Figure 2B-2 for a more detailed block diagram of this system.

State equations can be written for the blocks in Figure 2B-3. They are listed as follows:

$$\frac{dTe}{dt} = \frac{1}{\tau_e}(T_a + T_s - T_e)$$

$$\frac{dTa}{dt} = \frac{1}{\tau_a}(K_a E - T_a)$$

$$\frac{dXp}{dt} = \frac{1}{\tau_p}(K_p E - X_p)$$

$$\frac{dTs}{dt} = X_p - L$$

E = 1 when Te < TSET

= 0 when Te > TSET + SD

= unchanged when TSET < Te > TSET + SD

Where,

T_e = temperature of the bimetal element, ^{o}F (^{o}C)

τ_e = time constant of the bimetal element, sec.

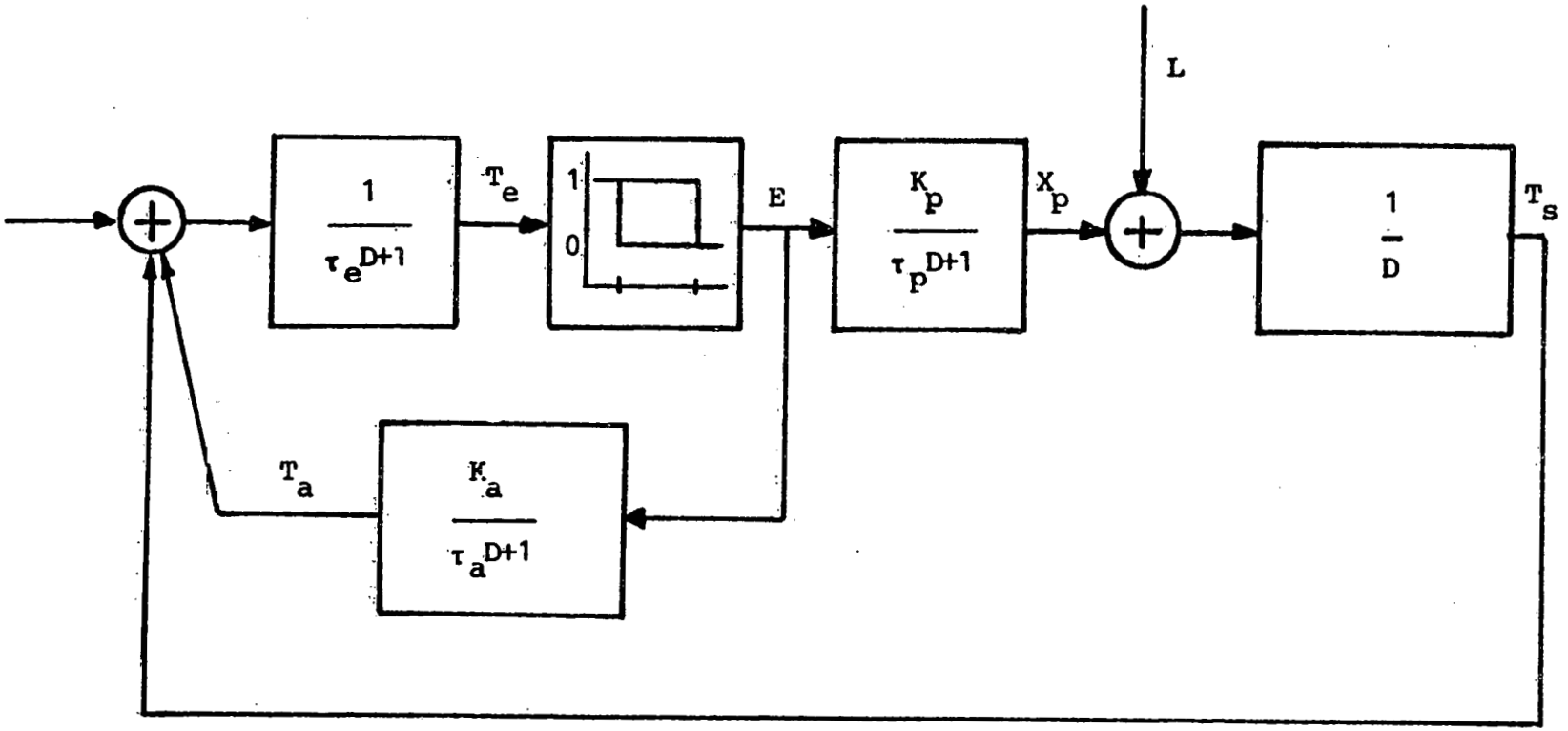

Figure 2B-2 Closed-loop Feedback Model with Expressions

T_a = temperature rise of the anticipator, ^{o}F (^{o}C)

τ_a = time constant of the anticipator, sec.

K_a = steady state temperature rise of the anticipator, ^{o}F (^{o}C)

X_p = output of the heating plant, $^{o}F/hr$ ($^{o}C/s$)

τ_p = time constant of the heating plant, sec.

K_p = steady state temperature rise of the heating plant, $^{o}F/hr$ ($^{o}C/s$)

T_s = temperature rise of the conditioned space, ^{o}F (^{o}C)

L = losses of the conditioned space $^{o}F/hr$ ($^{o}C/s$)

E = switch

SD = switch differential, ^{o}F (^{o}C)

TSET = set point temperature, ^{o}F (^{o}C)

This system of linear differential equations is solved and a rather lengthy expression for T_e as a function of time is obtained. This expression and more details concerning its derivation can be found in the Appendix. The expression for T_e is computer coded, and by an iteration scheme, on-times and off-times can be calculated for different losses L. Once an on-time and an off-time are known for a given load, cycle time, cycle rate and percent on-time are calculated by the following:

cycle time = on-time + off-time

cycle rate = 60/cycle time

% on-time = (on-time/cycle time) x 100

These results can be plotted and the influence of the different parameters on the system can be observed.

The expressions for T_e and the initial conditions contain nine parameters. Each of these will be defined or discussed and six of them will be studied to determine their influence on the system. It is assumed that each parameter has a range of values over which it can reasonably be expected to vary and each parameter will be assigned a base value. The parameter to be studied will be allowed to vary while all others are held constant at their base value. In this way, its influence on cycling can be isolated. This will also permit comparisons to be made between parameters. The list that follows gives a brief description or explanation of each parameter, its range of values and its base value. These are also summarized in Table 2B-1. The NEMA Standards [1972] may also be consulted for a more comprehensive list of definitions pertaining to the thermostat.

1. Thermostat set point - TSET, ^{o}F (^{o}C)

This is the temperature setting on the thermostat which an occupant would adjust to his or her preference. It will be set at $68^{o}F$ ($20^{o}C$) for the computer simulation and will not vary. TSET is used in the initial conditions for calculating both on time and off time.

2. Time constant of the bimetal element - τ_e, min.

This is the time the bimetal element takes to reach 63% of its steady state value when subjected to a step change in temperature. In the thermostat, this temperature change

Table 2B-1 Summary of Thermostat Parameters

Parameter	Range	Base Value
TSET	-	68 ^{o}F
τ_e	3 - 10 min	5 min
τ_a	0 - 3 min	1.5 min
τ_p	0 - 15 min	0 min
SD	1 - 3 ^{o}F	1.5 ^{o}F
K_a	1 - 3 ^{o}F	2 ^{o}F
K_p	4 - 16 ^{o}F/hr	10 ^{o}F/hr
L	0 - K_p	-
E	-	1 or 0

is caused by a combination of the conditioned space, the wall to which the thermostat is mounted and the heat from the anticipator. McBride [1979] calculates τ_e to be around six minutes, while Didion [1978] suggests values of three-five minutes. This section will let τ_e vary over three-ten minutes with five minutes being the assigned base value.

3. Time constant of the anticipator - τ_a, min.

There is some confusion about τ_a. McBride [1979] defines τ_a to be the time required for the actual anticipator heater to reach 63% of its steady state value. As the heater is an electrical resistance heater, it reaches steady state in a matter of seconds and McBride's τ_a is essentially zero. Didion [1978], on the other hand, defines τ_a to be the time required for the bimetal element to sense 63% of the steady state temperature of the heater. His τ_a varies from several minutes to almost half an hour. This section will conform to Didion's definition of τ_a and let τ_a vary from zero-three minutes and will assume very long values of τ_a are uncommon. The base value for τ_a will be 1.5 minutes.

4. Time constant of the heating/cooling plant - τ_p, min.

This is the time it takes the heating/cooling plant to produce 63% of its steady state output. For τ_p=0-2 minutes, the plant corresponds to electrical resistance heating or to central air conditioners and heat pumps.

For τ_p = 4-6 minutes, a forced hot air system is implied and for τ_p = 15-30 minutes, a radiant heating system is implied. The range of τ_p for this section will be 0-15 minutes with 0 minutes the base value.

5. Switch Differential - SD, ^{o}F (^{o}C)

Again, there is some confusion concerning this term. Manual differential and operating differential are NEMA terms but switch differential is not. Manual differential is defined in the NEMA Standards [1972] as "the difference in scale settings between cut-in and cut-out points determined by manually raising and lowering the thermostat setting with no electrical load." Operating differential (OD) is defined as "the difference between cut-in and cut-out points measured at the thermostat under specified operating conditions." Didion [1978] equates SD with manual differential and states that OD = RR (τ_e) + SD where RR is the temperature ramp. He cites .75-2^{o}F (.42-1.1^{o}C) as a suitable range. McBride [1979], however, equates SD with OD and claims .5-1.5^{o}F (.3-.8^{o}C) as a range. This section will equate SD with OD and let SD vary over 1-3^{o}F (.6-1.7^{o}C) with 1.5^{o}F (.8^{o}C) as a base value. SD is used in the initial conditions for calculating both on-time and off-time.

6. Anticipator temperature rise - K_a, ^{o}F (^{o}C)

This is the number of degrees above ambient that the anticipator heater adds to the air within the thermostat

cover. Didion [1978] states that 3-10°F (1.7-5.6°C) is the range for K_a while McBride [1979] calculates K_a to be about 3°F (1.7°C). This section will let K_a vary 1-3°F (.6-1.7°C) with 2°F (1.1°C) as the base value. Note that this parameter can be adjusted manually in some thermostats and is considered to be the dominant factor that controls cycling. See McBride [1979] for a good discussion of the anticipator temperature rise.

7. Steady state plant output - K_p, °F/hr (°C/hr)

This section will let K_p vary from 4°F/hr - 16°F/hr (2.2°C/hr-8.9°C/hr) with a base value of 10°F/hr (5.6°C/hr).

8. Losses in the conditioned space - L, °F/hr (°C/hr)

All of the effects that oppose the output of the heating or cooling plant are lumped together and are called the space losses. These effects include mass transfer (leakage) and heat transfer into and out of the conditioned space as well as the thermal storage effects of the walls, furnishings, etc. (That these effects can be lumped together is not exactly true, especially the thermal mass effects, but this assumption is deemed adequate for this model.) L varies in increments of $K_p/10$ in order to generate different percent on-times.

9. Switch - E

The switch is activated by the movement of the bimetal element and sends an on or off signal to both the heating/cooling plant and the anticipator. In the heating mode,

both devices are either switched on or off. In the cooling mode, one device is on while the other is off. E has a value of one or zero, indicating on or off respectively.

Section C - Results

Figures 2C-1 through 2C-12 show the results of studying the six parameters: SD, τ_e, τ_a, τ_p, K_a and K_p. Two different type plots for each of these parameters are shown. The first type plot for each parameter shows cycle rate versus percent on-time. These plots all have the general shape of the NEMA curve and clearly show the influence of each parameter on the cycling of the system. This influence will be discussed in more detail.

The second type plot for each parameter shows on-time versus percent on-time. All of these plots indicate that on-time tends to a non-zero value as percent on-time tends to zero. This can probably be attributed to the anticipator initiating on-time and the switch differential causing the on-time to have a finite value even though the percent on-time is tending to zero. This indicates that the thermostat has the dominant role in controlling the cycling of the system. With the aid of Figures 2C-1 through 2C-12, the influence of the six parameters can be discussed in more detail. The switch differential varies over a relatively small range but changes in SD have a strong influence on cycling. This is seen in Figure 2C-1. As SD gets smaller, the cycle rate increases. This is to be expected since SD

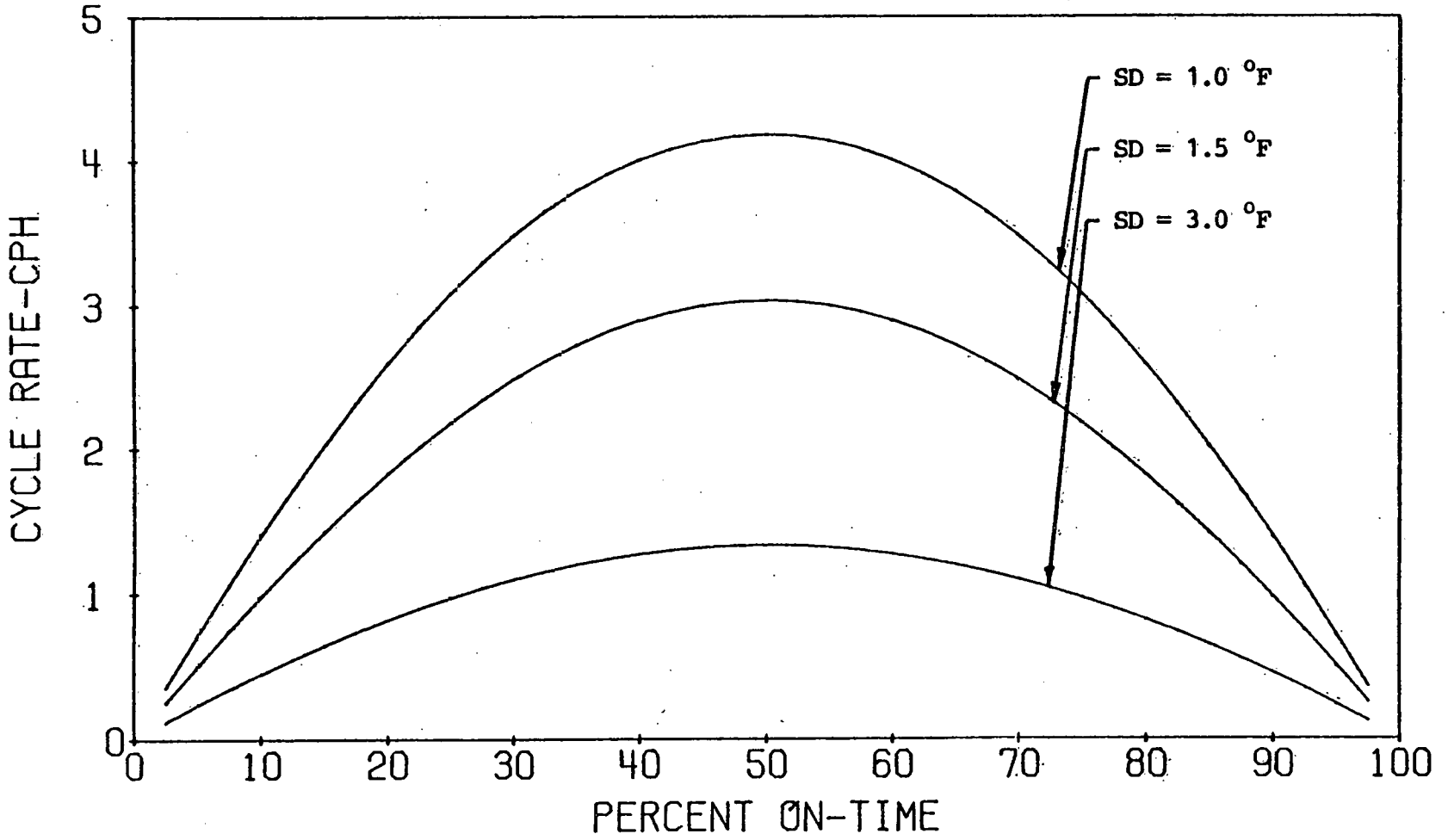

Figure 2C-1 Switch Differential - Percent On-time vs Cycle Rate

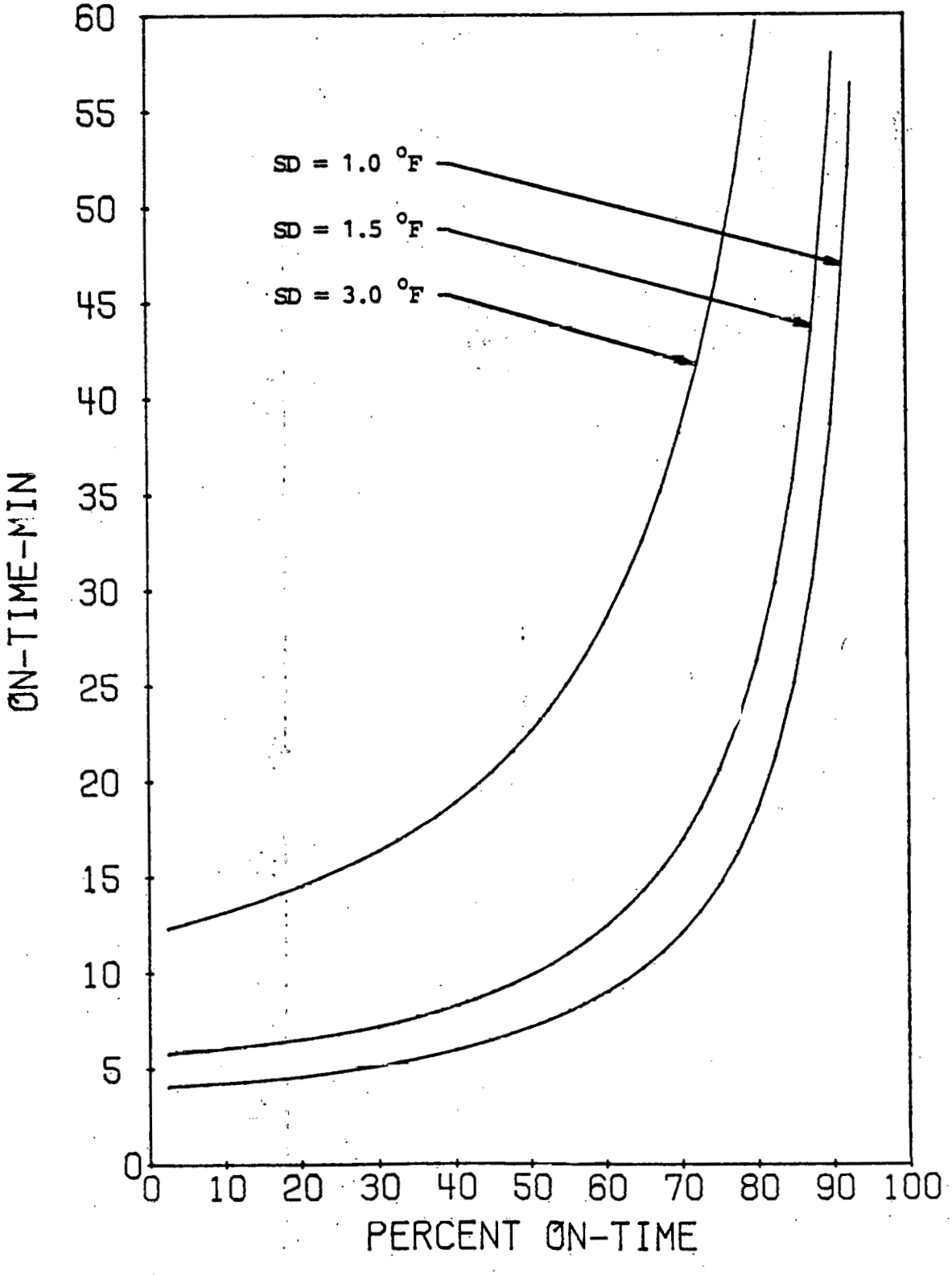

Figure 2C-2 Switch Differential - Percent On-time vs On-time

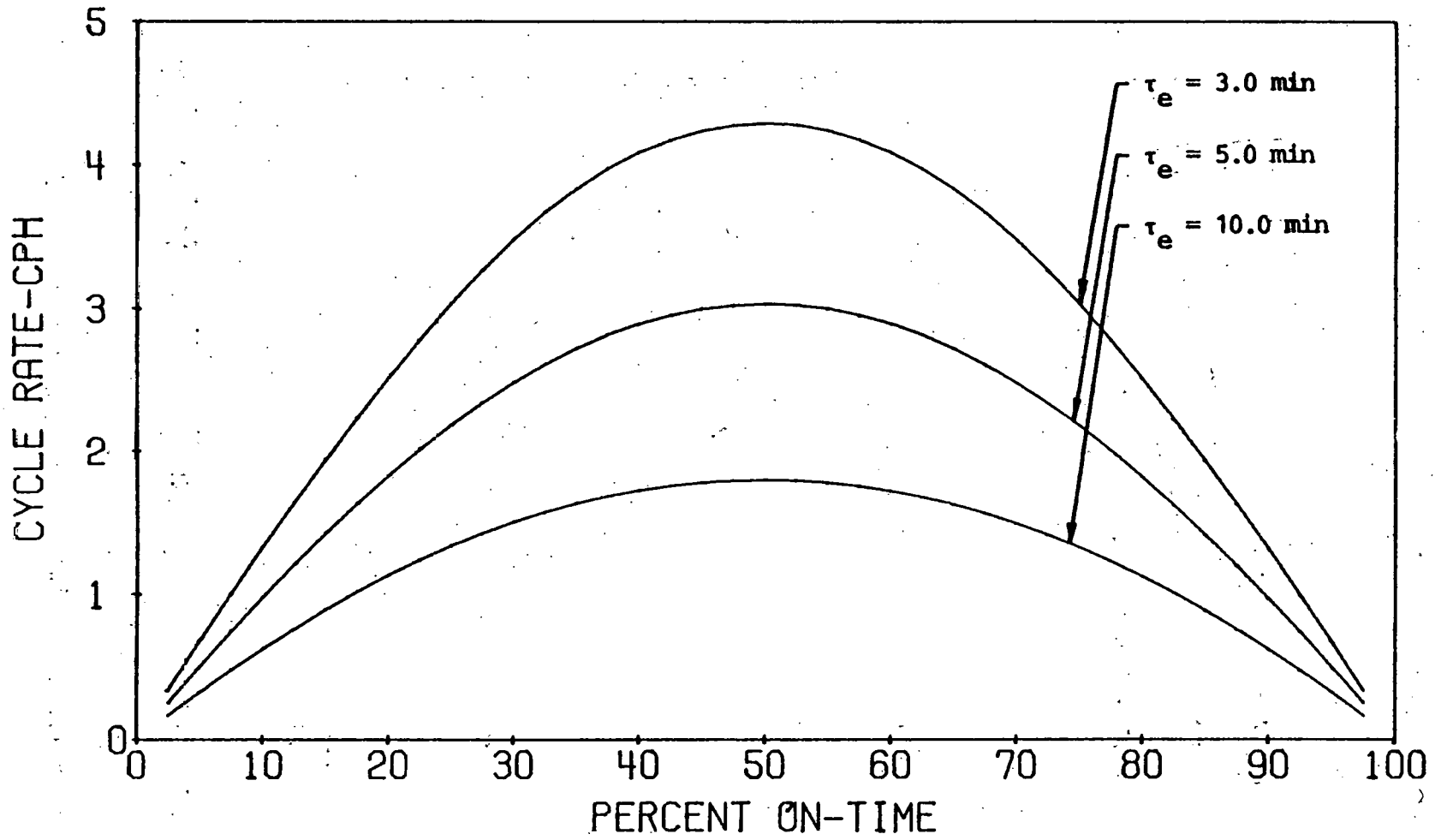

Figure 2C-3 Bimetal Time Constant - Percent On-time vs Cycle Rate

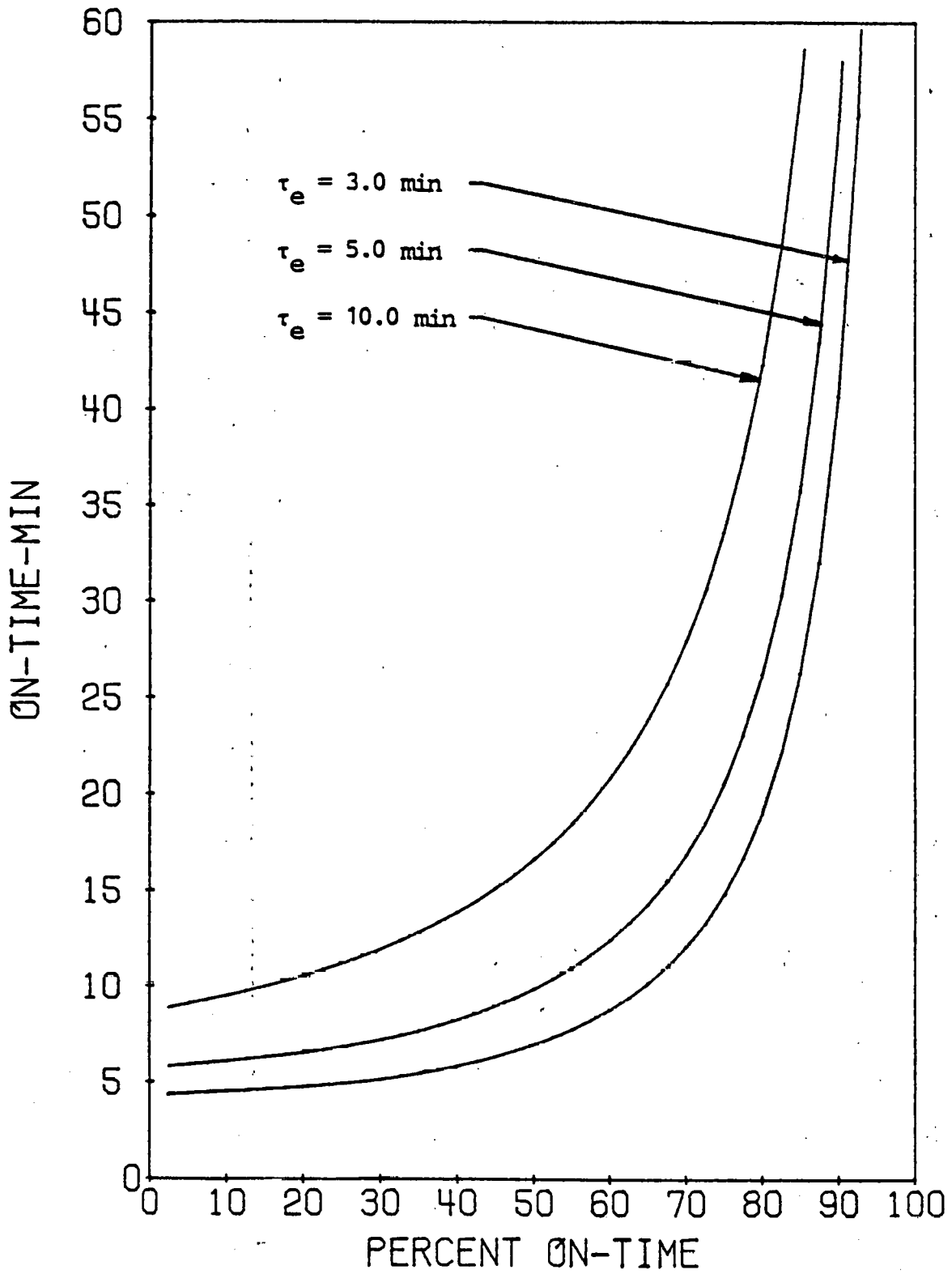

Figure 2C-4 Bimetal Time Constant - Percent On-time vs On-time

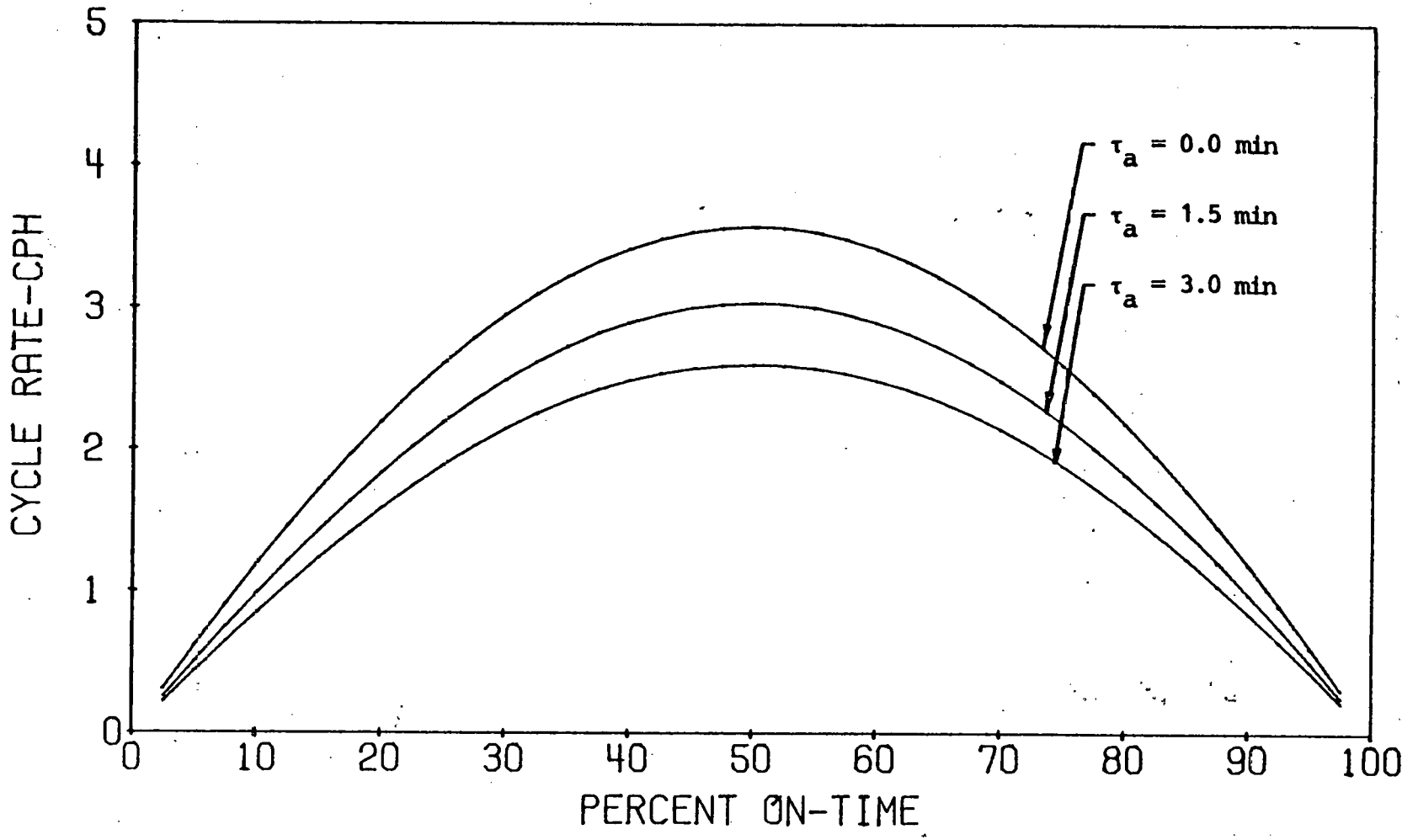

Figure 2C-5 Anticipator Time Constant - Percent On-time vs Cycle Rate

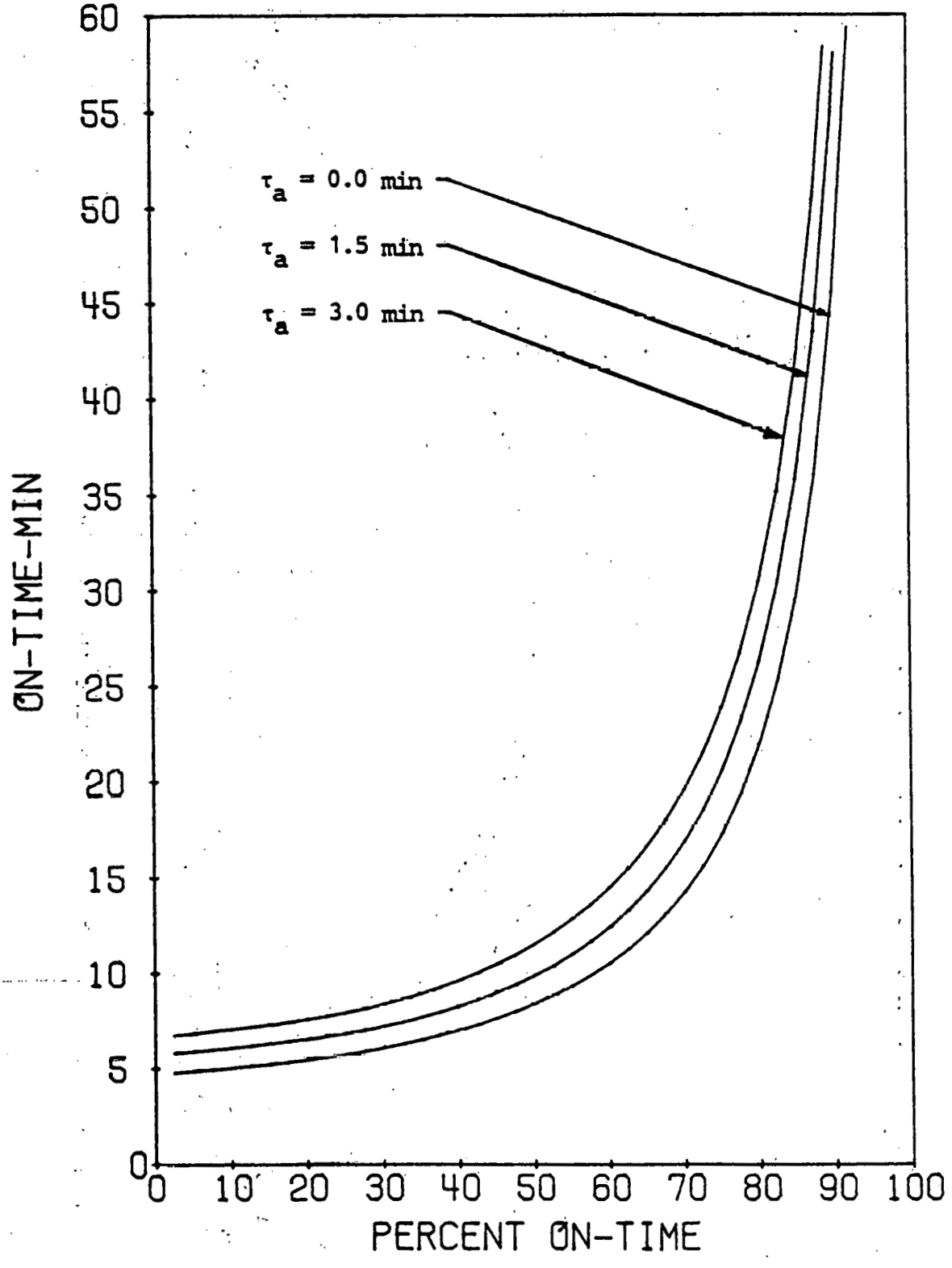

Figure 2C-6 Anticipator Time Constant - Percent On-time vs On-time

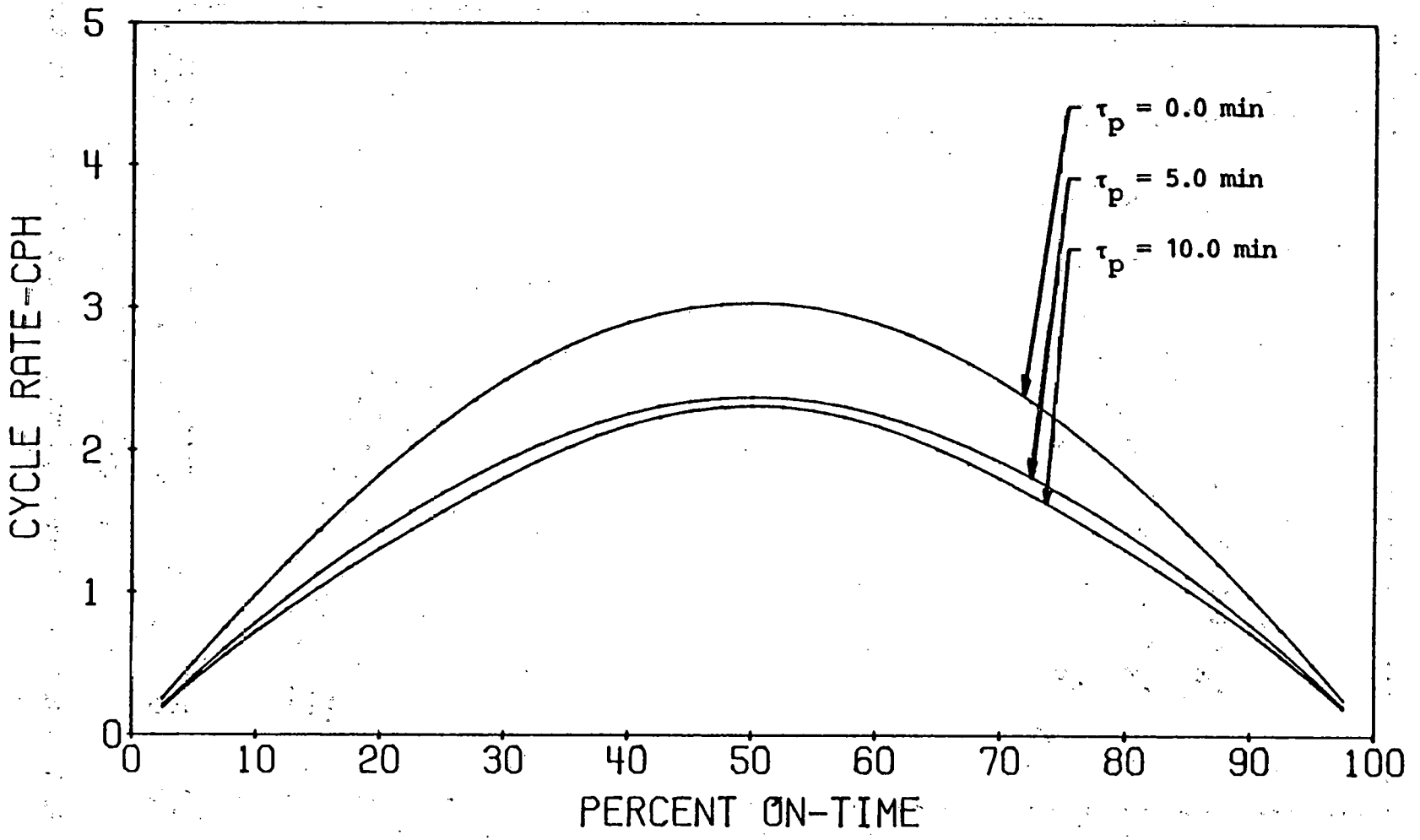

Figure 2C-7 Plant Time Constant - Percent On-time vs Cycle Rate

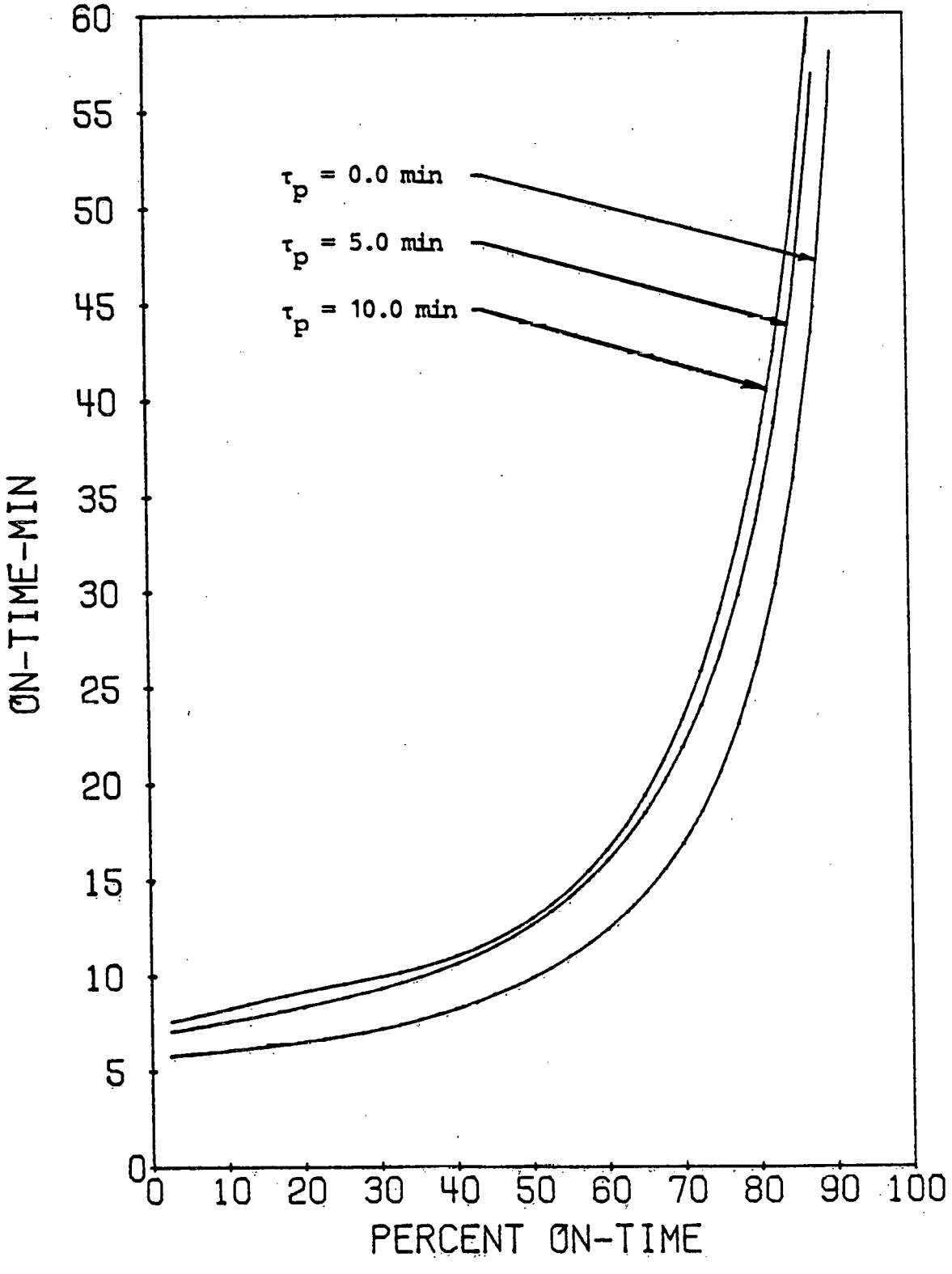

Figure 2C-8 Plant Time Constant - Percent On-time vs On-time

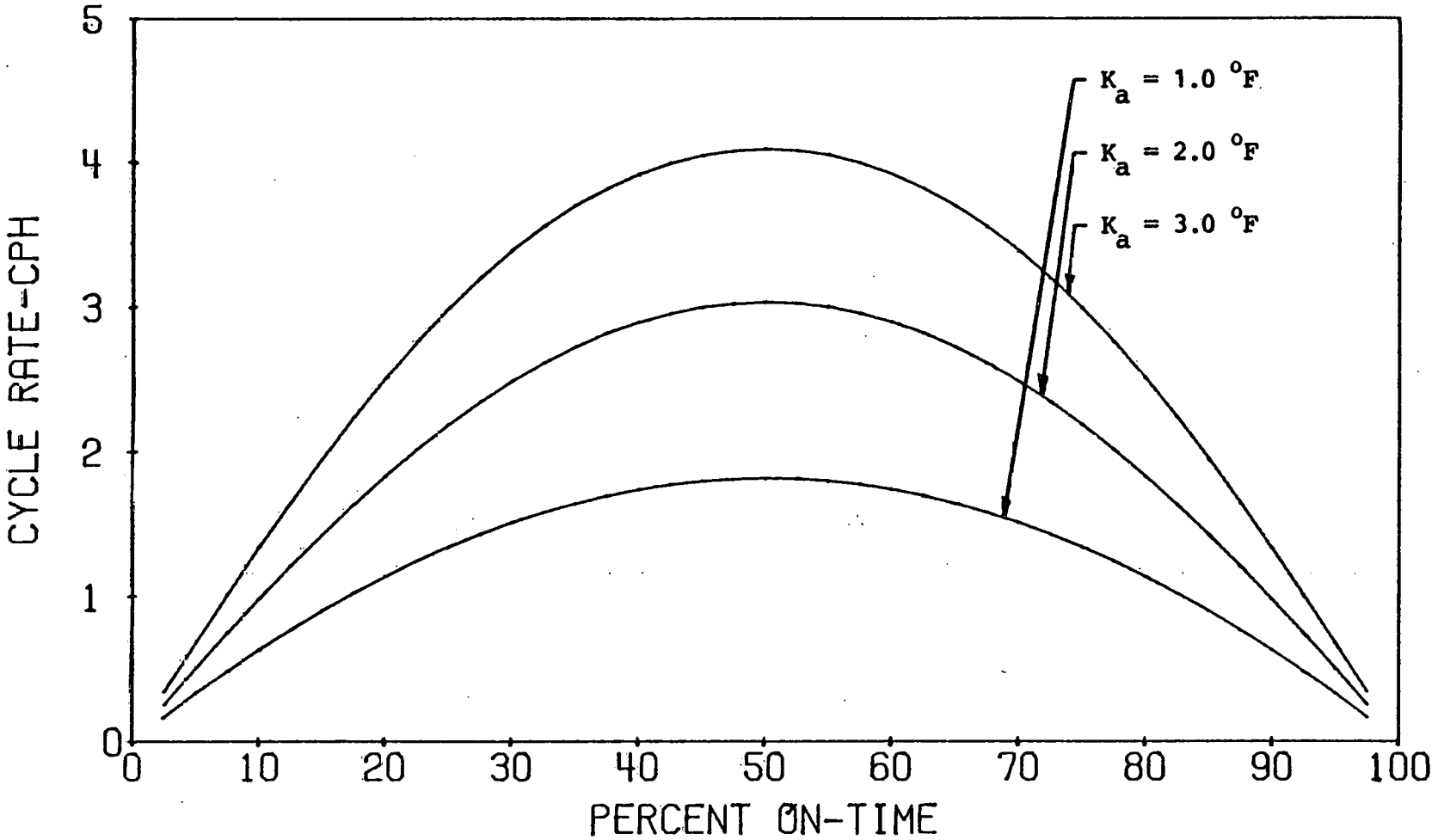

Figure 2C-9 Anticipator Gain - Percent On-time vs Cycle Rate

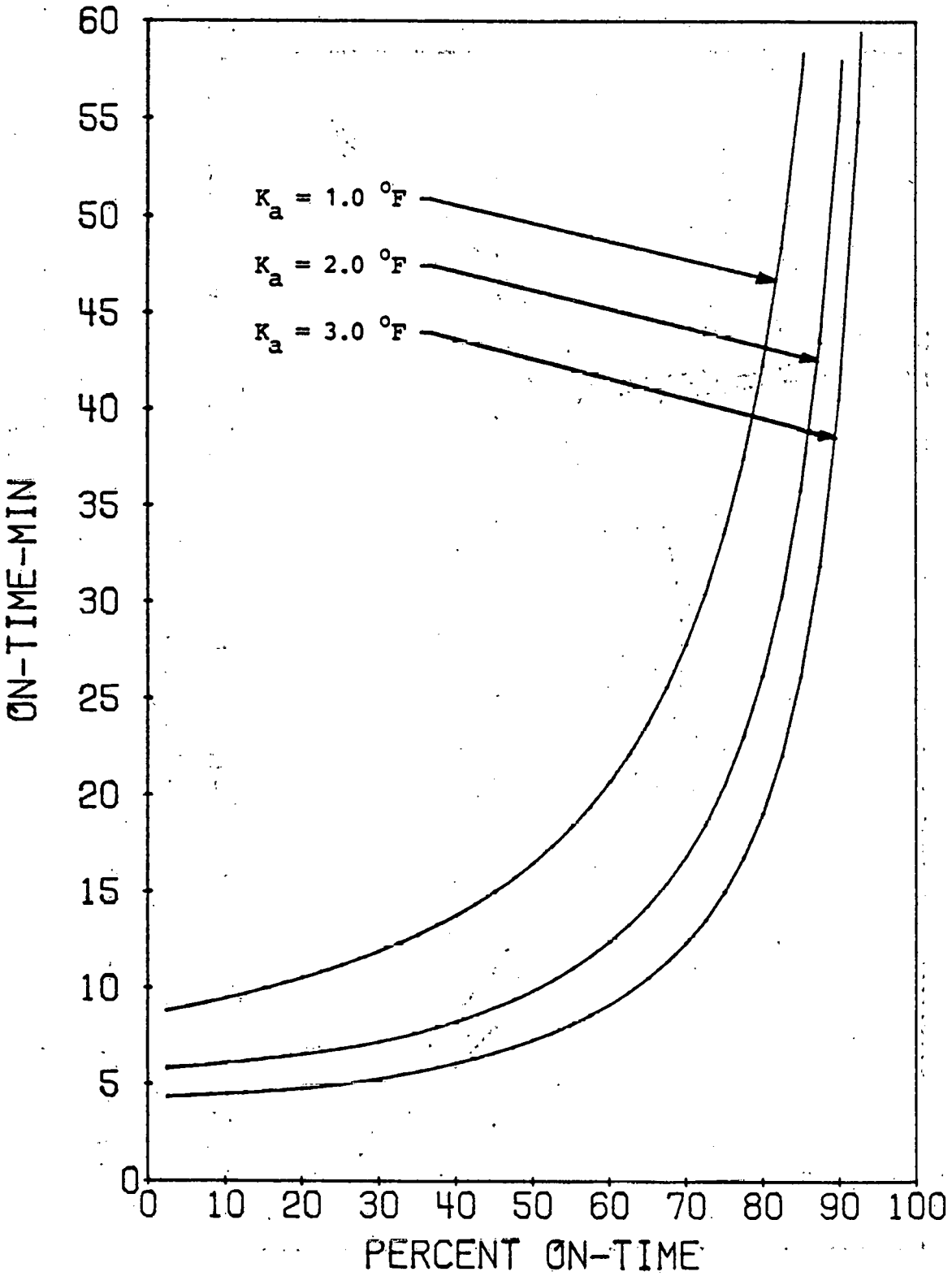

Figure 2C-10 Anticipator Gain - Percent On-time vs On-time

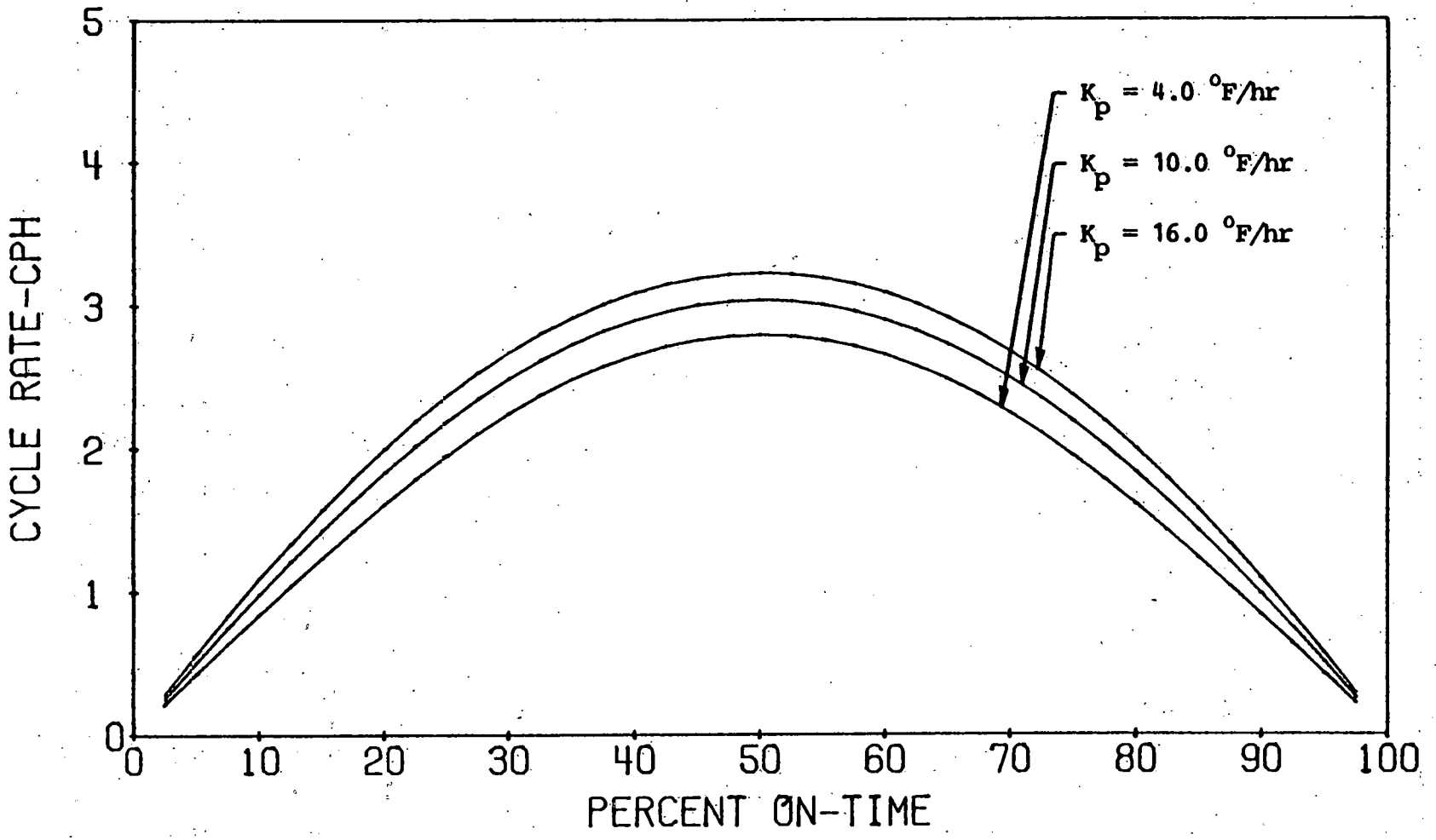

Figure 2C-11 Plant Gain - Percent On-time vs Cycle Rate

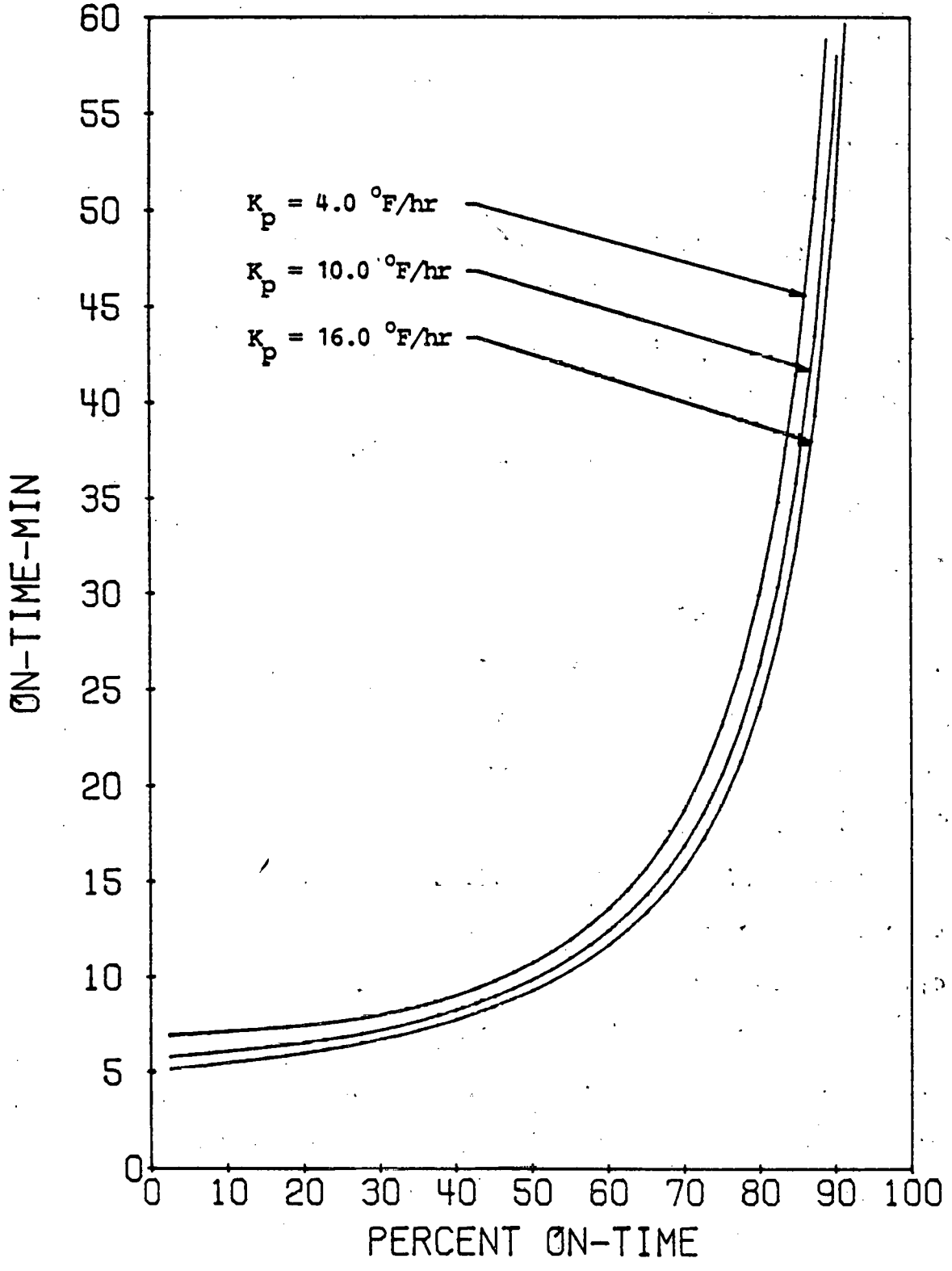

Figure 2C-12 Plant Gain - Percent On-time vs On-time

is essentially the difference between turning the equipment on and off.

The time constant of the bimetal element also has a significant effect on cycling if it is allowed to vary over the extremes of its range. But for relatively small changes in τ_e, its effect on cycling is secondary to that of SD. See Figure 2C-3.

Figure 2C-5 shows the effect of the anticipator time constant. It can be seen that its effect is not very significant. The extreme case of τ_a=0 does not increase the cycle rate more than 1 cph over the case where τ_a=3 minutes.

The influence of the heating/cooling plant time constant is also not very significant in affecting the cycle rate. In fact, as τ_p increases from 5 minutes to 20 minutes, the cycle rate stays about the same at 2.4 cph maximum. This is seen in Figure 2C-7.

Figure 2C-9 shows the effect of the anticipator temperature rise. After SD, K_a has the largest effect on cycling relative to its range of variation. As K_a increases from 2°F to 9°F (1.1°C - 5.0°C), the cycle rate increases from about 3 cph to almost 8 cph. This is important because in some thermostats K_a can be adjusted manually so that several different cycle rates can be produced for the same percent on-time.

The last parameter to be studied is K_p, the steady state plant output. As can be seen in Figure 2C-11, K_p

has little effect on the cycle rate. This agrees with the conclusions reached by McBride [1979] on the effect of the temperature ramp on cycling.

These results are summarized in Table 2C-1. Each parameter is listed, its influence on the system noted and the relative importance of each parameter on cycling is indicated by a ranking. This ranking is somewhat arbitrary, but it does help to compare the influence of each parameter on cycling.

In summary, it has been seen that the parameters that have the largest effect on the cycle rate are associated with the thermostat. This indicates that the thermostat is the major factor in determining the cycling of the system. Furthermore, it has been seen that the on-time of the system tends to a non-zero value as percent on-time tends to zero. This also emphasizes the dominant role of the thermostat.

As far as the DOE test procedures are concerned, it was seen that the duty cycle for test D could be explained by ideal thermostat dynamics. Since the above results confirm the major role of the thermostat in the system, this further justifies the prescribed duty cycle. That is, a six minute on - twenty-four minute off cycling scheme should be representative of actual field operation of air conditioning equipment operating at 20% on-time.

Table 2C-1 Qualitative Results of Computer Simulation

Parameter	Effect on Cycling	Magnitude of Effect	Rank
SD	As SD decreases, cycle rate increases	Largest effect relative to its range	1
K_a	As K_a increases, cycle rate increases	Large effect, manually adjustable	2
τ_e	As τ_e decreases, cycle rate increases	Large effect over extremes of range	3
τ_a	As τ_a decreases, cycle rate increases	Relatively small effect	4
τ_p	As τ_p increases, cycle rate decreases	Little effect after 5 minutes	5
K_p	As K_p increases, cycle rate increases	Smallest effect of parameters	6

CHAPTER III - SELECTED MEASUREMENT ERRORS

Section A - Introduction

For more than a year, the air conditioning industry has been testing their products according to the DOE test procedures in order to label them with an SEER. In this time, there have been many questions and concerns about the test procedures and the measured results. The industry, in general, has made a determined effort to understand and comply with the test procedures. Large amounts of time and money have been spent to obtain new equipment, build or redesign test chambers and formulate new testing strategies. In spite of this effort, test results continue to be questioned because many manufacturers have found that by simply changing their test installation, while still conforming to the governing procedures, they obtain different results (DOE Workshops [1980]). This is a real problem. But a far more serious problem could arise if a manufacturer were to have a unit tested by an independent testing laboratory, such as ETL, and the results for the same unit, when tested by the manufacturer, did not agree. As this has happened, it is imperative that this problem be resolved so that manufacturers may have confidence in their test results and may have those results reproduced by an

independent testing laboratory as well as by competitors. (It should be noted that some manufacturers have obtained good agreement between their results and those of ETL.)

The majority of these problems stem from the measurement of the cyclic capacity of a test unit, $Q_{cyc,dry}$. This quantity represents the amount of cooling done in a six minute on period and its defining equation is:

$$Q_{cyc,dry} = \frac{60\, c_p V A \int_0^{t_{on}} \Delta T \, dt}{v\,(1+W_n)} \qquad (3A\text{-}1)$$

where V = Velocity, ft/sec (m/sec)

c_p = Specific heat, Btu/lbm-^{o}F (KJ/kg -^{o}C)

ΔT = Temperature difference across the coil, ^{o}F (^{o}C)

t_{on} = On time, min

v = Specific volume ft^3/lbm (m^3/kg)

W_n = Humidity ratio

Measurements for the calculation of the integral in Eq. 3A-1 come from the transient test D. All the other terms are calculated from measurements taken during the preceding test C. These measurements are governed by ASHRAE Standard 37-78, ARI Standard 210-79 and specific provisions in the test procedures. However, the above two standards were written for steady state testing and do not address some of the problems of transient measurements. The test procedures are unclear on matters concerning the test set-up such as implementation of the dampers and thermocouple grid placement. Therefore, different results

for $Q_{cyc,dry}$ could be obtained from the same unit by testing it in two different test set-ups, although both might conform to the standards and the test procedures. As a result, questions and problems have arisen.

The purpose of this chapter is to examine several sources of measurement error in the test procedures. This will not include errors due to test tolerances, inherent equipment inaccuracies, etc. (See Thomas [1980] for this error analysis.) The errors that will be discussed are mainly concerned with the test set-up and are the primary cause of the questions and problems mentioned above. Section B will discuss various "minor" sources of error and related questions dealing with the test procedures. Several of these questions will lead into Sections D through G in which four "major" sources of error will be analytically studied. They are: thermocouple response, grid placement, dampers and nonuniform velocity and temperature distributions. Section C will describe a simple heat exchanger model that will be used to aid in studying these four areas of measurement error. Section H will discuss experimental data related to these four areas and will compare this data with the purely analytical results of the previous sections.

Section B - Several Questions and Problems

The intent of this section is to briefly discuss several transient measurement problems and questions as a

prelude to the later sections of this chapter. Most of these concerns have been raised while trying to understand and conduct the DOE tests (DOE Workshops [1980]). It is hoped that this and subsequent sections will resolve some of these concerns.

The first concern deals with ASHRAE Standard 37-78 and ARI Standard 210-79. These standards were written for steady state testing and do not address some of the problems of cyclic testing. For example, where may the thermocouple grid be placed in relationship to the pressure taps or the dampers? This and many other questions could be eliminated by new standards written for cyclic testing.

The on-time for the cyclic test is six minutes and this has been questioned. Chapter I showed that the six minute on - twenty-four minute off cycling scheme is representative of field cycling at a 20% load. Furthermore, much air conditioner and heat pump data appear to reach steady state operating conditions by six minutes (Thomas [1980], Nguyen [1981]). If this is true generally, then an on-time less than six minutes might not allow some units to reach steady state. An on-time greater than six minutes would allow steady state conditions to reduce the transient effects. Since the intent of the test is to measure the transient effects, it appears that the present duty cycle is properly defined.

After being calculated from measurements taken during the steady state test C, do V, c_p, v and W_n remain constant during test D?

While it is a good assumption that c_p is constant during test D, there is some question as to the constancy of the humidity related terms. However, the difficulty of accurate transient measurement of humidity justifies the assumption of constancy. This work will also consider v and W_n to be constants and $1/v(1+W_n)$ will often be written simply as the density, ρ.

V is not constant in a cyclic test. Fans need several seconds before they are up to speed. However, V is usually regarded as constant and represents another good trade-off made by NBS.

Assuming V to be time independent, can it also be assumed uniform over the cross section where temperature measurements are being made?

Without good air mixing and straightening, V will not generally be uniform. This nonuniformity may affect thermocouple response time and lead to substantial errors. This will be discussed in Section G.

Without good air mixing, the temperature of the cooled air stream (T_{out}) will probably not be uniform either. Depending on the thermocouple grid location and the velocity distribution, significant errors could result. See Section G.

At the start of the six minute on-time, the temperature difference across the evaporator coil (ΔT_o) is not always zero. This is a result of the dampers and refrigerant control. However, the operation of the dampers is not clearly defined in

the test procedures so that depending on construction, tightness, placement, etc., many different values for ΔT_o could be obtained. The implications of this will be discussed in Section F.

Room temperature (T_r) and outdoor temperature ($T_{outdoor}$) are allowed to fluctuate $\pm$ 0.5 ^oF (0.3 ^oG) and could fluctuate more during actual testing. The effect of this fluctuation has not yet been analyzed. It is recommended that this effect be investigated so that its effect on capacity may be known. In the subsequent sections, T_{in} and $T_{outdoor}$ will be assumed to be constant and uniform.

What type of errors are associated with the data acquisition system?

Proper selection, maintenance and understanding of the data acquisition system should minimize any errors associated with recording data. However, there are at least four potential trouble spots that should be mentioned. Several devices measure a quantity, such as power, by the use of "counts." It is conceivable that a full count could be lost due to the timing of the measurement. Depending on the value of that count, its loss could significantly affect the measurement.

Many integration schemes use the count method and the above caution applies. However, with the increasing use of computers, numerical integration will often be used to calculate the integral in Eq. 3A-1. Hence, care should be taken to insure that an accurate numerical integration scheme is used.

Since thermocouples produce such small voltages, small electrical variations can affect their accuracy. Therefore, a fluctuating reference junction temperature and noise are possible sources of error. Four methods of maintaining the reference temperature are the ice bath, the electronic ice bath, the triple point of water and the oven. Whichever method is used, it is important that its temperature remain as stable as possible. To minimize the effects of noise, appropriate grounding and shielding should be used.

As far as errors associated with equipment calibration, tolerances and inherent inaccuracies are concerned, Thomas [1980] has prepared a useful error analysis related to the test procedures which should be consulted. In the present work, no error will be assumed concerning the data acquisition system.

How does thermocouple response time affect the capacity measurement?

This will be discussed in detail in Section D.

Where should the thermocouples be placed?

This will be discussed in Section E.

What effect do thermal mass and heat transfer through duct walls have on the capacity measurement?

This will also be discussed in Section E.

How significant are radiation effects?

The literature indicates that radiation effects are generally small (Johnson, et.al. [1957], Moffat [1957]). Several calculations will consider this statement to see

how well it applies to the test procedures. Consider the radiative exchange between the walls and the coil. Suppose an extreme example where the walls are at 80°F (27°C), the coil is at 45°F (7°C), the emissivity of the walls is ε= .4 the view factor between the walls and the coil is F=.4 and the surface area of the walls is A_w=50 ft^2(4.7m^2). Then,

$$\dot{q} = \varepsilon F A_w \sigma (T_w^4 - T_c^4) \qquad (3B\text{-}1)$$

$$= 274 \text{ Btu/hr (80 W)}$$

$$= 27 \text{ Btu/6 min (8 W/6 min)}$$

where

$$\sigma = 1.714 \times 10^{-9} \text{ Btu/hr-ft}^2\text{-}^\circ\text{R} \quad (5.670 \times 10^{-8} \text{ W/m}^2 \text{ K}^4)$$

Under these extreme conditions, a two-ton unit would have its capacity reduced by less than 1%.

Now consider the effect of radiant heat transfer between the walls, the thermocouple and the coil. A steady state energy balance would yield the following:

energy radiated from walls = energy radiated to coil by thermocouple + energy convected from thermocouple

$$\varepsilon_w F_{w \text{ to } tc} A_w \sigma (T_w^4 - T_{tc}^4) = \varepsilon_w F_{tc \text{ to coil}} A_{tc} \sigma (T_{tc}^4 - T_{coil}^4) + h A_{tc} (T_{tc} - T_{air}) \qquad (3B\text{-}2)$$

Solving for the term $(T_{tc}-T_{air})$ and applying the reciprocity law for view factors, the following results:

$$(T_{tc} - T_{air}) = \qquad (3B\text{-}3)$$

$$\frac{\varepsilon_w F_{tc \text{ to wall}} A_{tc} \sigma (T_w^4 - T_{tc}^4) - \varepsilon_{tc} A_{tc} F_{tc\text{-coil}} \sigma (T_{tc}^4 - T_{coil}^4)}{h A_{tc}}$$

Let

$$T_w = 60^\circ F\ (16^\circ C)$$

$$T_{tc} = 55^\circ F\ (13^\circ C)$$

$$T_{coil} = 45^\circ F\ (7^\circ C)$$

$$\epsilon_w = .4$$

$$A_{tc} = .0003\ ft^2\ (3x10^{-5} m^2)$$

$$F_{tc\text{-}wall} = .7$$

$$\epsilon_{tc} = .2$$

$$F_{tc\text{-}coil} = .15$$

$$h = 20\ Btu/hr\text{-}ft^2\text{-}^\circ F\ (114\ W/m^{2\circ}C)$$

Substituting these values in Eq. 3B-3, $(T_{tc}-T_{air}) = .02^\circ F$ $(-.01^\circ C)$. For a two-ton unit, this change in measured temperature results in a change of measured capacity of less than .5%. If the walls were at $80^\circ F$ $(27^\circ C)$, the change in measured capacity would be less than 1.5%. The values used in this example are generous and in actual operation, radiation effects would be smaller. In this work, radiation effects will be considered negligibly small.

The use of insulation is desirable in the test set-up. Any heat transfer into the cooled airstream will cause its temperature to rise which will reduce the measured capacity of the unit. In order to measure as nearly as possible the actual capacity, all such effects should be minimized. Therefore, as much insulation as practical should be used to effectively eliminate the effects of heat transfer. This will be discussed in more detail in Section E.

Section C - Heat Exchanger Assumptions

Before the measurement errors of Sections D through G can be analyzed, some assumptions about the heat exchanger are needed. Many authors and numerous data indicate that the heat exchanger can be modeled as a first order system, at least as a first approximation (Hart [1978], Murphy [1977]). Figures 3C-1 and 3C-2 show two temperature drop across the coil versus time plots obtained from two different sources (Thomas [1980]). It is observed that they are roughly exponential in shape. The data points in Figure 3C-1 begin at the origin, show a steady state temperature difference of about 24°F (13°C) and have a time constant of about 60 seconds. (The time constant is defined as the time it takes to reach 63% of the steady state value.) On the other hand, the data points in Figure 3C-2 do not begin at the origin, show a steady state temperature difference of about 16°F (9°C) and have a time constant of about 75 seconds. Both appear to have reached steady state by six minutes of on-time.

With these considerations, the following modeling assumptions will be made. It should be remembered that this heat exchanger model is quite arbitrary. The intent of this model is to provide a base for comparisons which will be made in the next four sections.

1. The heat exchanger will be modeled as a first order system with T_{out} equal to the temperature of the cooled air stream.

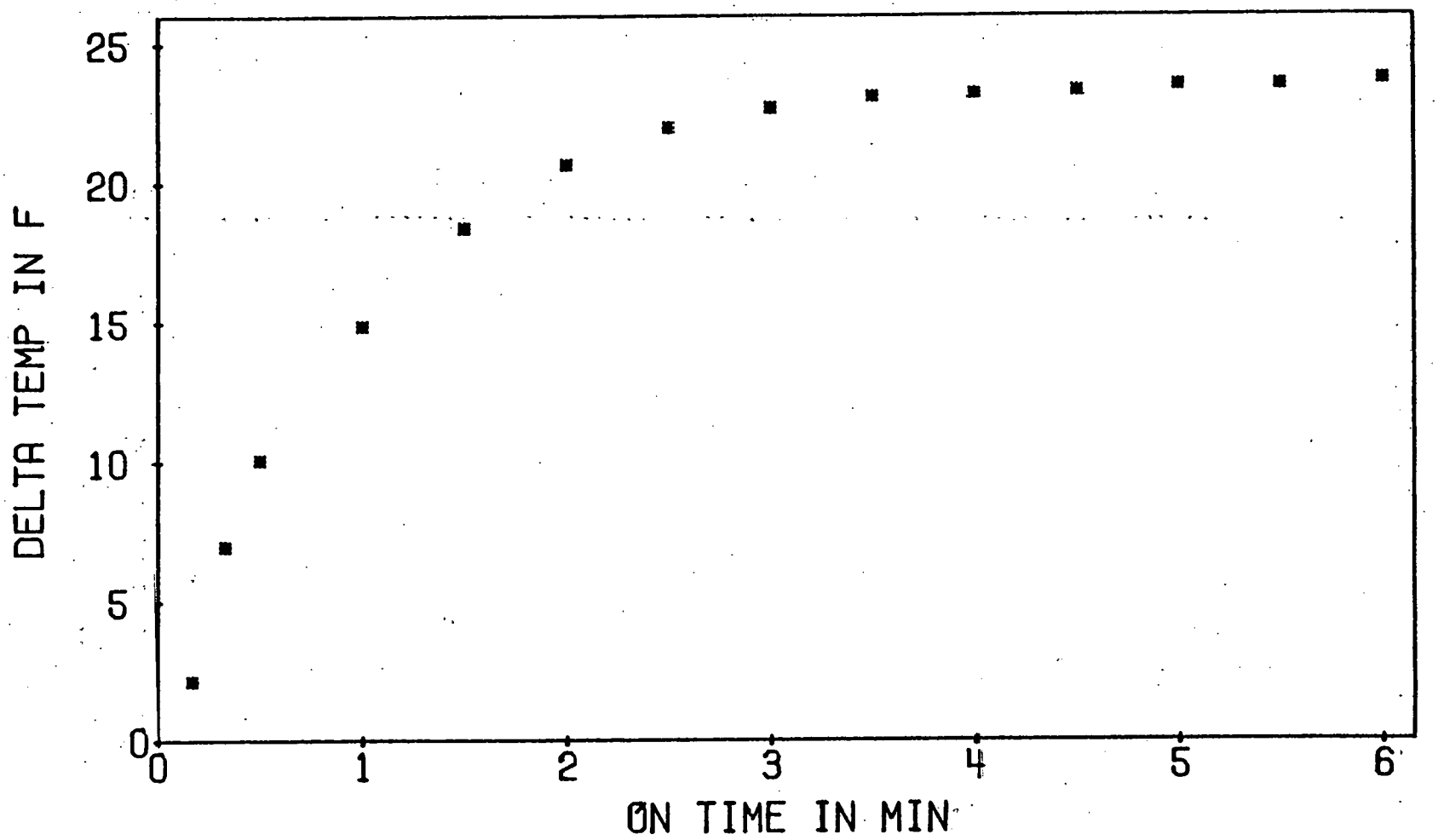

Figure 3C-1 ΔT vs TIME Curve with $\Delta T_o=0$ (Experimental)

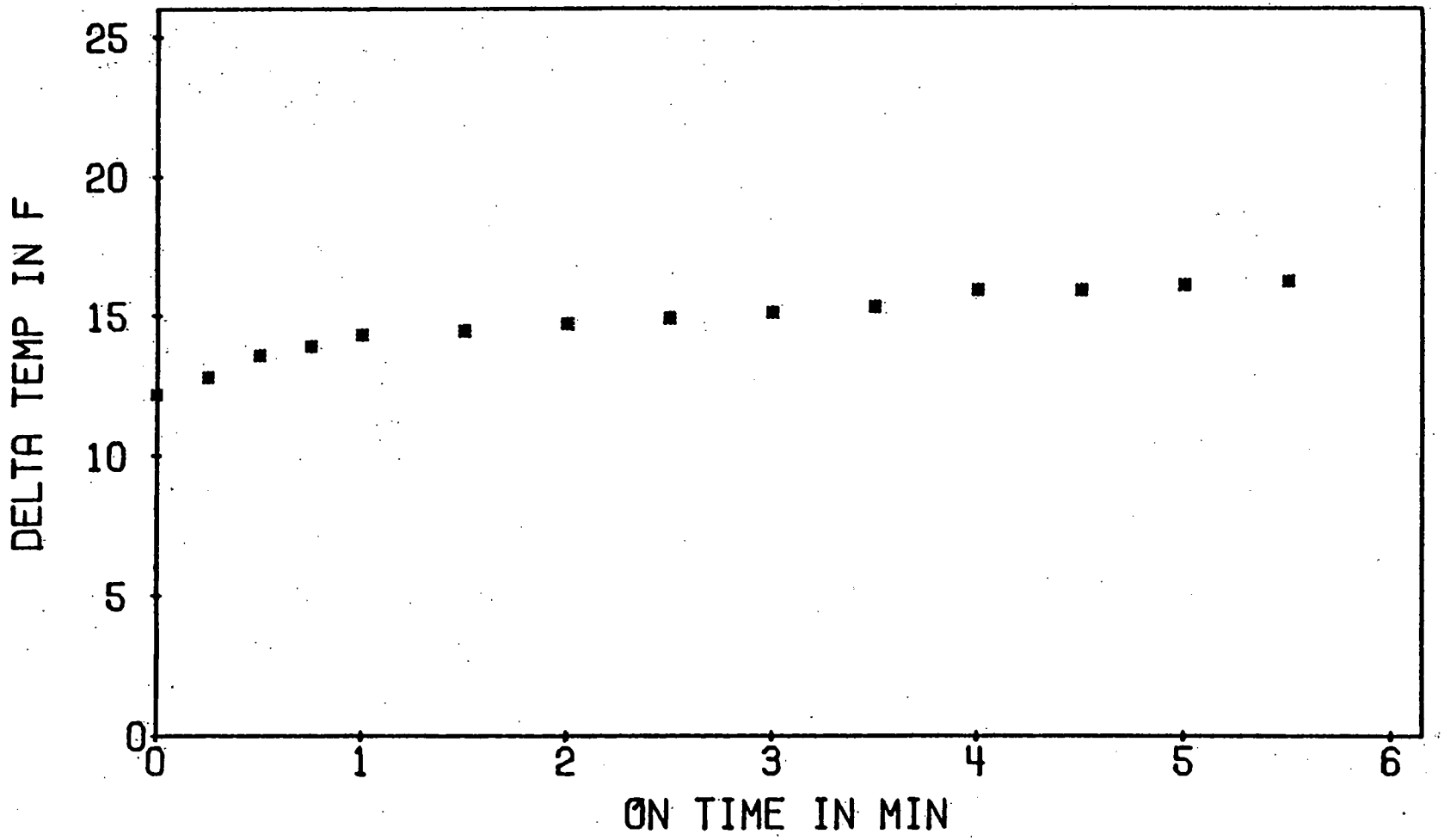

Figure 3C-2 ΔT vs TIME Curve with $\Delta T_o \neq 0$ (Experimental)

2. The time constant, τ_h, will vary between 30 and 90 seconds. The fact that it is not zero will be attributed to the thermal mass of the coil and refrigerant dynamics.

3. Room temperature, T_r, will equal 80°F (27°C).

4. Steady state temperature, T_{ss}, will equal 60°F (16°C).

5. The temperature difference across the heat exchanger, $\Delta T=T_r-T_{out}$, will equal 20°F (11°C) at steady state.

6. The initial temperature of the coil and the surrounding air, T_o, will vary from 60°F (16°C) to 80°F (27°C) but will equal 80°F (27°C) unless otherwise stated.

7. Only the heat exchanger (coil) will be considered in the forthcoming analysis of capacity measurement. This means the effects of a blower assembly will not be considered, i.e. air-handler units will not be discussed.

A block diagram for this system can be written as:

$$T_r \longrightarrow \boxed{\frac{T_{ss}/T_r}{\tau_h\, D+1}} \longrightarrow T_{out}$$

In equation form, this is written as

$$\tau_h \frac{dT_{out}}{dt} + T_{out} = T_{ss} \qquad (3C\text{-}1)$$

Solving this differential equation gives:

$$T_{out}=T_{ss}+(T_o-T_{ss})e^{-t/\tau_h} \qquad (3C\text{-}2)$$

Therefore, the temperature difference across the coil is

$$\Delta T=(T_r-T_{ss}) - (T_o-T_{ss})e^{-t/\tau_h} \qquad (3C-3)$$

Figure 3C-3 shows a plot of ΔT vs TIME for τ_h=30, 60 and 90 seconds. These curves will be called ideal curves because they are considered to have been generated under ideal conditions, i.e. perfect thermocouple response, perfect air mixing, no thermal storage or heat transfer effects, no dampers, etc. The ideal capacity can be found by integrating Eq. 3C-3 over six minutes.

$$QIDEAL = \rho c_p VA \int_o^{t_{on}} \Delta T \, dt \qquad (3C-4)$$

$$= \rho c_p VA \, (T_r-T_{ss}) \, t_{on} + \tau_h (T_o-T_{ss})(e^{-t_{on}/\tau_h}-1)$$

For numerical comparison, let

ρ = Density of air = .071 lbm/ft^3 (1.14 kg/m^3)

c_p = Specific heat = .24 Btu/lbm^{o}F (1 KJ/kg^{o}C)

V = Velocity = 15 ft/sec (4.6 m s)

A = Cross-sectional area = 1 ft^2 (.09m^2)

Substituting these values into Eq. 3C-4,

QIDEAL = 1687 Btu (494 W.hr) for τ_h=30 sec

QIDEAL = 1534 Btu (450 W.hr) for τ_h=60 sec

QIDEAL = 1389 Btu (407 W.hr) for τ_h=90 sec

QIDEAL for τ_h= 30 seconds will be used throughout the remaining sections as a base value. It roughly corresponds to a 1½ ton unit. Analytical predictions for capacity which include the effects of finite thermocouple response, thermal mass effects, etc. will be compared to QIDEAL.

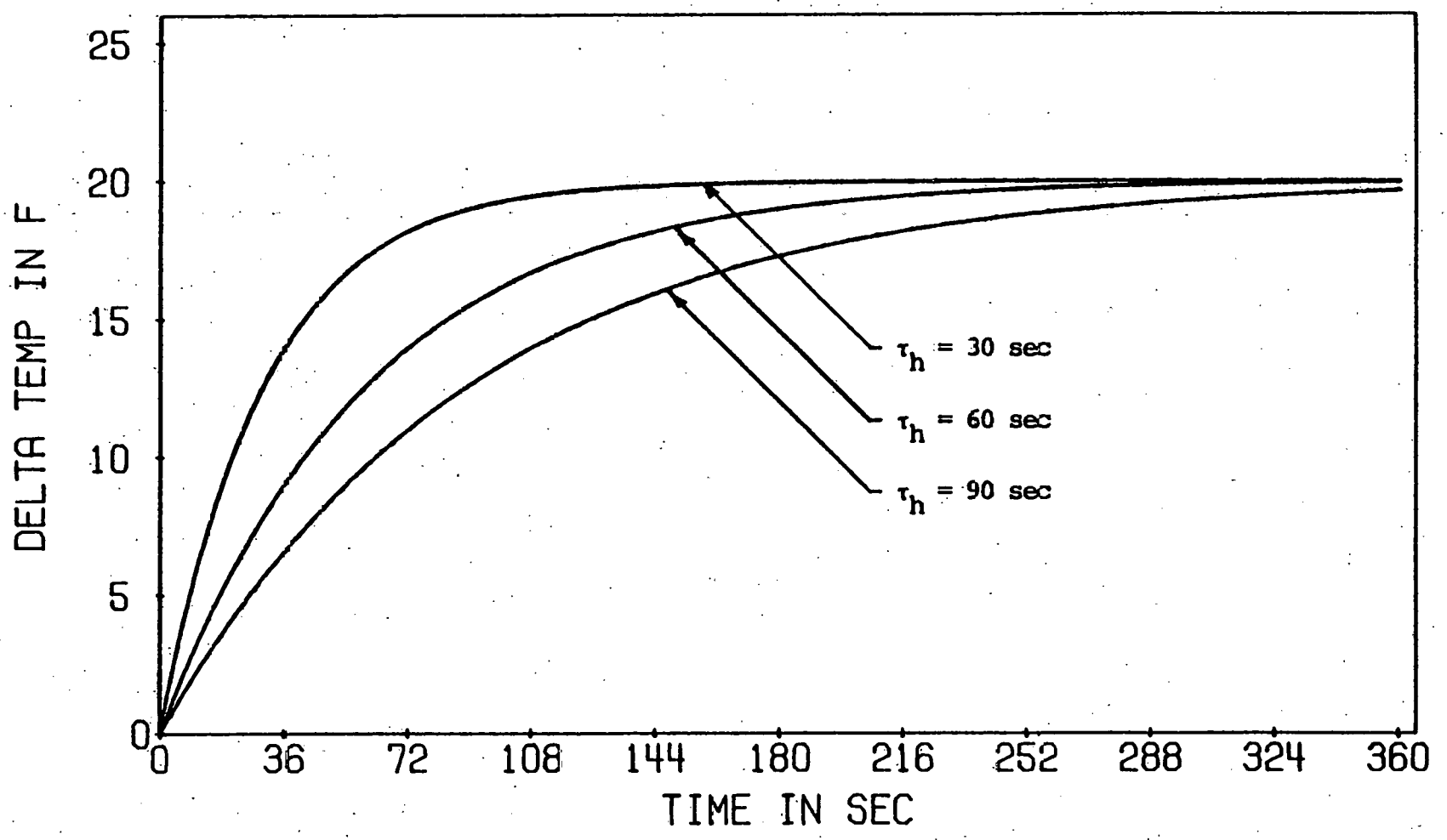

Figure 3C-3 ΔT vs TIME Curves (Analytical)

This will provide a relative magnitude of error which is caused by these different effects.

Since QIDEAL will be referred to frequently, Table 3C-1 will summarize the numerical values used in its calculation.

Section D - Thermocouple Response

One of the transient measurement concerns of test D is the response time of the temperature sensing device. Since this response time is finite, it is important to determine its influence on the cyclic capacity measurement.

The following quote from the Federal Register briefly defines the response time for the test procedures.

> "Instrumentation shall have a response time of 2.5 seconds or less. Response time is the time required for the instrumentation to obtain 63% of the final steady state temperature difference when subjected to a step change in temperature difference of 15°F or more " (Federal Register [1979]).

The instrumentation commonly used consists of thermocouples and an appropriate recording device. Two important factors are implied in the above definition. First, the medium in which the response time of the measuring device (hereafter, a thermocouple) is found is air. The distinction is important because if some other medium were used, such as water, the response time would be quite different. Second, it is implied that the velocity of the air stream is comparable to that which passes through the air conditioning unit. If an unrepresentative velocity were used, the response time could also be unrepresentative.

Table3C-1 Numerical Values for QIDEAL

$QIDEAL = \rho c_p VA \int_0^{t_{on}} \Delta T \, dt$ where $\Delta T = (T_r - T_{ss}) - (T_o - T_{ss}) \, e^{-t/\tau_h}$	
$\rho = .071$ lbm/ft^3	$c_p = .24$ Btu/lbm-^{o}F
V = 15 ft/sec	A = 1 ft^2
$T_r = 80$ ^{o}F	$T_o = 80$ ^{o}F
$T_{ss} = 60$ ^{o}F	$\tau_h = 30$ sec
$\Delta T_{ss} = 20$ ^{o}F	$\Delta T_o = 0$ ^{o}F
$t_{on} = 6$ minutes	
$\int_0^{t_{on}} \Delta T \, dt = 110$ F-min	
QIDEAL = 1687 Btu	

Response Time

A defining equation for thermocouple response can be found in most heat transfer books such as Kreith [1973]. A lumped parameter analysis is usually made and errors due to heat conduction through the leads and radiant energy exchange are considered negligible. These simplifications give

$$\frac{T_{meas}-T_{ss}}{T_o-T_{ss}} = e^{-t/\tau_t} \qquad (3D-1)$$

where

$$\tau_t = \frac{mc_p}{hA_s} \qquad (3D-2)$$

and

T_{meas} = Output temperature as measured by the thermocouple

T_o = Initial temperature of the thermocouple

τ_t = Time constant of the thermocouple

m = Mass of the thermocouple

c_p = Specific heat of the thermocouple

h = Convective heat transfer coefficient

A_s = Surface area of the thermocouple

As can be seen in Eq. 3D-2, the time constant is a function of m, A_s and h.

Depending on how the thermocouple is made, its junction can be modeled as a cylinder, a sphere or some other geometrical body. See Figure 3D-1. Assuming constant properties of a copper-constantan thermocouple, the time

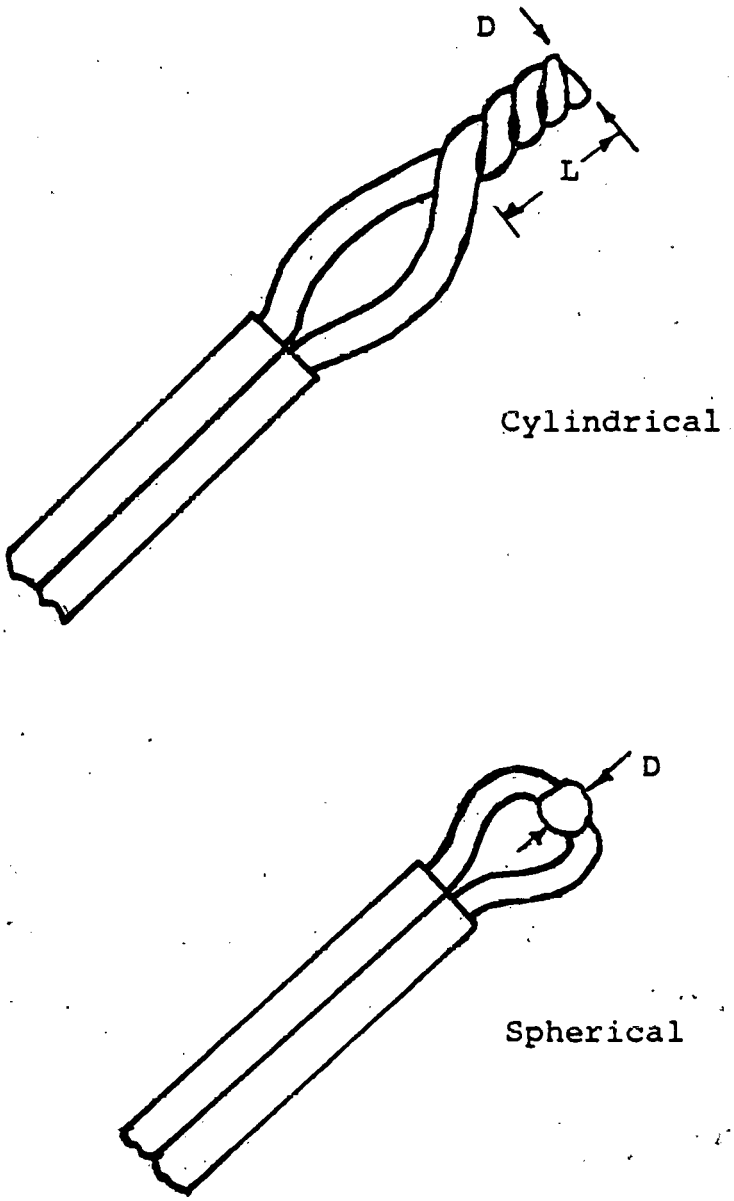

Figure 3D-1 Cylindrical and Spherical Thermocouple Junctions

constant can be analytically studied after making appropriate substitutions for the surface area, the heat transfer coefficient, etc. Specifically, its dependence on velocity and wire thickness is desired.

First, consider a cylindrical junction. Its volume and surface area are given by

$$\text{Vol} = \frac{\pi D^2 L}{4} \tag{3D-3}$$

$$A_s = \pi DL \tag{3D-4}$$

where

D = Diameter of wire

L = Length of junction

The convective heat transfer coefficient is found by considering a free right circular cylinder normal to an air flow. A big assumption is made here. It will be assumed that the wire leads to the junction are small compared to the junction (which is not true) so that classical correlations may be used. Kreith [1973] recommends the following correlation.

$$\frac{\bar{h}D}{k} = C\left(\frac{VD}{\nu}\right)^n \tag{3D-5}$$

where

$\bar{h}$ = Average convective heat transfer coefficient, Btu/hr $ft^2{}^oF$ ($W/m^2{}^oC$)

k = Thermal conductivity of air, .016 Btu/hr $ft^2{}^oF$ (.027 W/m^oC)

ν = Kinematic viscosity of air, $.16 \times 10^{-3} ft^2/sec$ ($.15 \times 10^{-4} m^2/sec$)

C = Empirical constant, .615

n = Empirical constant, .466

Substitution of these expressions into Eq. 3D-2 yields

$$\tau_t = \left(\frac{\rho c_p \nu^n D^{2-n}}{4kC}\right) V^{-n} \qquad (3D\text{-}6)$$

where ρ = density = 558 lbm/ft^3 (8938 kg/m^3) c_p = .096 Btu/lbm$^\circ$F (402 W s/kg$^\circ$C)

Assuming that the diameter of the junction is twice the diameter of the wire and letting the wire vary from 22 AWG (.1253 in) to 30 AWG (.0100 in), the curves in Figure 3D-2 are generated.

Now, consider a spherical junction. The volume and surface area are given by

$$\text{Vol} = \frac{\pi D^3}{6} \qquad (3D\text{-}7)$$

$$A_s = \pi D^2 \qquad (3D\text{-}8)$$

The convective heat transfer coefficient is found by considering a free sphere in flowing air. The same assumption as before is made concerning the leads. Kreith recommends the same correlation as before but with different empirical constants (C = .37, n = .6). After the appropriate substitutions,

$$\tau_t = \left(\frac{\rho c_p \nu^n D^{2-n}}{6kC}\right) V^{-n} \qquad (3D\text{-}9)$$

Assuming that the diameter of the sphere is twice the wire thickness, the curves in Figure 3D-3 are found.

Figures 3D-2 and 3 both indicate that thermocouple response is quite dependent on velocity and wire thickness.

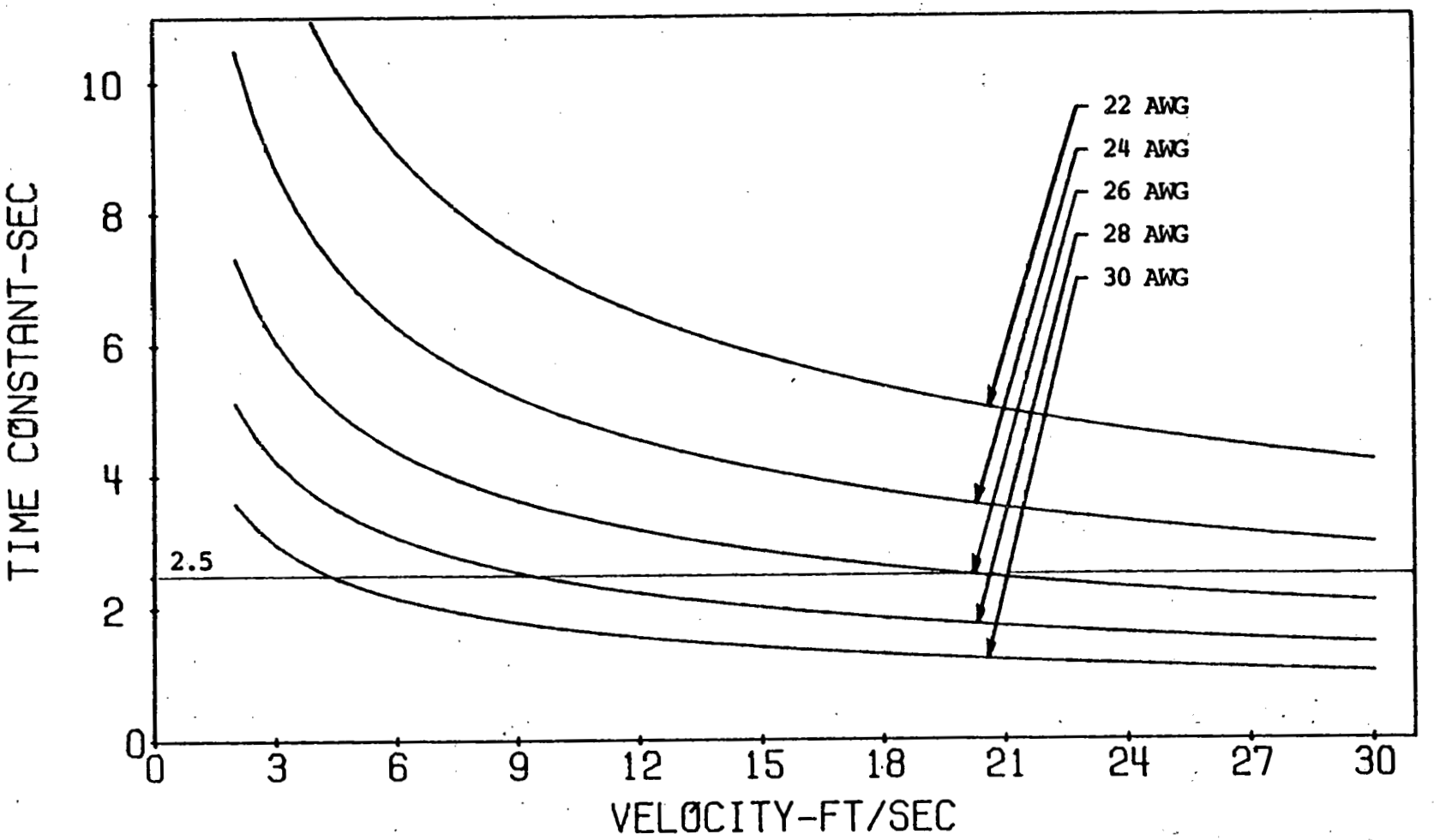

Figure 3D-2 Thermocouple Response for Cylindrical Junction

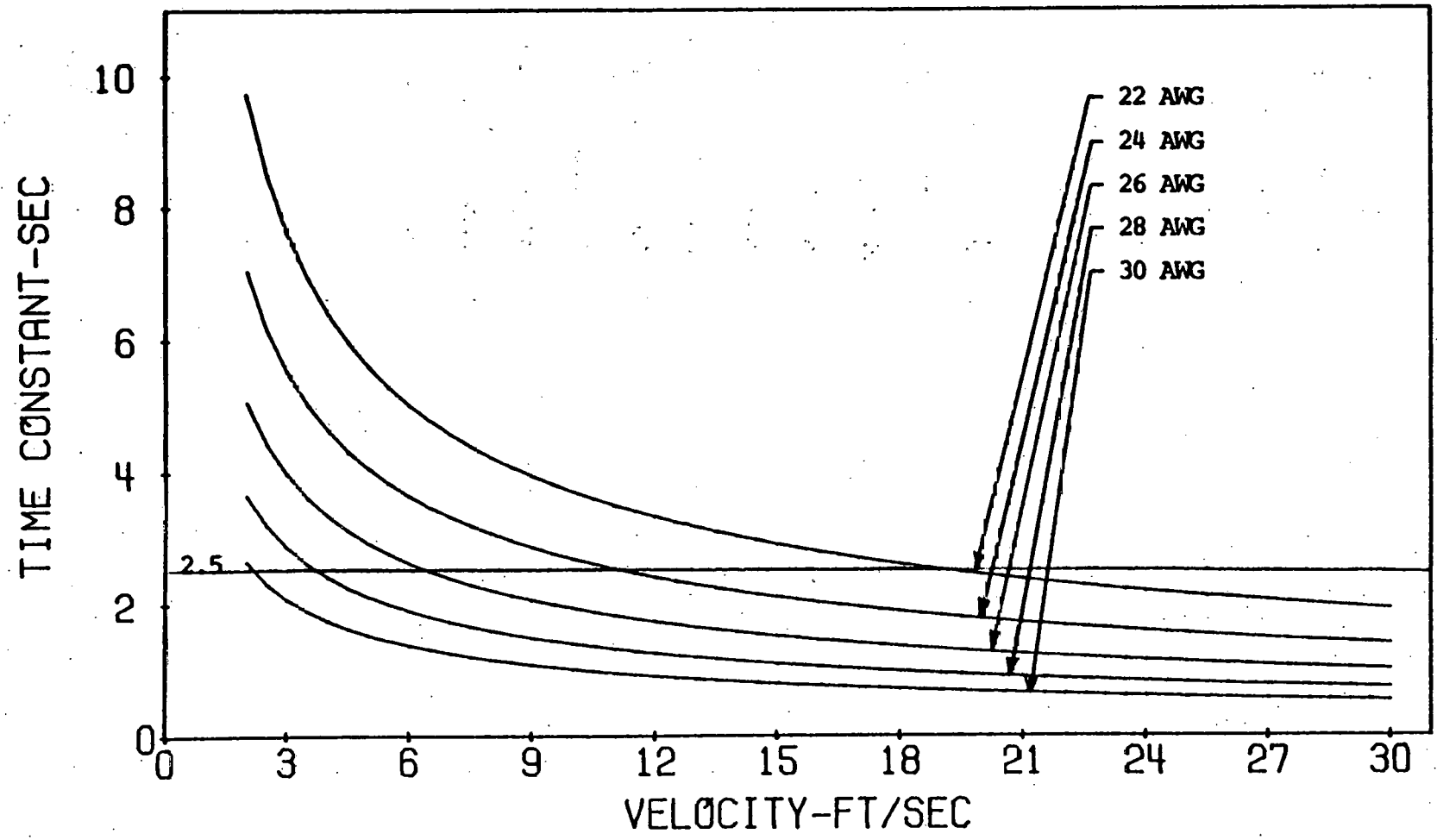

Figure 3D-3 Thermocouple Response for Spherical Junction

Comparing the two sets of curves, it appears that a spherical junction responds more rapidly than a cylindrical junction of the same wire thickness. If a cylindrical junction is used, 28 AWG wire or smaller is needed to have a response time of 2.5 seconds or less over the range of velocities typically found in unitary air conditioners and heat pumps. For a spherical junction, 24 AWG wire or smaller should be used. To minimize response time, 30 AWG wire is recommended.

It can also be inferred from Figures 3D-2 and 3 that under conditions of low velocity, the time response will be quite long. Murphy and Goldschmidt [1978] report it to be on the order of 60 seconds. If a thermocouple happened to be placed in an area of low velocity, its long time response could cause a significant error in the transient temperature measurement at that location. In fact, if several of the thermocouples in a thermocouple grid (which is commonly used in the DOE tests) were located in areas of low velocity, the transient temperature measurement of the grid could be distorted and lead to large errors.

Effects of Response Time

The fact that thermocouple response is finite means that the actual cyclic capacity of a unit and the cyclic capacity as calculated from thermocouple measurement could differ. This difference will now be examined. Eq. 3D-1 implies that a thermocouple can be modeled as a first order system.

Combined with the first order heat exchanger model, the following block diagram represents the measurement of the cooled air.

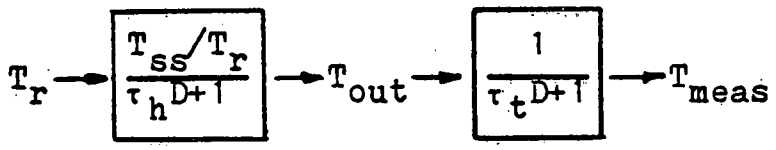

This can be written in equation form.

$$\tau_t \frac{dT_{meas}}{dt} + T_{meas} = T_{ss} + (T_o - T_{ss})\, e^{-t/\tau_h} \qquad (3D\text{-}10)$$

This can be solved for T_{meas}.

$$T_{meas} = T_{ss} + \frac{\tau_h}{\tau_h - \tau_t}(T_o - T_{ss})\, e^{-t/\tau_h} + \qquad (3D\text{-}11)$$

$$\left((T_o - T_{ss}) - \frac{\tau_h}{\tau_h - \tau_t}(T_o - T_{ss})\right) e^{-t/\tau_t}$$

This solution assumes that at t=0, the temperature of the thermocouple is the same as that of the coil and the surrounding air. The temperature difference is now easily written.

$$\Delta T = (T_r - T_{ss}) - \frac{\tau_h}{\tau_h - \tau_t}(T_o - T_{ss})\, e^{-t/\tau_h} - \qquad (3D\text{-}12)$$

$$\left((T_o - T_{ss}) - \frac{\tau_h}{\tau_h - \tau_t}(T_o - T_{ss})\right) e^{-t/\tau_t}$$

With Eq. 3D-12, a ΔT vs TIME curve can be plotted and the effect of τ_t can be observed. Figure 3D-4 shows three such curves corresponding to τ_t=0, 2.5 and 8 seconds, respectively. Recall that τ_t=0 sec. indicates perfect response so that the top curve in Figure 3D-4 is an ideal curve (as defined in Section C). As can be seen, longer

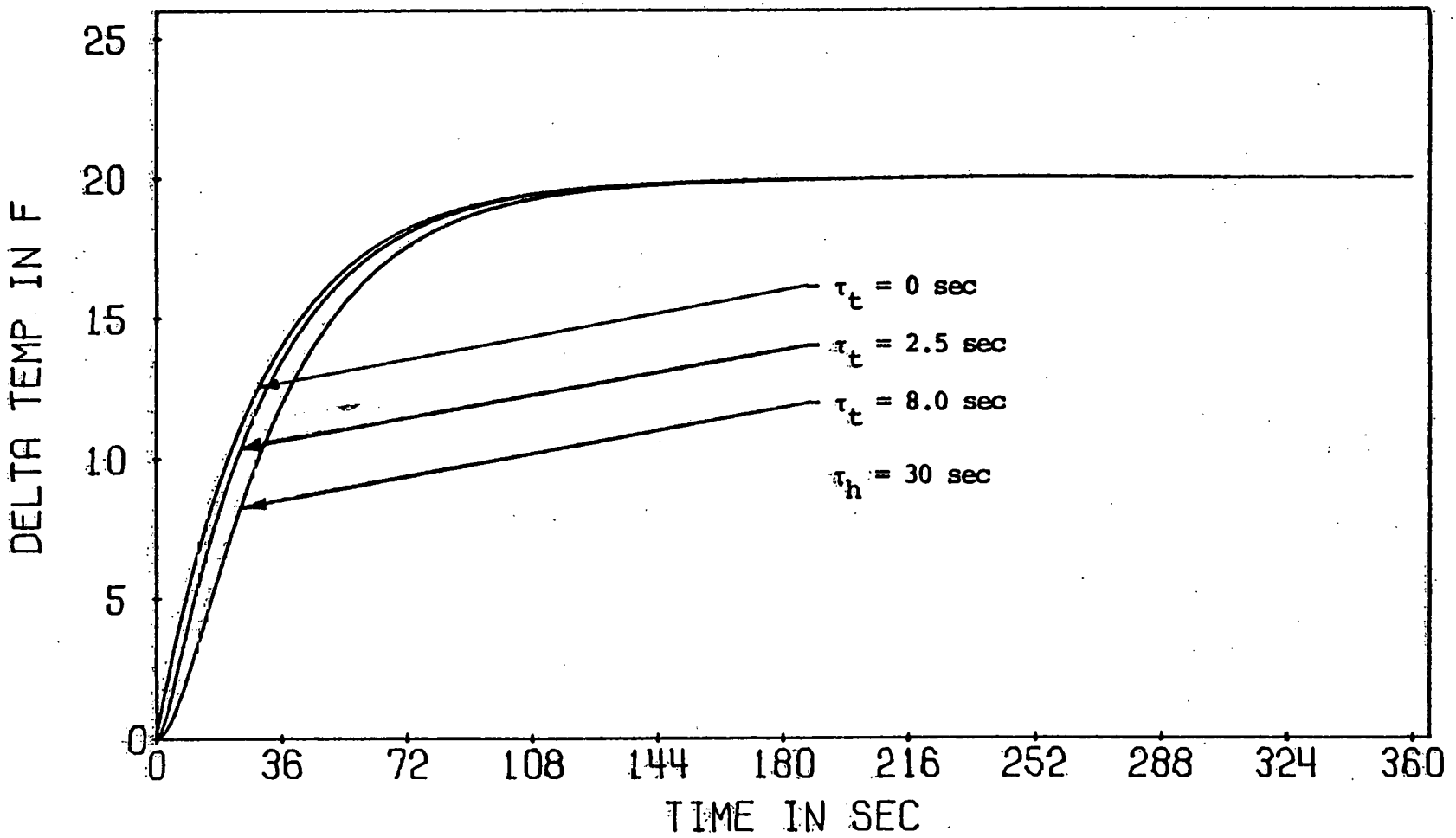

Figure 3D-4 Effect of τ_t on ΔT vs TIME Curves

response time causes the measured temperature to lag the actual temperature.

Capacity can also be computed by integrating Eq. 3D-12 over six minutes.

$$QMEAS = \rho c_p VA \int_0^{t_{on}} \Delta T \, dt \qquad (3D\text{-}13)$$

$$= \rho c_p VA \{ (T_r - T_{ss}) t_{on} + \frac{\tau_h^2}{\tau_h - \tau_t} (T_o - T_{ss})(e^{-t_{on}/\tau_h} - 1)$$

$$+ \tau_t \left((T_o - T_{ss}) - \frac{\tau_h}{\tau_h - \tau_t} (T_o - T_{ss}) \right) (e^{-t_{on}/\tau_t} - 1) \}$$

Note that if $\tau_t = 0$, QMEAS = QIDEAL. For $\tau_t \neq 0$, the error due to response time will be given by

$$\text{Percent error} = \frac{QIDEAL - QMEAS}{QIDEAL} \times 100 \qquad (3D\text{-}14)$$

Figure 3D-5 shows the percent error involved when various combinations of τ_h and τ_t are considered. The numerical values used are the same as those found in Table 3C-1.

As can be seen, the error in measuring $Q_{cyc,\ dry}$ due to thermocouple response is rather modest, on the order of 1%, when response time is kept at 2.5 seconds or less. With due consideration to wire thickness, junction shape and velocities, the thermocouple measurement error can be made negligibly small and accurate and reliable measurements can be made. However, if these things are not considered, significant error can result.

Section E - Grid Placement

The transient temperature measurement of Test D is usually made with thermocouple grids normally consisting

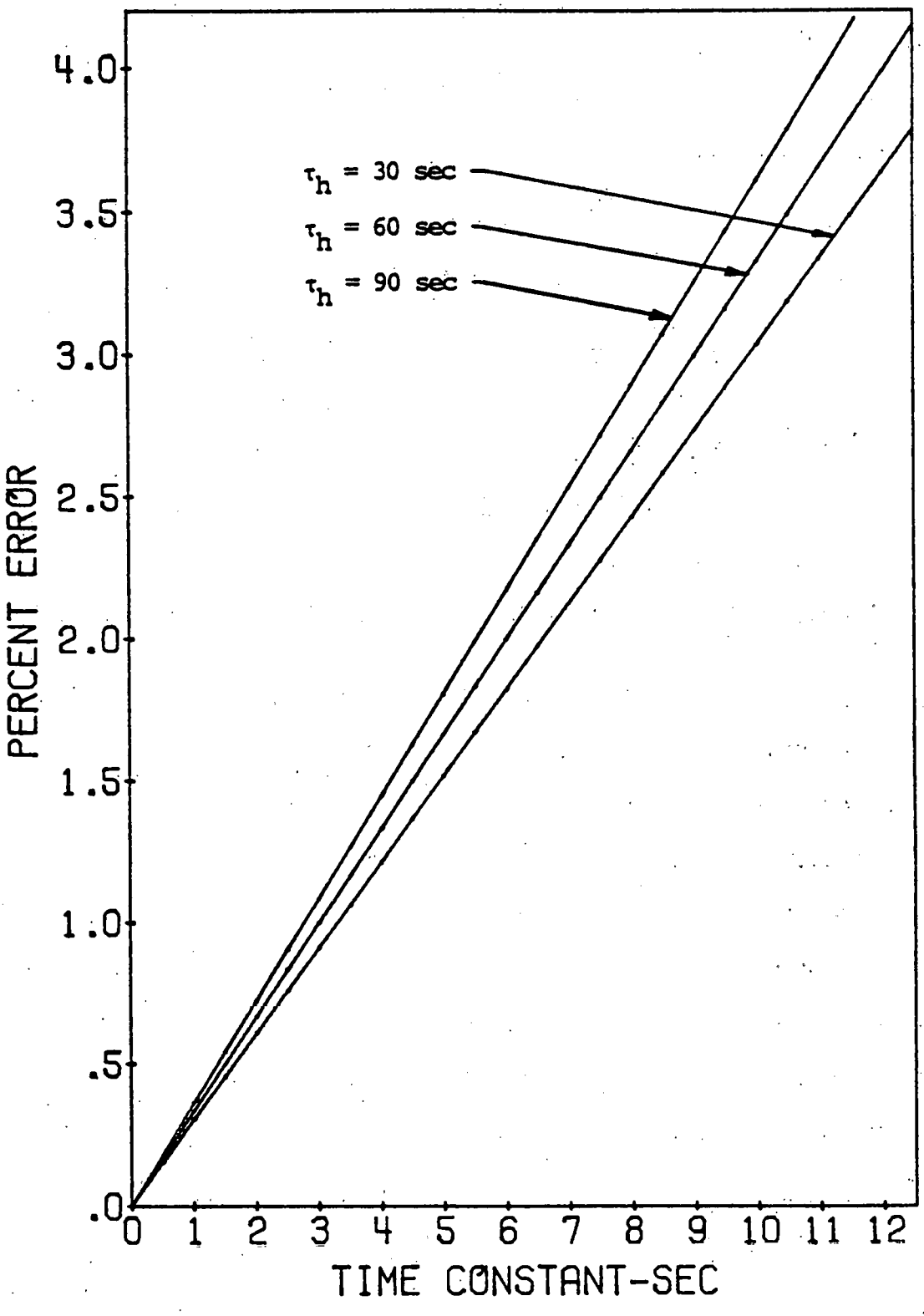

Figure 3D-5 Effect of τ_t on Measured Capacity

of 9-16 thermocouples per grid. As noted in Figure 3E-1, the thermocouples in these grids can be connected individually to the recording device or they can be connected in parallel or in series to each other and then to the recording device. Each arrangement gives different temperature information. Individual thermocouples would yield a rough temperature profile across the cross section, depending on how many thermocouples were used. However, a recording device with sufficient channels would be needed and an additional algorithm for determining the temperature difference would also be needed before the capacity could be computed. A parallel arrangement provides electronic averaging so that the output temperature is the average of the temperatures sensed by the thermocouples in the grid. The temperature difference still needs to be found. A series arrangement, often called a thermopile, is used to either increase sensitivity or to measure temperature differences. Since the output temperature is the temperature difference, this arrangement is preferred by some. This work will consider a grid to mean any of the above arrangements whose ultimate output is the temperature difference.

The major concern with thermocouple grids has not been their make-up, but their placement with respect to the evaporator coil in the test set-up. Since most manufacturers test several different types of equipment in their test chambers, modifications in the test set-up are often necessary. For this reason, the test procedures do not

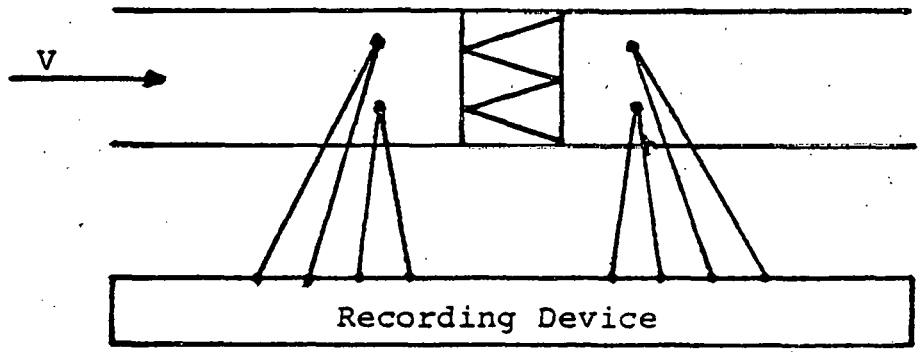

Individual Connections

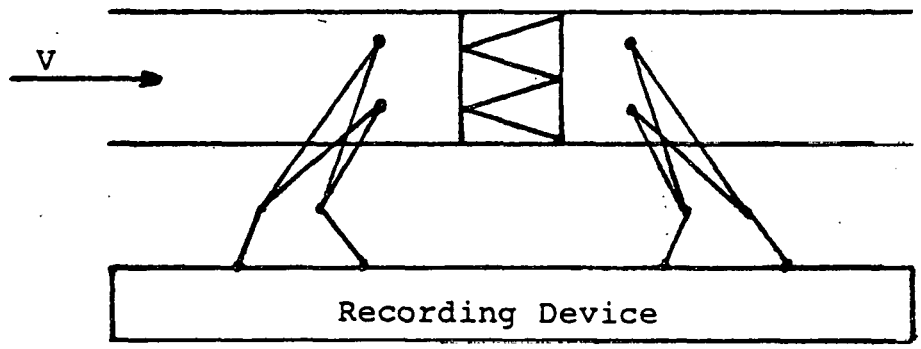

Parallel Arrangement

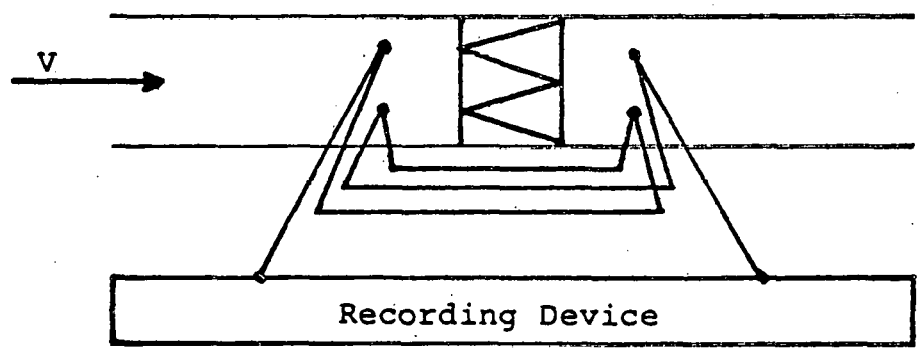

Series Arrangement

Figure 3E-1 Common Thermocouple Grid Arrangements

specify a location for the grids. However, some manufacturers, while testing the same unit, have obtained different measured capacities by moving the grids from one location to another (DOE Workshops [1980]). This section will consider the problem of grid placement and the potential differences in measured capacity due to grid location. (Grid placement with respect to the dampers will be discussed in Section F.)

There appear to be five phenomena that could affect the measured capacity of a unit due to the placement of the grid. If the grid were moved, these effects might change, further affecting the measured capacity. They are:

1. Nonuniform velocity and temperature distributions over the cross section of the grid.
2. Lag time due to the separation of the grid from the coil.
3. Mass transfer (leakage) into the duct.
4. Heat transfer through the duct wall.
5. Thermal storage effects of the walls and other massive objects.

The first of these effects will be considered in detail in Section G. For the remainder of this section, the velocity and temperature will be considered uniform over the cross-section.

Lag Time

Due to the separation of the downstream grid from the coil, a lag time will exist. This will delay the

temperature measurement of a slug of air since a slug of air leaving the coil takes a finite amount of time to reach the grid. In most test facilities, this separation is not more than 10-15 ft (3.1-4.6m). Since typical velocities range from 5 ft/sec - 20 ft/sec (1.5m/s - 6.1m/s), lag times will be on the order of .5-3 seconds or less. The effect of lag time on transient capacity measurement was found to be minimal. (Eqs. 3D-12, 13 were slightly modified to account for lag time.) For a lag time of 5 seconds, the error in measured capacity was less than 1%. Consequently, lag time will be neglected in this work.

With regard to the upstream grid, lag time effects will also be small. Furthermore, assuming that the inlet grid always measures 80°F (27°C), changing its placement will have a negligible effect on measured capacity.

Leakage

The big effect of mass transfer, room air leaking, into the duct, is caused by the leakage between the downstream temperature measuring location and location where the flow rate is measured.

For a condition where the initial temperature drop across the coil is zero, it can be shown that the effect on capacity of air leakage into the test set up between the coil and the temperature grid is zero.

Figure 3E-1A shows a schematic diagram of the energy entering the duct between coil and temperature measuring location.

An energy balance gives

$$\dot{m}_1 C_p T_{out} + \dot{m}_2 C_p T_r = (\dot{m}_1+\dot{m}_2) C_p T_M \qquad (8)$$

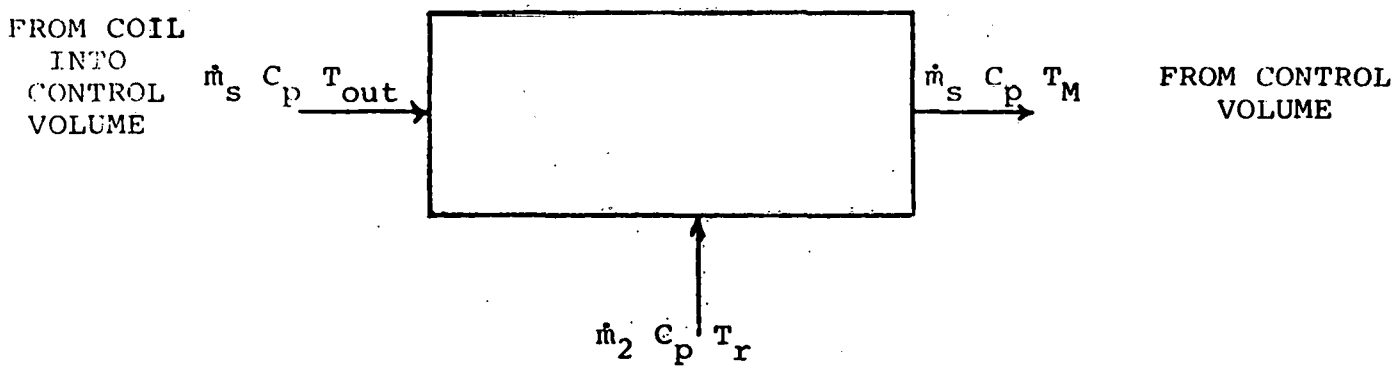

Figure 3E-1A Control Volume Between Coil and Downstream Measuring Location

Solving for T_M gives

$$T_M = \frac{\dot{m}_1}{\dot{m}_1+\dot{m}_2} T_{out} + \frac{\dot{m}_2}{\dot{m}_1+\dot{m}_2} T_R \quad (9)$$

The temperature drop as measured by the two sets of sensors would be

$$(T_r - T_M) = \Delta T_m = \frac{\dot{m}_1}{\dot{m}_1+\dot{m}_2} [T_R - T_{out}] \quad (10)$$

but $T_R - T_{out} = \Delta T$ or

$$T_m = \frac{\dot{m}_1}{\dot{m}_1+\dot{m}_2} \Delta T \quad (11)$$

The calculated capacity would be

$$Q = \dot{m}_1 C_p \int_o^{t_{on}} \Delta T_m \, dt \quad (12)$$

Substituting 10 into 11 and assuming $\dot{m}_1$ is constant gives

$$Q = \dot{m}_1 C_p \int_o^{t_o} \Delta T \, dt = Q_{IDEAL} \quad (13)$$

The effect of adding mass after the downstream measuring point is to increase the mass flow rate being measured. This would tend to make the calculated cooling capacity too large. The calculated capacity would be

$$Q_{CAL} = \dot{m}_3 C_p \int_o^{t_{on}} \Delta T \, dt \quad (14)$$

and the percent error would be

$$\text{Percent error} = \frac{Q_{IDEAL} - Q_{CAL}}{Q_{IDEAL}} = 100 \quad (15)$$

$$= 1 - \frac{\dot{m}_3}{\dot{m}_1} \quad (16)$$

if $\dot{m}_3 = \dot{m}_1 + X\dot{m}_1$. Then

$$\text{percent error} = -X \quad (17)$$

where X is percent leakage.

Therefore, a 2% leakage error would give capacity which is 2% too large. The present standards allows a 2% leakage rate.

Heat Transfer Effects

During the on-time of test D, energy will be transferred by conduction and convection from the room air, through the insulation (if any) and the duct wall and into the cooled air stream. The net effect of this transfer is a decrease in measured capacity. The magnitude of this decrease will be examined by considering the overall heat transfer coefficient (U), the surface area of the test set-up and the temperature difference between room air and cooled air. As was mentioned above, this analysis will be done without regard to thermal storage effects.

The overall heat transfer coefficient is defined by the following equation:

$$U = \frac{1}{R_o+R_I+R_w+R_i} \qquad \text{(all areas assumed equal)} \qquad \text{(3E-1)}$$

where

$R_o = \frac{1}{h_o}$ = Reciprocal of the outside film coefficient

R_I = R-value of insulation

R_w = R-value of duct wall $\frac{\text{thickness}}{\text{conductivity}}$

$R_i = \frac{1}{h_o}$ = Reciprocal of the inside film coefficient

Estimates for h_o range from about .3 Btu/hr ft^2 °F (1.7 W/m^2°C) (Murphy and Goldschmidt [1978]) to 1.63 Btu/hr ft^2 °F (9.25 W/m^2°C) (ASHRAE Fundamentals [1977]). This work will assume H_o=1 Btu/hr ft^2 °F (5.7 W/m^2°C). Values for h_i vary from 0 Btu/hr ft^2 °F (ASHRAE Fundamentals [1977]) to about

4 Btu/hr ft^2 ^{o}F (22.7 W/m^{2o}C) (McAdams [1954]). This work will assume h_i=2.25 Btu/hr ft^{2o}F (12.8 W/m^{2o}C) (Murphy and Goldschmidt [1978]). R-values for insulation (from ASHRAE Fundamentals [1977]) and the corresponding U-values are summarized in Table 3E-1.

With a given surface area, maximum heat transfer will occur when the unit has reached steady state because this is when ΔT has a maximum value. A more realistic value for ΔT can be found by integration.

$$\overline{\Delta T} = \frac{1}{t_{on}} \int_0^{t_{on}} \Delta T \, dt \qquad (3E\text{-}2)$$

Using this value for the temperature difference, the energy transferred to the cooled air is given by

$$\dot{q} = UA\overline{\Delta T} \qquad (3E\text{-}3)$$

In six minutes, $\dot{q}/10$ will be the additional energy affecting the cyclic capacity. Figure 3E-2 shows the amount of additional energy for various combinations of U-value and ΔT.

An example will illustrate this effect. Suppose the ducting of a test set-up is made of 24 gage sheet metal and is without insulation. Between the coil and the thermocouple grid, let there be 15 ft^2 (1.4m^2) of surface area. Recalling the numerical evaluation of QIDEAL in Section B, ΔT can be computed by Eq. 3E-2.

$$\Delta T = \frac{1}{6 \text{ min}} (110^o\text{F-min}) \quad \left(\frac{1}{360\text{s}} (3667^o\text{C-s}) \right)$$
$$= 18.3^o\text{F} \qquad\qquad (10.2^o\text{C})$$

Table 3E-1 Heat Transfer Coefficients

$\dot{q} = UA\Delta T$ where $U = \frac{1}{R_o + R_I + R_w + R_i}$	
$R_o = \frac{1}{h_o} = \frac{1}{1} = 1$	$R_i = \frac{1}{h_i} = \frac{1}{2.25} = .44$
$R_w = \frac{\text{thickness}}{\text{conductivity}}$; $R_{\text{sheet metal}} \doteq 0$; $R_{\text{cardboard}} \doteq .5$	
R_I (insulation)	U-value (Btu/hr-ft^2-°F)
0 (no insulation)	.69
3.5 (1 in. glass wool)	.20
7.1 (2 in. polystyrene)	.12
14.2 (4 in. polystyrene)	.06
3.5 (1 in. glass wool)	.18 (cardboard wall)

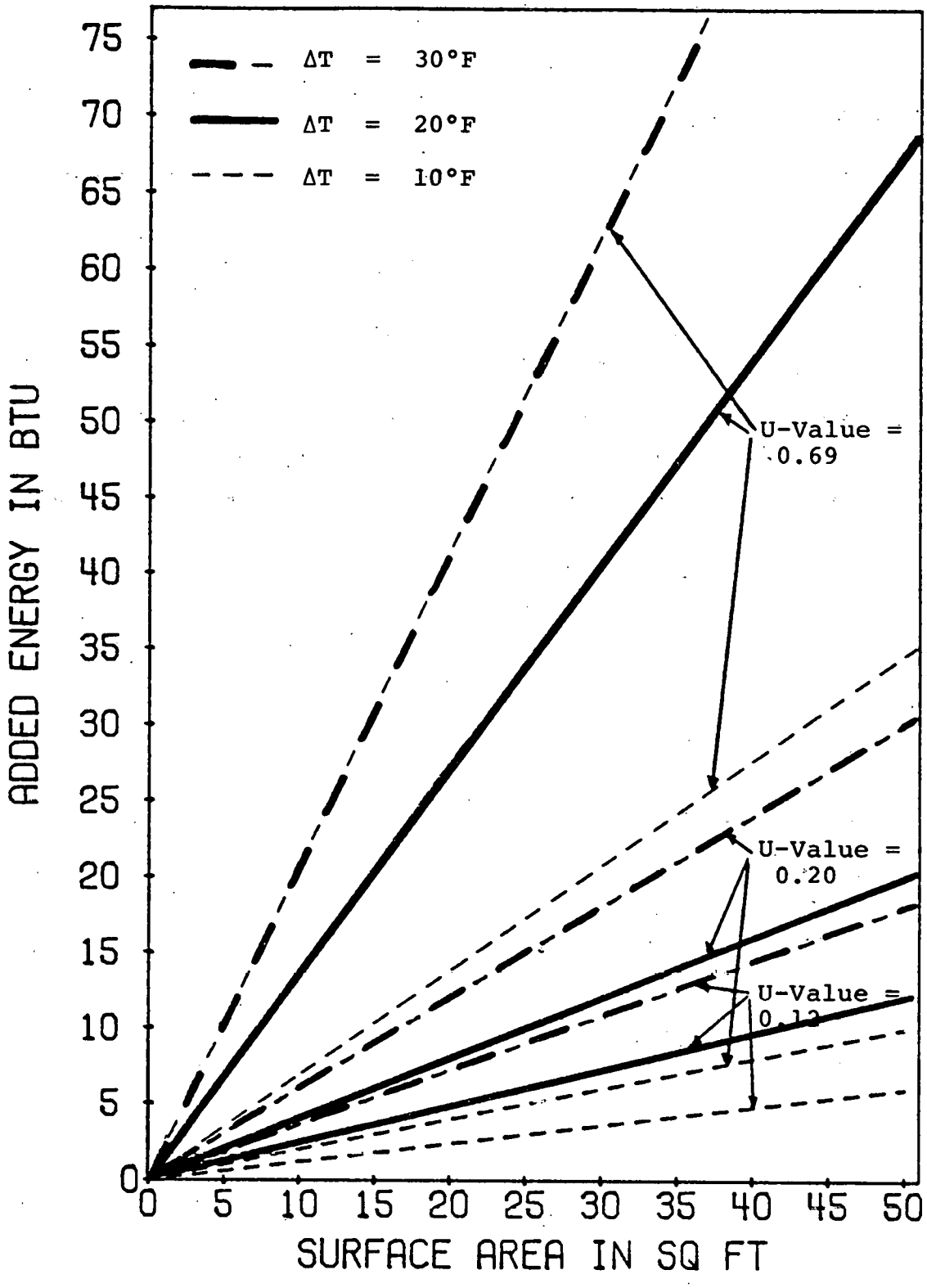

Figure 3E-2 Heat Transfer Through Duct Wall for Different U-values

Hence,

$$q = (.69 \text{ Btu/hr ft}^{2}\text{F})(15 \text{ Ft}^2)(18.3^{\circ}\text{F})$$

$$= 189 \text{ Btu/hr}$$

$$= 19 \text{ Btu/6 min}$$

$$(3.9 \text{ W/m}^{2}\text{C})(1.4\text{m}^2)(10.2^{\circ}\text{C})$$

$$(56 \text{ W})$$

$$= (5.6 \text{ W}/360 \text{ s})$$

The percent error due to heat transfer is

$$\text{Percent error} = \frac{\text{Additional energy}}{\text{QIDEAL}} \times 100$$

$$= \frac{19}{1687} \times 100 \qquad \left(\frac{5.6}{494} \times 100 \right)$$

$$= 1.1\% \qquad (1.1\%)$$

If the same test installation had insulation of R-7, the percent error would be 0.2%, a substantial improvement in measured capacity.

Figure 3E-2 indicates that for an uninsulated test set-up with a large amount of surface area between the coil and the grid, a substantial amount of energy could be added to the cooled air resulting in 5-10% errors. It can also be seen that insulation of R-7 drastically reduces the added energy so that its maximum effect (50 ft^2 and $\Delta T=30^{\circ}F$) on measured capacity amounts to 1% of QIDEAL. For typical test set-ups with insulation of R-7, the error in measured capacity should be much less than 1%.

Thermal Storage Effects

During the 24 minute off-time of test D, the duct walls and other massive objects, such as the air mixer, will

be storing thermal energy. This causes their temperatures to rise, so that at start-up, they may have returned to room temperature. During the on-time, this stored energy will be released into the cooler air stream with the net effect of decreasing measured capacity. The amount of energy released is given by Eq. 3E-4.

$$Q = mc_p\Delta T \qquad (3E\text{-}4)$$

where

m = Mass of the wall or object, lbm (kg)

c_p = Specific heat, Btu/lbm ^{o}F (J/kg ^{o}C)

ΔT is the average initial temperature of the mass less its average final temperature. ΔT is very much dependent on the insulation, the inside film coefficient, heat conduction along the ducting, etc. This makes it rather difficult to measure or estimate the value of ΔT. This analysis will simply assume different values of ΔT that could occur during testing and calculate the corresponding effect on measured capacity.

Suppose the ducting in a test installation is made of 24 gage sheet metal which weighs 1.16 lbm/ft^2 (5.7 kg/m^2) and has a c_p= 11 Btu/lbm ^{o}F (.13 Wh/kg ^{o}C). Further suppose that there are 15 ft^2 (1.4m^2) of well insulated sheet metal between the coil and the grid and ΔT=20^{o}F (11^{o}C). Then by Eq. 3E-4,

$$Q = (15\ ft^2)(1.16\ lbm/ft^2)(.11\ Btu/lbm^oF)(20^oF)$$

$$= 38.3\ Btu$$

$$(1.4m^2)(5.7\ kg/m^2)(.13\ Wh/kg^oC)(11^oC)$$

$$= (11.4\ Wh)$$

The effect of this added energy on QIDEAL is

$$\text{Percent error} = \frac{38.3}{1687} \times 100 \qquad (\frac{11.4}{494} \times 100)$$

$$= 2.3\% \qquad = (2.3\%)$$

Suppose a 15 lbm (6.8 kg) mixer were placed in the test set-up of the above example and it experienced a $\overline{\Delta T}$ = 10 ^oF (5.6 ^oC). It would also add energy.

$$Q = (15\ lbm)(.11\ Btu/lbm\ ^oF)(10^oF)$$

$$= 16.5\ Btu$$

$$(6.8\ kg)(.13\ Wh/kg\ ^oC)(5.6\ ^oC)$$

$$= (5.0\ Wh)$$

So,

$$\text{Percent error} = \frac{16.5}{1687} \qquad (\frac{5.0}{494})$$

$$= 1\% \qquad = (1\%)$$

These two errors are additive. Hence, in this example, thermal storage effects contributed about 3.3% error in measured capacity.

Figures 3E-3 and 4 show the released energy from massive objects under different conditions. It can be seen from these two plots that if a test set-up had a heavy air mixer (for example) and a large amount of sheet metal surface area exposed to the cold air stream, errors on the order of 5-15% could occur. Insulation will not minimize these effects. In fact, insulation tends to maximize these effects because the thermal mass is maintained at a lower temperature, increasing ΔT. A practical solution to minimize thermal storage effects is to eliminate, as much as possible, the thermal mass that is exposed to the cold air stream. For example, the insulation could be placed inside the sheet metal or a different, less massive, structural material such as cardboard or fiberglass could be used for that portion of the ducting between the coil and the grid. Air mixers and flow straighteners could also be made from a lightweight material such as plastic.

In summary, it has been seen that the placement of the thermocouple grid can cause changes in the measured capacity. By moving the grid downstream, more surface area is exposed which increases the effects of leakage, heat transfer and thermal storage. For a typical, uninsulated test set-up with a mixer a decrease in measured capacity on the order of 5% might occur, due only to the

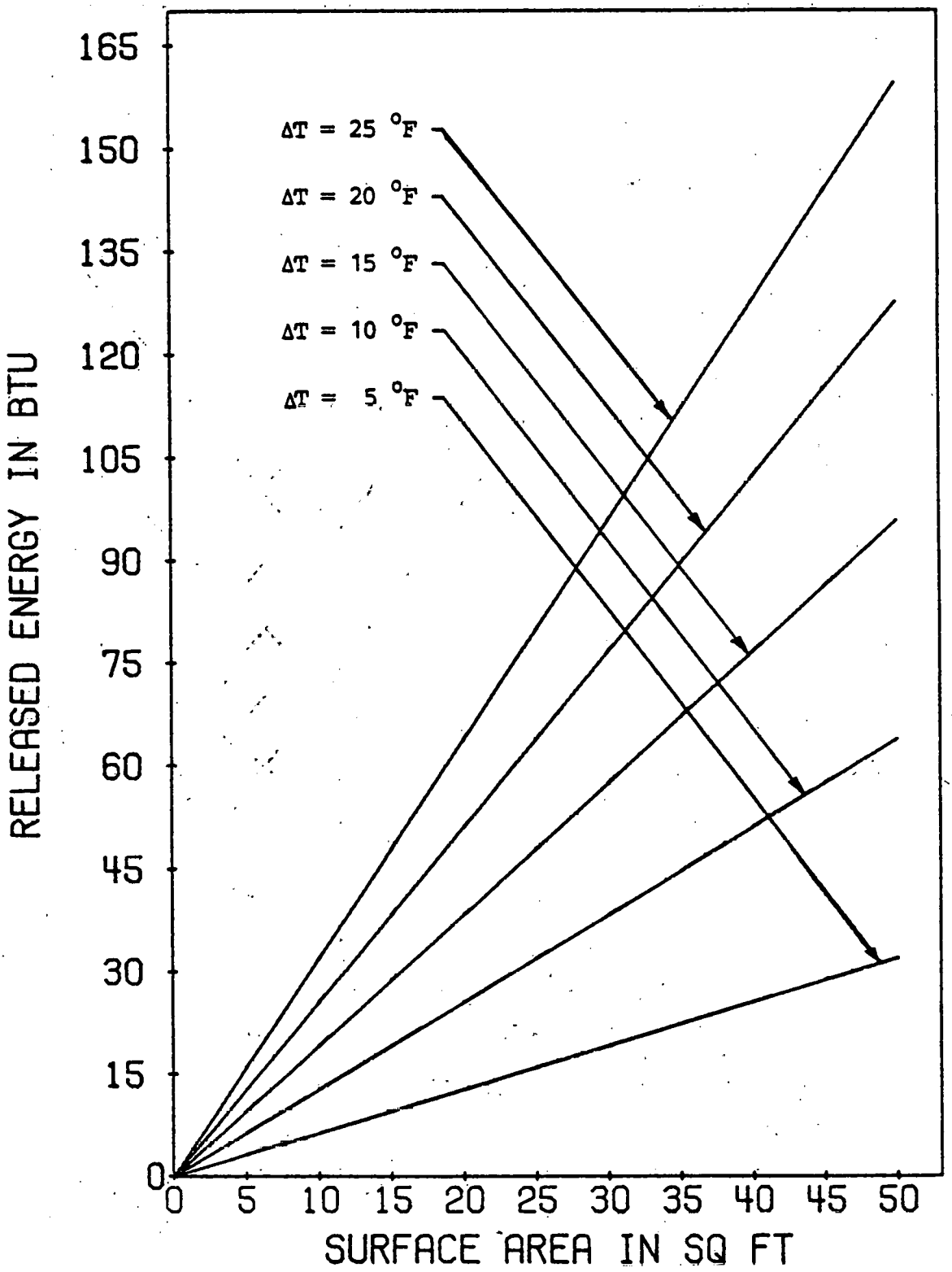

Figure 3E-3 Energy Released from 24 Gage Sheet Metal per Surface Area

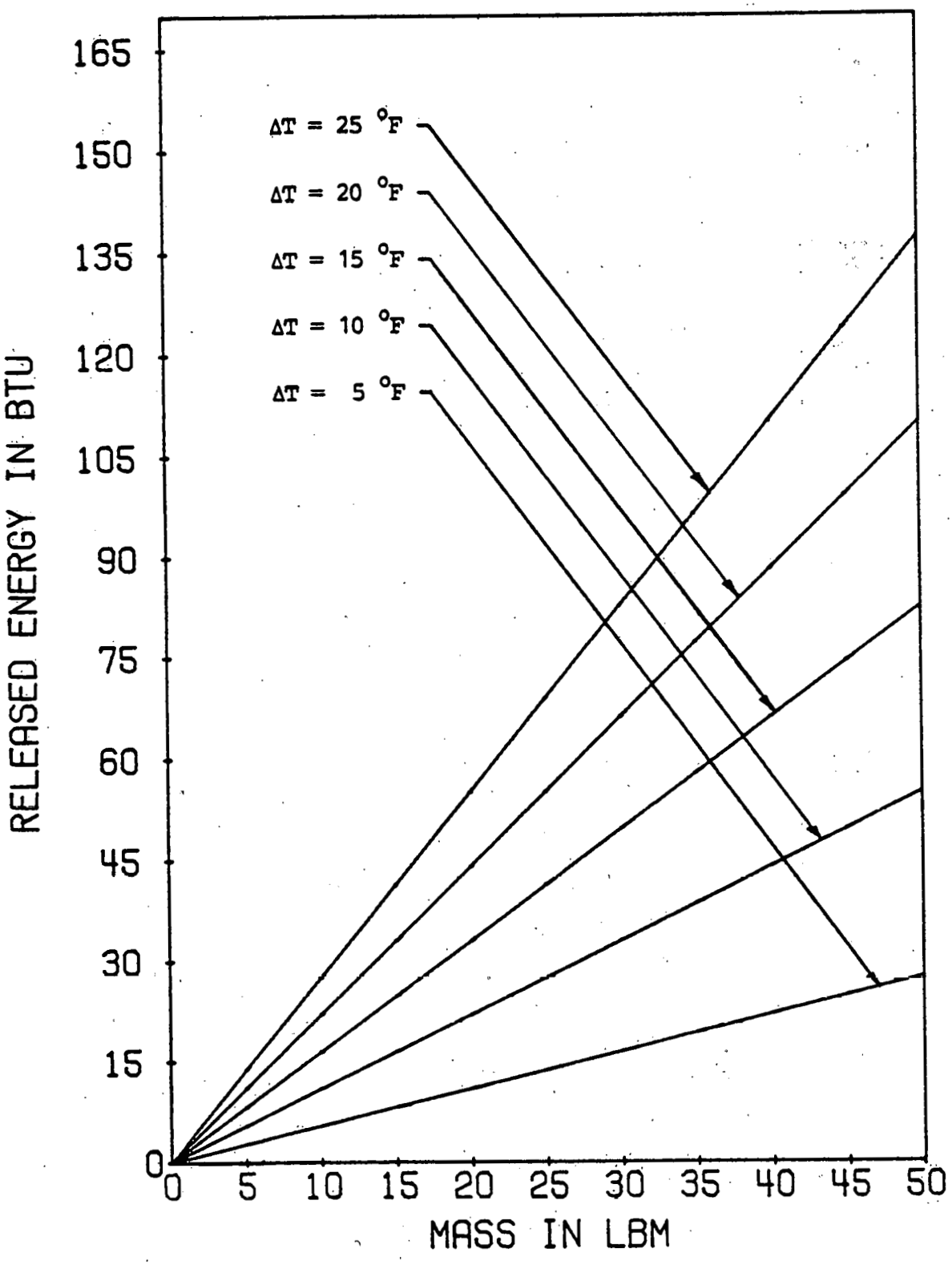

Figure 3E-4 Energy Released from 24 Gage Sheet Metal per Mass

location of the grid. If the grid were moved, this estimate could increase or decrease. But, with proper attention to joints, seams, cracks, etc., mass transfer errors can be essentially eliminated. With insulation of R-7 or better, heat transfer effects will be less than 1% over a considerable range of locations. However, thermal storage effects could still be on the order of 2-3% (or more) unless some of the thermal mass were removed. It is hoped that with these considerations, the effects of grid placement on measured capacity can be minimized.

Section F - Dampers

The following quote is taken from the Federal Register and concerns the dampers.

> "The test installation shall be designed such that there will be no air flow through the cooling coil due to natural or forced convection while the indoor fan is 'off.' This shall be accomplished by installing dampers upstream and downstream of the test unit to block the off period air flow " (Federal Register [1979]).

This portion of the test procedures has caused considerable confusion because neither the intent nor the practical application of the dampers is made clear. The purpose of this section is to attempt to resolve some of this confusion.

Apparently, the dampers were added to the test procedures with the intent to credit a manufacturer with the off-time cooling done by the unit and to aid in obtaining repeatable and reproducible results (Didion [1980-A]).

Ideally, by blocking the air flow over the coil, heat transfer between the trapped air and the coil and the compartment walls is essentially stopped so that the coil, the compartment walls and the trapped air remain cold, nearly at the steady state operating temperature.[1] Therefore, at start-up, the coil does not have to be "cooled down" by heat transfer to the refrigerant, allowing heat transfer from the air to the refrigerant (through the cold coil) to begin immediately. Furthermore, the cold compartment walls add little energy to the air flow. Hence, cooler air is produced more quickly and the measured efficiency of the unit during test D is increased.

Of course, an ideal test set-up does not exist. Due to the temperature gradient between the room air and the trapped air, heat transfer will occur raising the temperature of the trapped air. Furthermore, at shut-down, some evaporator coils partially fill with hot refrigerant from the condenser due to a pressure gradient (Murphy and Goldschmidt [1979]). This further increases the heat transfer into the compartment. Nevertheless, dampers should maintain the coil, compartment walls and trapped air at a temperature below room temperature which, in many cases, will increase the measured capacity.

The implementation of the dampers is not prescribed or even mentioned in the standards which govern the test set-up and ambiguities do exist. For example, two mechanical dampers are implied, but several manufacturers use an

1- Air temperature may also depend on refrigerant control.

air trap instead of an upstream damper. Is an air trap as effective as a damper in blocking air flow over the coil? How should the dampers open in the duct as far as air flow is concerned? Should they be air tight? How quickly should they open or close? Where should the dampers be placed? Where should the thermocouple grids be placed in relationship to the dampers? These are valid questions whose answers are reflected in the variety of test set-ups found throughout the air conditioning industry.

In order to study the effects of dampers on the measured capacity of a unit, several assumptions regarding the analysis are needed. The following are these assumptions.

1. Two dampers or a damper and an air trap are equally effective because both block the inlet flow of room air.

2. All off-time heat transfer effects will be reflected in T_o, the temperature of the coil and the trapped air at start-up. (The temperature of the coil will be an average temperature and is assumed to be about the same as the trapped air at the end of the 24 minute off-time.)

3. Mass transfer (leakage) through the dampers will also be reflected in T_o. On-time leakage will be neglected.

4. The dampers will open immediately upon start-up and air flow will be considered constant, uniform and unaffected by the dampers once the dampers are open.

5. The upstream thermocouple grid will be placed outside of the upstream damper.

6. The time constant of the unit, τ_h, will not change because of dampers. This is an important assumption as far as modeling the dampers is concerned. It is, in effect, saying that the cold coil does not enhance or diminish the heat transfer capability of the refrigerant, especially at start-up. This is probably not true and could be a subject for future investigation. On the other hand, the dampers will allow the coil to be at a lower temperature than ambient at start-up. This means that a certain amount of energy will not have to be removed from the coil in the process of cooling it down to its steady state temperature. Instead, it will be assumed that this amount of energy will be removed from the air. For modeling purposes in this section, this energy will simply be added back into the measured capacity as QCOIL.

The effects to be studied are damper placement and thermocouple response in relationship to damper placement. Consider the sketch shown in Figure 3F-1 showing an arrangement where the downstream thermocouple grid is placed inside the damper. In order to obtain a ΔT vs TIME curve, the temperatures sensed by the thermocouple grid must be identified. Since the downstream grid is inside the damper, it will continue to sense T_o for D1/V seconds (Distance/Velocity = Time) after start-up. Then, it will sense the temperature of the slug of air between the coil and the upstream damper. But, before reaching the grid, this slug of air passes through the coil and is cooled according to the first order response discussed in Section C. This

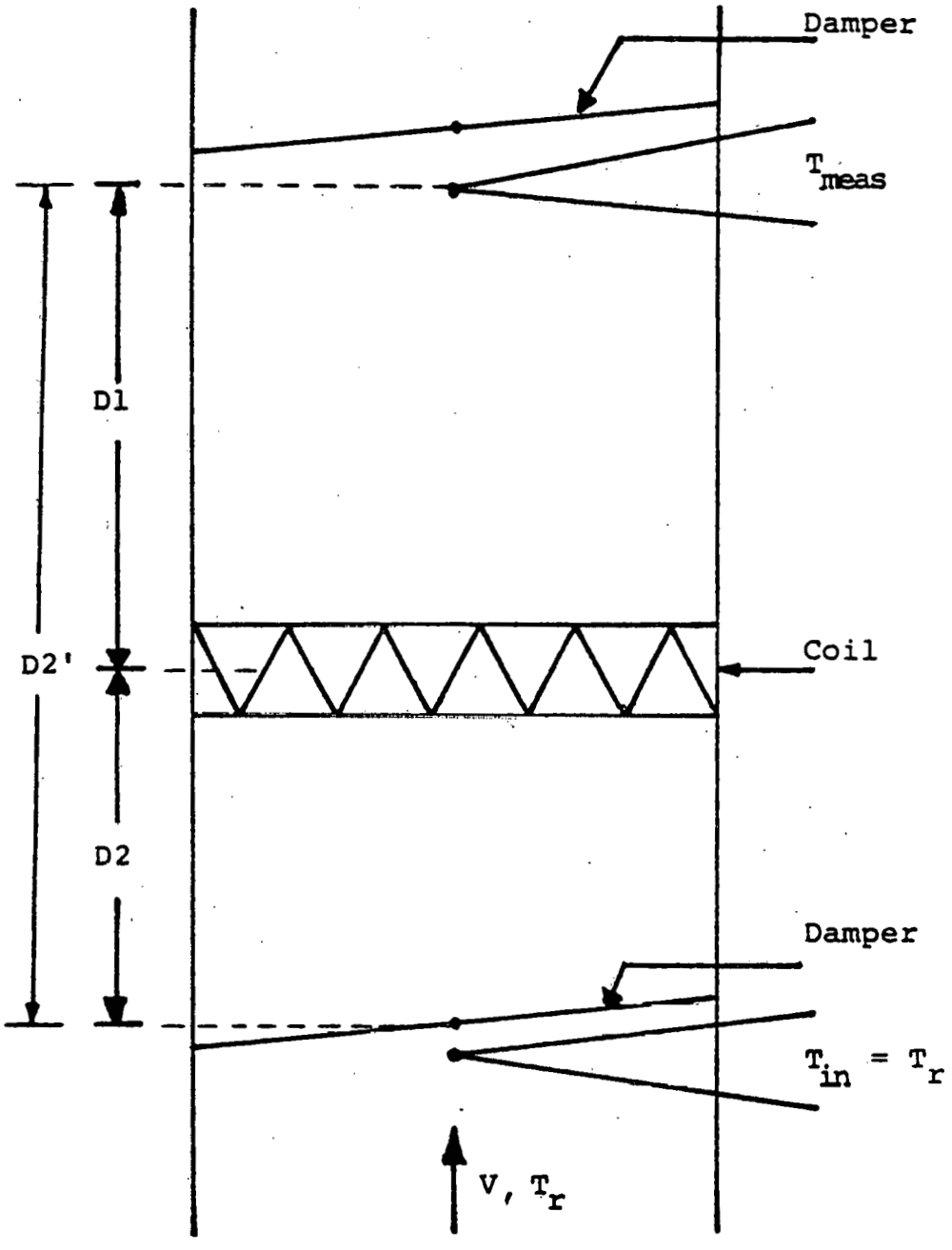

Figure 3F-1 Thermocouple Grid Inside Damper

cooled air is sensed for D2/V seconds. After this time has elapsed, room air at T_r, which has entered the coil and been cooled, is sensed by the grid. Eq. 3F-1 represents the temperature difference as a function of time, and is derived by applying Eq. 3D-12 for the above temperatures.

$$\Delta T = T_r - T_{meas}$$

$$= T_r - T_o \qquad \text{for } 0 < t < D1/V$$

$$= (T_r - T_{ss}) - \frac{\tau_h}{\tau_h - \tau_t}(T_o - T_{ss})\, e^{-t/\tau_h}$$

$$- (T_o - T_{ss})\left(1 - \frac{\tau_h}{\tau_h - \tau_t}\, e^{\frac{-D1/V}{\tau_h}}\right) e^{-(t-D1/V)/\tau_t}$$

$$\text{for } D1/V < t < D2'/V$$

$$= (T_r - T_{ss}) - \frac{\tau_h}{\tau_h - \tau_t}(T_r - T_{ss})\, e^{-t/\tau_h}$$

$$- \left(T_2 - T_{ss} - \frac{\tau_h}{\tau_h - \tau_t}(T_r - T_{ss})\, e^{\frac{-D2'/V}{\tau_h}}\right) e^{-(t-D2'/V)/\tau_t}$$

$$\text{for } t > \frac{D2'}{V} \qquad \text{(3F-1)}$$

where

T_2 = Temperature sensed by thermocouple at $t = D2'/V$

$D2' = D1 + D2$

Using Eq. 3F-1, ΔT vs TIME curves can be plotted. Furthermore, Eq. 3F-1 can be integrated over time so that capacity can be computed. By varying D1, D2 and T_o, the effects of dampers on measured capacity can be studied.

To illustrate these ideas, consider the following example. Numerical values are assumed representative of some units. Let:

T_r = 80°F (26.7°C) T_{ss} = 60°F (15.6°C)

T_o = 70°F (21.1°C) τ_h = 30 sec

V = 15 ft/sec (4.6 m/s)

D1 = 5 ft (1.5 m) D2 = 5 ft (1.5 m)

ρ = .071 lbm/ft^3 (1.14 kg/m^3)

Mass of coil = 24 lbm

c_p = .24 Btu/lbm°F (1004.8 W s/kg°C) (air)

c_p of coil = .11 Btu/lbm°F (460.5 W s/kg°C)

A = 1 ft^2 (.09 m^2) τ_t = 1, 2.5 and 5 sec.

Substituting these values into Eq. 3F-1 and letting the on-time run from 0-6 minutes, the curves in Figures 3F-2 and 3 are obtained. Figure 3F-2 shows the response in the first 10 seconds. All three curves begin at ΔT_o=10°F (5.6°C). After the cold air has been drawn out and replaced by the room air, the curves begin to differ according to the time constant of the thermocouple. Figure 3F-3 shows the response over the full six minutes. In particular, note the dip in the curves which is caused by the thermocouple response time.

The expression for ΔT is integrated over the six minutes and the capacities for this example are obtained. The results are tabulated in Table 3F-1. QIDEAL represents the capacity that would be calculated assuming ideal conditions such as T_o=80°F (26.7°C), τ_t= 0 sec, no thermal mass effects, etc. QMEAS is the measured capacity and the

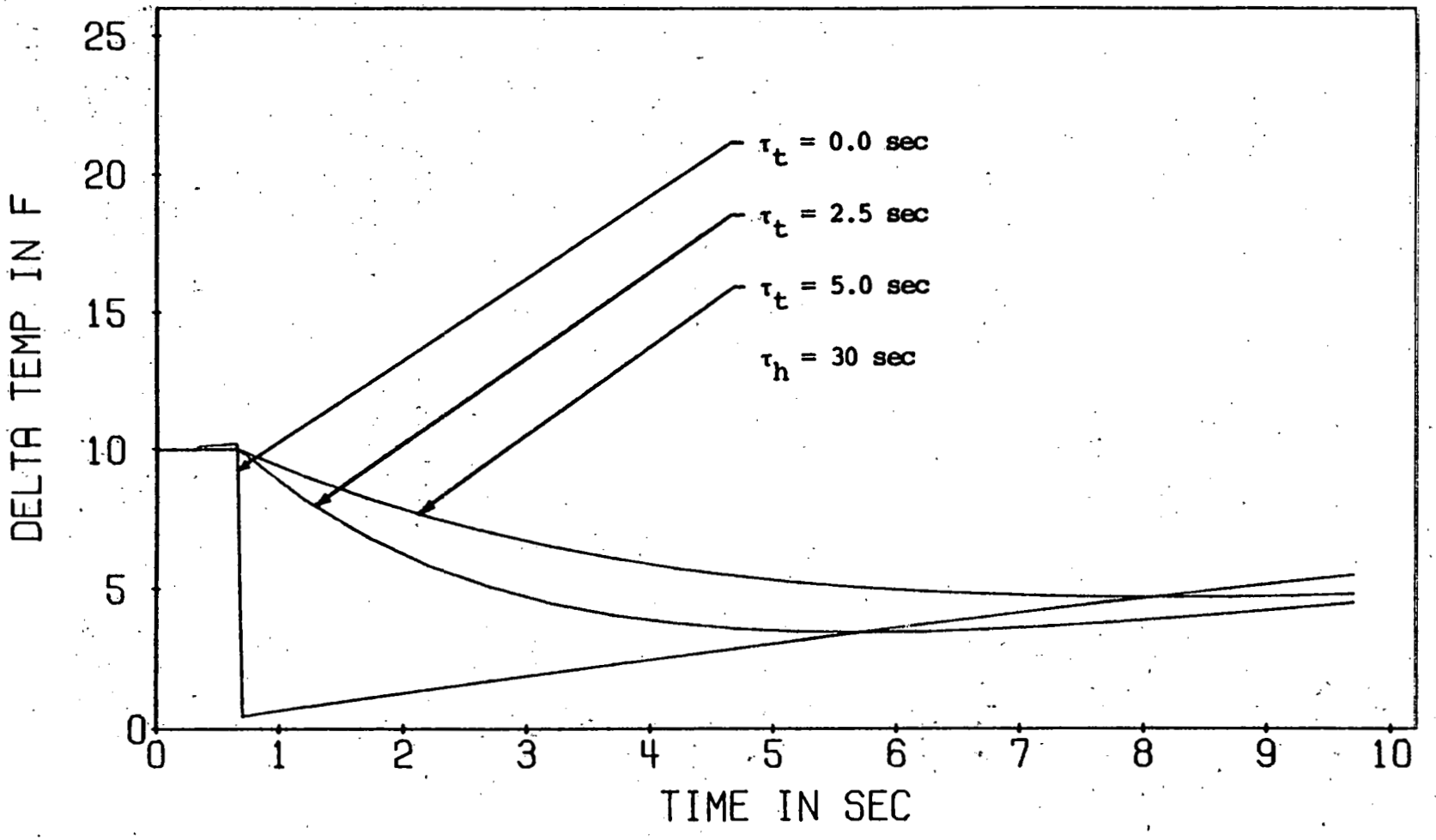

Figure 3F-2 ΔT vs TIME Curves with Grid Inside Damper - First 10 Seconds

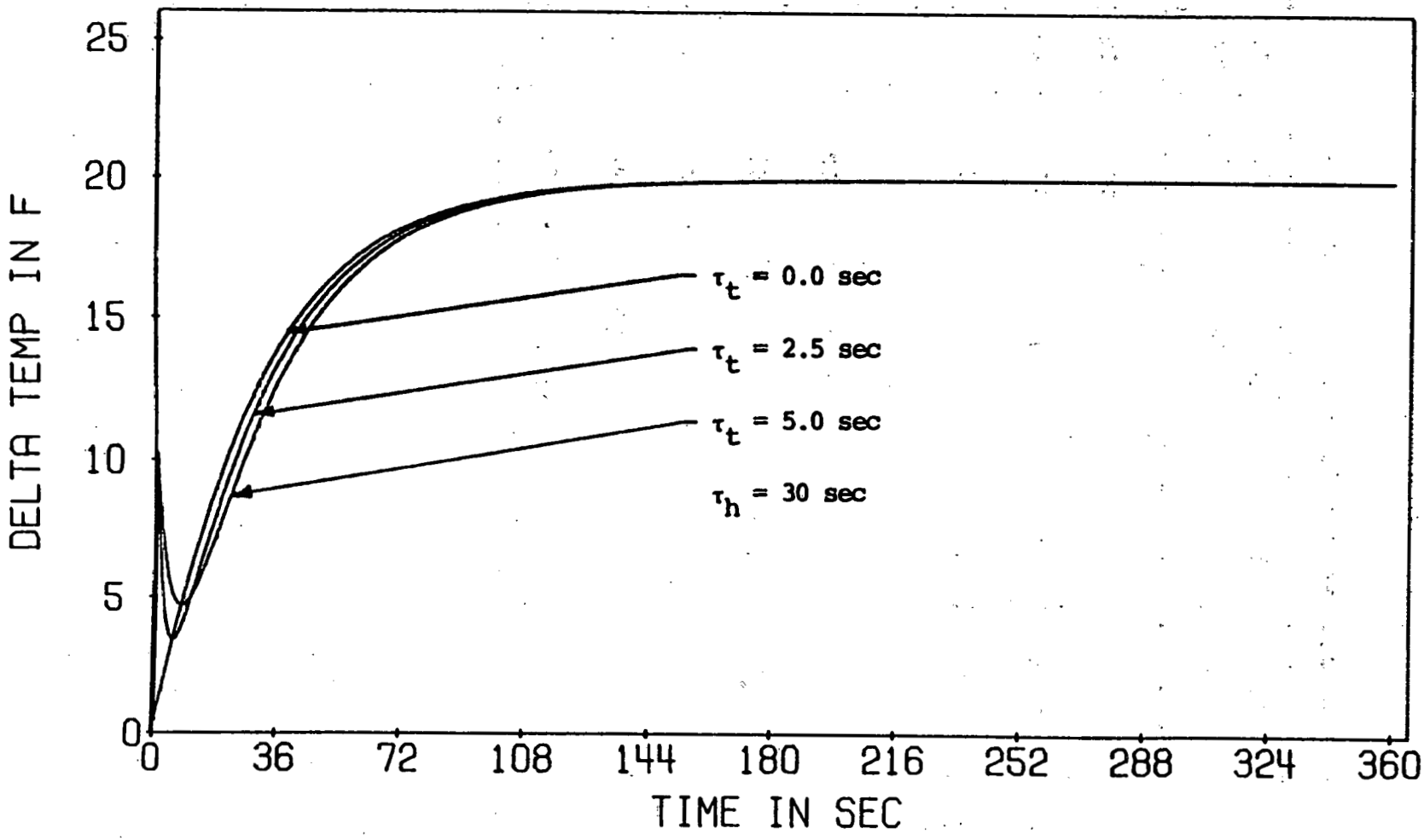

Figure 3F-3 ΔT vs TIME Curves with Grid Inside Damper - Full 6 Minutes

Table 3F-1 Capacities for Grid Inside Dampers

QIDEAL Btu	QMEAS Btu	%ERROR	QCOIL Btu	%ERROR w/coil	T_o °F	τ_t SEC
1686.96	1686.96	.00	0	.00	80	0
1686.96	1680.74	.37	0	.37	80	2.5
1686.96	1674.56	.73	0	.73	80	5.0
1686.96	1688.64	-.10	26.40	-1.66	70	0
1686.96	1682.45	.27	26.40	-1.30	70	2.5
1686.96	1676.27	.63	26.40	-0.93	70	5.0
1686.96	1690.33	-.20	52.80	-3.33	60	0
1686.96	1684.15	.17	52.80	-2.96	60	2.5
1686.96	1677.97	.53	52.80	-2.60	60	5.0

difference between QIDEAL and QMEAS is the error. It is expressed by

$$\text{Percent error} = \frac{(\text{QIDEAL} - \text{QMEAS})}{\text{QIDEAL}} \times 100$$

If the percent error is positive, the measured capacity is less than the ideal capacity. If the percent error is negative, the capacity has increased.

When the temperature of the coil is less than room temperature, less energy is taken from the coil to cool it down to its steady state temperature. This allows more air to be cooled. For purposes of computation, this extra cooling energy will be credited to the unit by adding it back into QMEAS as QCOIL, which is calculated by Eq. 3F-2.

$$\text{QCOIL} = m_c \, c_{pc} \, (T_r - T_o) \qquad \text{(3F-2)}$$

where

m_c = mass of the coil, lbm (kg)

c_{pc} = specific heat of coil, Btu/lbm^{o}F (W s/kg^{o}C)

A new percent error is also calculated to reflect this addition.

The results of computing the capacity with QCOIL are also shown in Table 3F-1. It can be seen that when the mass of the coil is not considered, the dampers have little effect. Including the coil mass (QCOIL) does increase the measured capacity. Hence, the measured capacity can be increased by lowering T_o, but it is decreased by longer thermocouple response time. Under normal conditions with the dampers causing T_o=70^{o}F (21.1^{o}C), a 1.3% increase in capacity is observed.

The effect of moving the dampers to various locations can also be studied. Tables 3F-2, 3 and 4 summarize the results of seven different damper locations. Each Table corresponds to a different value of T_o. For T_o=80°F (26.7°C), little effect of location is noted, with thermocouple response time causing the percent error. Interestingly, from T_o=70 to 60°F (21.1 to 15.6°C), capacity increased as response time decreased. This can be explained by recalling the ΔT vs. TIME curves in Figure 3F-3. For shorter response times, there is less lag to the actual temperature and the initial gain in area under the curve is not balanced by the subsequent loss in area under the curve as time marches on. Finally, it can be seen that different damper locations do not cause much change in the measured capacity.

Next, consider the arrangement shown in Figure 3F-4. Now the thermocouple grid is placed some distance outside the downstream damper. As before, the temperatures sensed by the grid must be specified. For D3/V seconds (Distance/Velocity=Time), the grid senses the temperature of the air outside the dampers which is assumed to be room temperature. In the next D1/V seconds, the slug of trapped air downstream of the coil, at T_o, passes through the grid. This is followed by the slug of trapped air upstream of the coil which has been cooled by the heat exchanger. Finally, cooled room air reaches the grid. Again, applying Eq. 3D-12 to the above temperatures Eq. 3F-3 results.

Table 3F-2 Grid Placement - $T_o = 80^oF$

QIDEAL Btu	QMEAS Btu	%ERROR	QCOIL Btu	%ERROR w/coil	D1 Ft	D2 Ft	τ_t Sec
1686.96	1686.96	.00	0	.00	5	5	0
1686.96	1686.92	.00	0	.00	10	5	0
1686.96	1686.81	.01	0	.01	20	5	0
1686.96	1686.95	.01	0	.01	5	10	0
1686.96	1686.95	.00	0	.00	5	20	0
1686.96	1686.92	.00	0	.00	10	10	0
1686.96	1686.81	.01	0	.01	20	20	0
1686.96	1680.74	.37	0	.37	5	5	2.5
1686.96	1680.70	.37	0	.37	10	5	2.5
1686.96	1680.55	.38	0	.38	20	5	2.5
1686.96	1680.70	.37	0	.37	5	10	2.5
1686.96	1680.59	.38	0	.38	5	20	2.5
1686.96	1680.64	.37	0	.37	10	10	2.5
1686.96	1680.28	.40	0	.40	20	20	2.5
1686.96	1674.56	.73	0	.73	5	5	5.0
1686.96	1674.52	.74	0	.74	10	5	5.0
1686.96	1674.37	.75	0	.75	20	5	5.0
1686.96	1674.32	.74	0	.74	5	10	5.0
1686.96	1674.39	.75	0	.75	5	20	5.0
1686.96	1674.46	.74	0	.74	10	10	5.0
1686.96	1674.06	.76	0	.76	20	20	5.0

Table 3F-3 Grid Placement - $T_o = 70^oF$

QIDEAL Btu	QMEAS Btu	%ERROR	QCOIL Btu	%ERROR w/coil	D1 Ft	D2 Ft	τ_t Sec
1686.96	1688.64	-.10	26.40	-1.66	5	5	0
1686.96	1689.46	-.15	26.40	-1.71	10	5	0
1686.96	1691.03	-.24	26.40	-1.81	20	5	0
1686.96	1689.46	-.15	26.40	-1.71	5	10	0
1686.96	1691.10	-.25	26.40	-1.81	5	20	0
1686.96	1690.28	-.20	26.40	-1.76	10	10	0
1686.96	1693.41	-.38	26.40	-1.95	20	20	0
1686.96	1682.45	.27	26.40	-1.30	5	5	2.5
1686.96	1683.25	.22	26.40	-1.35	10	5	2.5
1686.96	1684.81	.13	26.40	-1.44	20	5	2.5
1686.96	1683.26	.22	26.40	-1.35	5	10	2.5
1686.96	1684.83	.13	26.40	-1.44	5	20	2.5
1686.96	1684.05	.17	26.40	-1.39	10	10	2.5
1686.96	1687.05	-.01	26.40	-1.57	20	20	2.5
1686.96	1676.27	.63	26.40	-0.93	5	5	5.0
1686.96	1677.07	.59	26.40	-0.98	10	5	5.0
1686.96	1678.63	.49	26.40	-1.07	20	5	5.0
1686.96	1677.07	.59	26.40	-0.98	5	10	5.0
1686.96	1678.64	.49	26.40	-1.07	5	20	5.0
1686.96	1677.86	.54	26.40	-1.03	10	10	5.0
1686.96	1680.83	.36	26.40	-1.20	20	20	5.0

Table 3F-4 Grid Placement - $T_o = 60^oF$

QIDEAL Btu	QMEAS Btu	%ERROR	QCOIL Btu	%ERROR w/coil	D1 Ft	D2 Ft	τ_t Sec
1686.96	1690.33	-.20	52.80	-3.33	5	5	0
1686.96	1691.99	-.30	52.80	-3.43	10	5	0
1686.96	1695.25	-.49	52.80	-3.62	20	5	0
1686.96	1691.99	-.30	52.80	-3.43	5	10	0
1686.96	1695.25	-.49	52.80	-3.62	5	20	0
1686.96	1693.63	-.40	52.80	-3.53	10	10	0
1686.96	1700.00	-.77	52.80	-3.90	20	20	0
1686.96	1684.15	.17	52.80	-2.96	5	5	2.5
1686.96	1685.81	.07	52.80	-3.06	10	5	2.5
1686.96	1689.07	-.12	52.80	-3.25	20	5	2.5
1686.96	1685.81	.07	52.80	-3.06	5	10	2.5
1686.96	1689.07	-.12	52.80	-3.25	5	20	2.5
1686.96	1687.45	-.03	52.80	-3.16	10	10	2.5
1686.96	1693.82	-.41	52.80	-3.54	20	20	2.5
1686.96	1677.97	.53	52.80	-2.60	5	5	5.0
1686.96	1679.63	.43	52.80	-2.70	10	5	5.0
1686.96	1682.82	.24	52.80	-2.89	20	5	5.0
1686.96	1679.63	.43	52.80	-2.70	5	10	5.0
1686.96	1682.89	.24	52.80	-2.89	5	20	5.0
1686.96	1681.27	.34	52.80	-2.79	10	10	5.0
1686.96	1687.64	-.04	52.80	-3.17	20	20	5.0

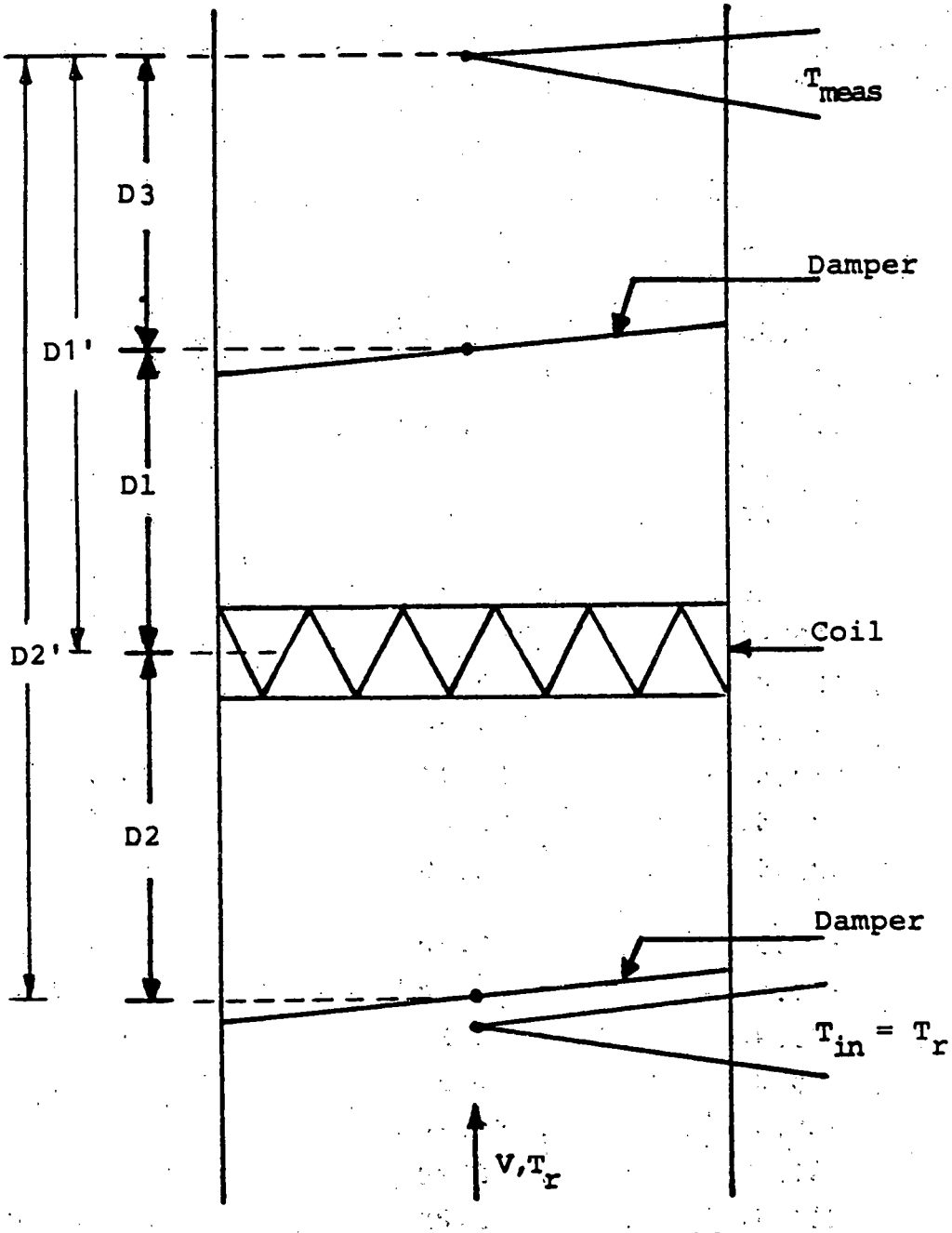

Figure 3F-4 Thermocouple Grid Outside Damper

$$T = T_r - T_{meas}$$

$$= 0 \qquad \text{for } 0 < t < D3/V$$

$$= (T_r - T_o) - (T_r - T_o)\, e^{-(t-D3/V)/\tau_t}$$

$$\text{for } D3/V < t < D1'/V$$

$$= (T_r - T_{ss}) - \frac{\tau_h}{\tau_h - \tau_t}(T_o - T_{ss})\, e^{-t/\tau_h}$$

$$- (T_1 - T_{ss} - \frac{\tau_h}{\tau_h - \tau_t}(T_o - T_{ss})\, e^{-D1'/V/\tau_h})\, e^{-(t-D1'/V)/\tau_t}$$

$$\text{for } D1'/V < t < D2'/V \qquad (3F\text{-}3)$$

where

$D1' = D3 + D1$

$D2' = D3 + D2 + D1$

T_1 = Temperature sensed by thermocouple at $t = D1'/V$

T_2 = Temperature sensed by thermocouple at $t = D2'/V$

Using the same numerical example as before with D3=5 ft (1.5 m), ΔT vs. TIME curves are plotted and are shown in Figures 3F-5 and 6. Referring to Figure 3F-5, $\Delta T_o = 0^\circ F$ ($0^\circ C$) at $t = 0$ for all the curves. But only the curve for $\tau_t = 0$ sec responds markedly to the slug of cooler air trapped by the dampers. Figure 3F-6 shows the response for the full six minutes of on-time. Again, note the dip due to thermocouple response.

Capacity is found by integrating Eq. 3F-3 over the on-time and Table 3F-5 shows the results for the capacity calculations. These results are almost identical with the

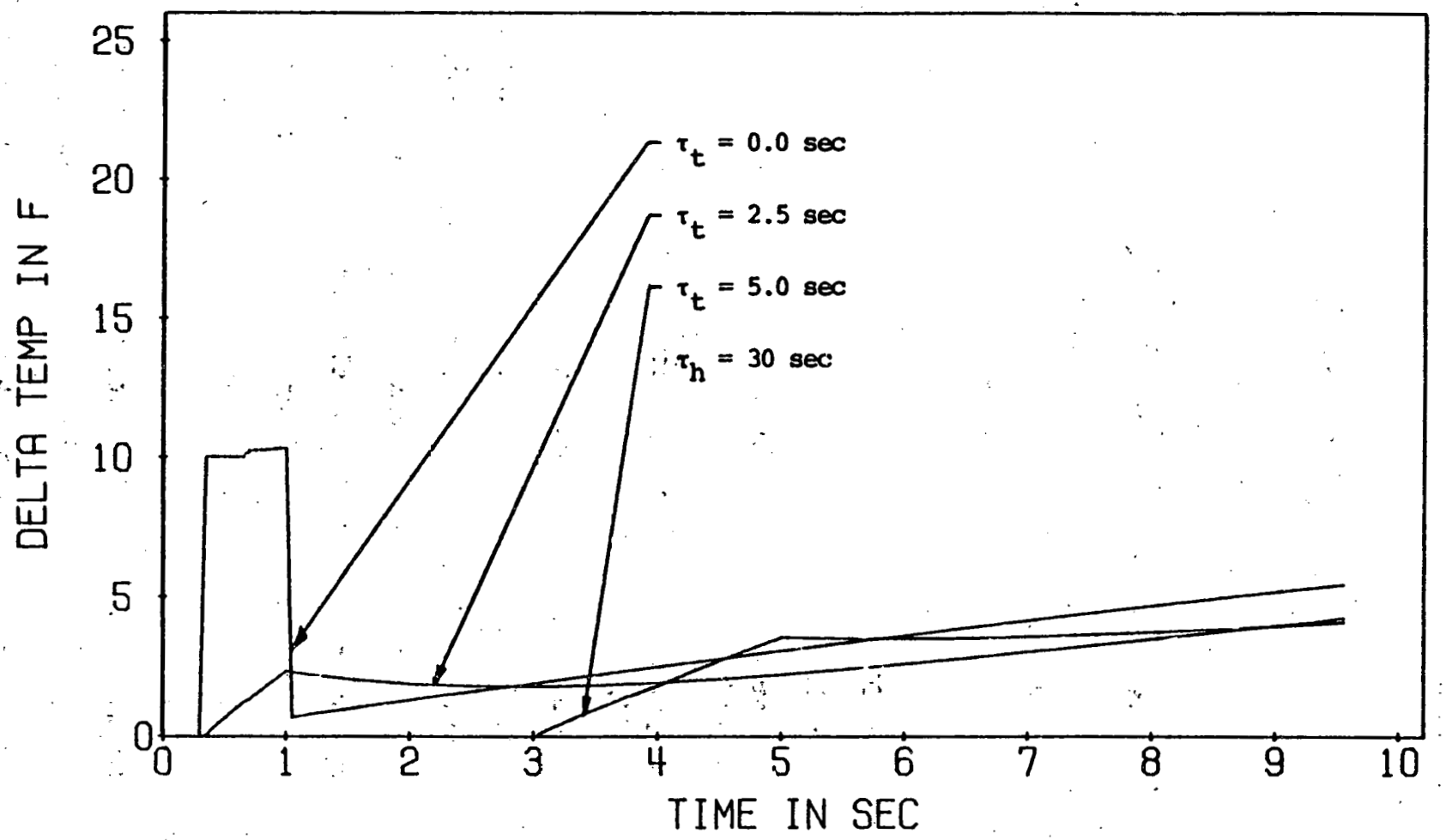

Figure 3F-5 ΔT vs TIME Curves with Grid Outside Damper - First 10 Seconds

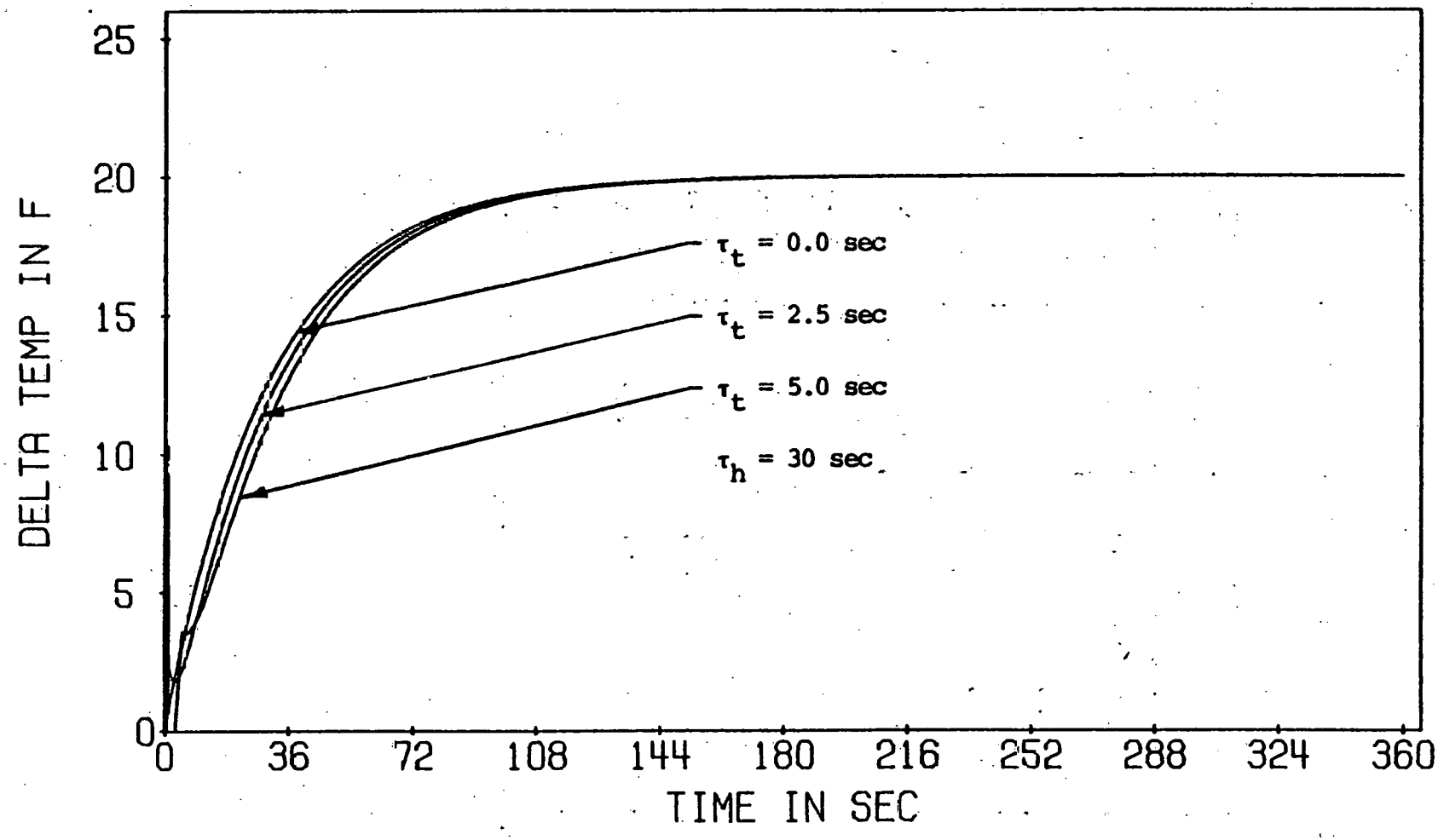

Figure 3F-6 ΔT vs TIME Curves with Grid Outside Damper - Full 6 Minutes

Table 3F-5 Capacities for Grid Outside Dampers

QIDEAL Btu	QMEAS Btu	%ERROR	QCOIL Btu	%ERROR w/coil	T_o °F	τ_t Sec
1686.96	1686.92	.00	0	.00	80	0
1686.96	1681.50	.32	0	.32	80	2.5
1686.96	1675.34	.69	0	.69	80	5.0
1686.96	1688.60	-.10	26.40	-1.66	70	0
1686.96	1681.60	.32	26.40	-1.25	70	2.5
1686.96	1675.40	.69	26.40	-0.88	70	5.0
1686.96	1690.28	-.20	52.80	-3.33	60	0
1686.96	1681.71	.31	52.80	-2.82	60	2.5
1686.96	1675.45	.68	52.80	-2.45	60	5.0

corresponding results when the thermocouple grid was placed inside the dampers.

Tables 3F-6, 7 and 8 show the results of the effects on measured capacity due to various damper and grid locations. As before, when T_o=80°F (26.7°C), location of the dampers or the grid has a negligible effect with the errors arising from thermocouple response. Again, measured capacity is increased as either T_o or response time decreases. However, very little change is observed by moving the thermocouple grid, and only a small change is observed by moving the location of the dampers.

Comparison of the two arrangements indicates that neither are strongly dependent on damper location as such, but rather on the value of T_o at start-up. (In practice, of course, T_o is dependent on damper placement.) Increases in measured capacity on the order of 1-3% can be made by obtaining lower values of T_o at start-up. Finally, it appears that the increases in capacity are slightly higher for the arrangement where the thermocouple grid is placed inside the downstream damper.

One final comment is in order. From the above discussion, it is apparent that T_o plays the major role in determining the effect of dampers on the measured capacity. In actual testing, T_o varies from room temperature to nearly 80% of T_{ss}. Its value is partly determined by off period refrigerant flow. However, it is mainly determined by the operation and placement of the dampers, insulation,

Table 3F-6 Grid Placement - $T_o = 80^oF$

QIDEAL Btu	QMEAS Btu	%ERROR	QCOIL Btu	%ERROR w/coil	D3 Ft	D1 Ft	D2 Ft	τ_t Sec
1686.96	1686.92	.00	0	.00	5	5	5	0
1686.96	1686.88	.00	0	.00	5	10	5	0
1686.96	1686.73	.01	0	.01	5	20	5	0
1686.96	1686.88	.00	0	.00	5	10	10	0
1686.96	1686.73	.01	0	.01	5	20	20	0
1686.96	1681.50	.32	0	.32	5	5	5	2.5
1686.96	1681.43	.33	0	.33	5	10	5	2.5
1686.96	1681.25	.34	0	.34	5	20	5	2.5
1686.96	1682.06	.29	0	.29	5	10	10	2.5
1686.96	1682.78	.25	0	.25	5	20	20	2.5
1686.96	1686.92	.00	0	.00	10	5	5	0
1686.96	1686.88	.00	0	.00	10	10	5	0
1686.96	1686.73	.01	0	.01	10	20	5	0
1686.96	1686.88	.00	0	.00	10	10	10	0
1686.96	1686.73	.01	0	.01	10	20	20	0
1686.96	1681.43	.33	0	.33	10	5	5	2.5
1686.96	1681.35	.33	0	.33	10	10	5	2.5
1686.96	1681.13	.35	0	.35	10	20	5	2.5
1686.96	1681.96	.30	0	.30	10	10	10	2.5
1686.96	1682.63	.26	0	.26	10	20	20	2.5

Table 3F-7 Grid Placement - $T_o = 70^oF$

QIDEAL Btu	QMEAS Btu	%ERROR	QCOIL Btu	%ERROR w/coil	DTC Ft	D1 Ft	D2 Ft	τ_t Sec
1686.96	1688.60	-.10	26.40	-1.66	5	5	5	0
1686.96	1689.40	-.14	26.40	-1.71	5	10	5	0
1686.96	1690.94	-.24	26.40	-1.80	5	20	5	0
1686.96	1690.21	-.19	26.40	-1.76	5	10	10	0
1686.96	1693.29	-.38	26.40	-1.94	5	20	20	0
1686.96	1681.60	.32	26.40	-1.25	5	5	5	2.5
1686.96	1681.69	.31	26.40	-1.25	5	10	5	2.5
1686.96	1682.07	.29	26.40	-1.27	5	20	5	2.5
1686.96	1682.47	.27	26.40	-1.30	5	10	10	2.5
1686.96	1684.27	.16	26.40	-1.41	5	20	20	2.5
1686.96	1688.55	-.09	26.40	-1.66	10	5	5	0
1686.96	1689.33	-.14	26.40	-1.71	10	10	5	0
1686.96	1690.83	-.23	26.40	-1.79	10	20	5	0
1686.96	1690.13	-.19	26.40	-1.75	10	10	10	0
1686.96	1693.15	-.37	26.40	-1.93	10	20	20	0
1686.96	1681.54	.32	26.40	-1.24	10	5	5	2.5
1686.96	1681.61	.32	26.40	-1.25	10	10	5	2.5
1686.96	1681.95	.30	26.40	-1.27	10	20	5	2.5
1686.96	1682.31	.27	26.40	-1.29	10	10	10	2.5
1686.96	1683.83	.17	26.40	-1.40	10	20	20	2.5

Table 3F-8 Grid Placement - $T_o = 60^oF$

QIDEAL Btu	QMEAS Btu	%ERROR	QCOIL Btu	%ERROR w/coil	DTC Ft	D1 Ft	D2 Ft	τ_t Sec
1686.96	1690.28	-.20	52.80	-3.33	5	5	5	0
1686.96	1691.92	-.29	52.80	-3.43	5	10	5	0
1686.96	1695.15	-.49	52.80	-3.62	5	20	5	0
1686.96	1693.54	-.39	52.80	-3.52	5	10	10	0
1686.96	1699.85	-.76	52.80	-3.89	5	20	20	0
1686.96	1681.71	.31	52.80	-2.82	5	5	5	2.5
1686.96	1681.95	.30	52.80	-2.83	5	10	5	2.5
1686.96	1682.89	.24	52.80	-2.89	5	20	5	2.5
1686.96	1682.88	.24	52.80	-2.89	5	10	10	2.5
1686.96	1685.75	.07	52.80	-3.06	5	20	20	2.5
1686.96	1690.22	-.19	52.80	-3.32	10	5	5	0
1686.96	1691.84	-.29	52.80	-3.42	10	10	5	0
1686.96	1695.03	-.48	52.80	-3.61	10	20	5	0
1686.96	1693.44	-.38	52.80	-3.51	10	10	10	0
1686.96	1699.68	-.75	52.80	-3.88	10	20	20	0
1686.96	1681.65	.32	52.80	-2.81	10	5	5	2.5
1686.96	1681.87	.30	52.80	-2.83	10	10	5	2.5
1686.96	1682.77	.25	52.80	-2.88	10	20	5	2.5
1686.96	1682.78	.25	52.80	-2.88	10	10	10	2.5
1686.96	1685.58	.08	52.80	-3.05	10	20	20	2.5

etc. In other words, the effect of the dampers is highly dependent on the test set-up. Therefore, the same coil could be tested by two different laboratories and different results might be obtained simply due to differences in their test set-ups. This has serious implications as far as the testing program is concerned because valid comparisons of units could not be made.

One simple way to begin correcting this problem is to eliminate the dampers altogether and let the indoor fan run continuously. As is seen in Tables 3F-2 and 6 where T_o=80°F (26.7°C), a condition that will usually be obtained under such a set-up, no increases or decreases in measured capacity are obtained except those that can be accounted for from thermocouple response time. By eliminating dampers and letting the indoor fan run continuously, T_o would consistently equal 80°F (26.7°C). Hence, in test D, all manufacturers would begin to measure cyclic capacity at the same point, namely at ΔT_o=0 when t =0. This set-up would also more closely approximate actual field operation of a unit. Furthermore, off-time cooling could easily be calculated by continuing to monitor ΔT vs TIME until ΔT again returned to zero (or within some increment of zero). Of course, the power consumed by the fan during the off-time would have to be accounted for.

Section G - Nonuniformity

This section will study the effects of a nonuniform velocity and temperature distribution on the measurement

of capacity during test D. While the defining equation for $Q_{cyc,\ dry}$ considers the velocity, V, uniform and constant, it is not hard to imagine considerable nonuniformity in V as the air flow passes through the coil with its tubes, fins, supports, etc. before reaching the thermocouple grid. It is not quite so obvious that the temperature distribution over the coil may also vary, causing a nonuniform temperature distribution to be sensed by the thermocouples. However, Murphy and Goldschmidt [1979] confirm the possibility of a nonuniform temperature distribution over the coil. It will also be observed in the data of the next section.

The defining equation for $Q_{cyc,\ dry}$ could be written more generally as follows:

$$Q_{cyc,dry} = \iint_A \int_t \rho\ c_p\ V\ (x,y)\ \Delta T\ (x,y,t)\ dt dA \qquad (3G\text{-}1)$$

where

A = cross-sectional area of the duct

t = time

ρ = density of air

c_p = specific heat of air

V = velocity of air (assumed independent of time)

ΔT = temperature difference across the coil

Assuming constant properties and the first order response of the heat exchanger from Section C over six minutes, Eq. 3G-1 can be simplified.

$$Q_{cyc,dry} = \qquad (3G\text{-}2)$$

$$\rho c_p \iint_A V(x,y)\ \{(T_r - T_{ss}(x,y))t_{on} + \tau_h (T_o - T_{ss}(x,y))(e^{-t_{on}/\tau_h} - 1)\}dA$$

Three more assumptions underlie Eq. 3G-2; T_o is constant over the coil, the time response of the heat exchanger is also constant, and the velocity is time independent. This equation can also be modified to account for the effect of thermocouple response time on the capacity. One simply substitutes Eq. 3D-13 for the bracketed expression in Eq. 3G-2. With analytical expressions for V and T_{ss}, Eq. 3G-2 could be integrated to yield an exact value for $Q_{cyc,dry}$. However, such expressions are not generally available, so they must be replaced with experimental or semi-empirical values and $Q_{cyc,dry}$ is computed by numerical integration or summation. Hence, $Q_{cyc,dry}$ might now be written as

$$Q_{cyc,dry} = \tag{3G-3}$$

$$c_p \sum_{i=1}^{M} V(i)\ (T_r - T_{ss}(i))t_{on} + \tau_h (T_o - T_{ss}(i))(e^{-t_{on}/\tau_h} - 1)\ dA(i)$$

where

M = number of finite area elements

It should be noted that if either the velocity or the temperature is uniform over the cross-sectional area, Eq. 3G-1 reduces to Eq. 3A-1, the DOE cyclic capacity equation. That is,

$$Q_{cyc,dry} = \rho c_p \iint_A \int_t V(x,y)\Delta T(x,y,t)\ dt\ dA$$

If $\Delta T(x,y,t) = \Delta T\ (t)$, then

$$Q_{cyc,dry} = \rho c_p \iint_A V(x,y)dA \int_t \Delta T\ (t)\ dt$$

but, $\iint_A V(x,y)dA = \bar{V}A$

So $Q_{cyc,dry} = \rho c_p \bar{V} A \int_t \Delta T\ (t)\ dt$

If $V(x,y) = V$, then

$$Q_{cyc,dry} = \rho c_p\ V \iint_A \int_t \Delta T\ (x,y,t)\ dt\ dA$$

$$= \rho c_p\ V \int_t \iint_A \Delta T\ (x,y,t)\ dA\ dt$$

but $\iint_A \Delta T\ (x,y,t)\ dA = \overline{\Delta T}\ (t)\ A$

So $Q_{cyc,dry} = \rho c_p\ VA \int_t \overline{\Delta T}\ (t)\ dt$

In order to study the effects of nonuniform velocity and temperature distributions on capacity measurement, consider Eq. 3G-3 and an 81 square grid placed over the cross-sectional area of a duct just downstream of the evaporator coil. See Figure 3G-1. Over each square and block of nine squares, velocity and temperature measurements are to be made and then substituted into Eq. 3G-3. First, several measuring schemes will be labeled and defined. Note that square refers to one of the 81 squares and block refers to nine squares with three squares on a side.

T81 - This will correspond to measurements made by a thermocouple grid composed of 81 thermocouples, each sensing the steady state temperature of a particular square in the grid. It will be assumed that each thermocouple can be monitored individually and that the average of any number of thermocouples can be found.

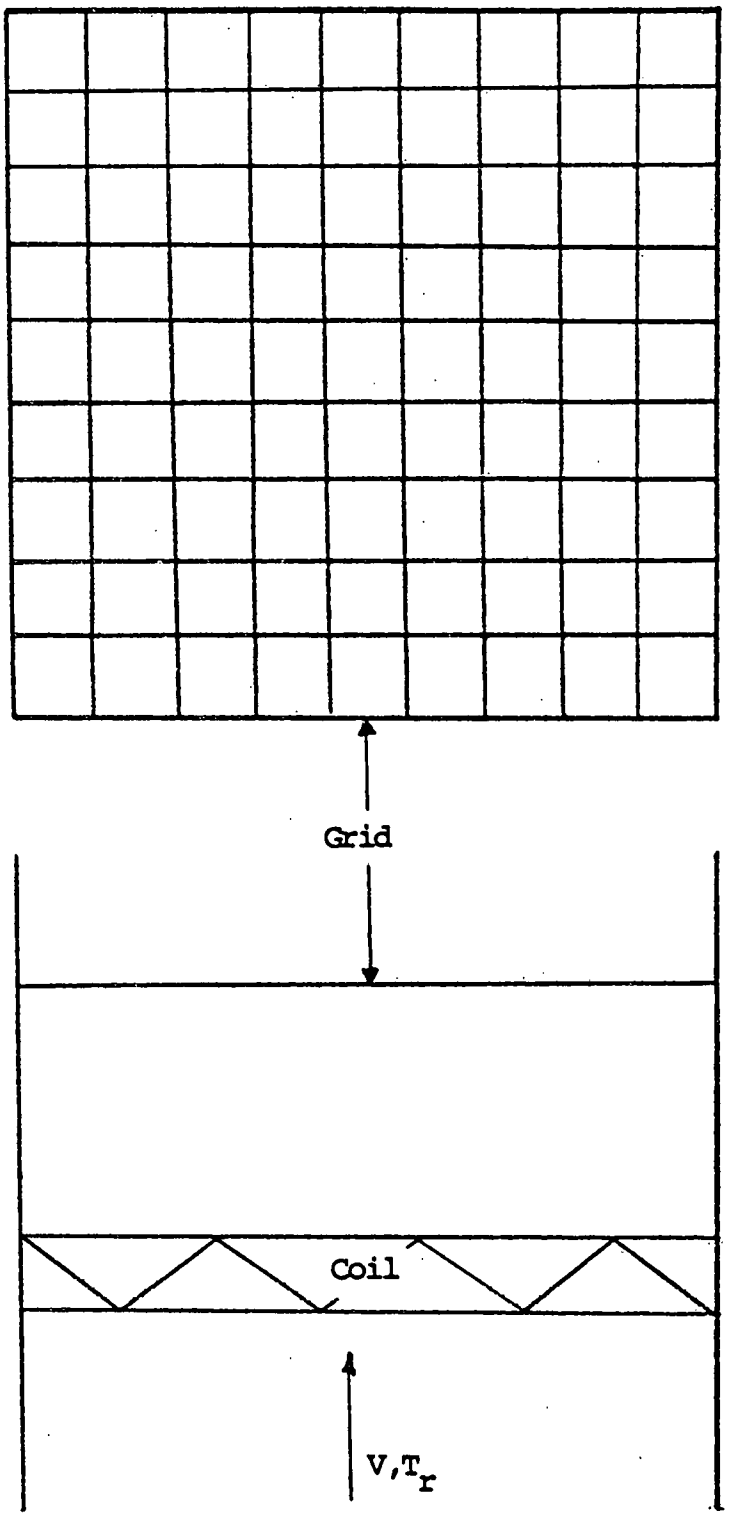

Figure 3G-1 81 Square Grid in the Duct

T9A - This will correspond to measurements made by a nine point thermocouple grid. Each thermocouple senses the average steady state temperature of the nine squares forming each block in the grid. It will be assumed that each thermocouple can be monitored individually or that they can all be averaged. See Figure 3G-2.

T9 - This will correspond to measurements made by a nine point thermocouple grid. Each thermocouple senses the steady state temperature of the center square only of its particular block. This temperature then represents the entire block. It will be assumed that each thermocouple can be monitored individually or that the average of the nine center squares can be obtained. See Figure 3G-3.

V81 - This will correspond to some measuring procedure where a velocity of the air flow through each of the 81 squares in the grid is found. These velocities can be used individually or they can be averaged.

V9A - This will correspond to some measuring procedure where an average velocity for each block is found. This average velocity will be assumed to be the numerical average of the velocities through the nine component squares of that block. Each velocity can be used individually or they can be averaged. See Figure 3G-2.

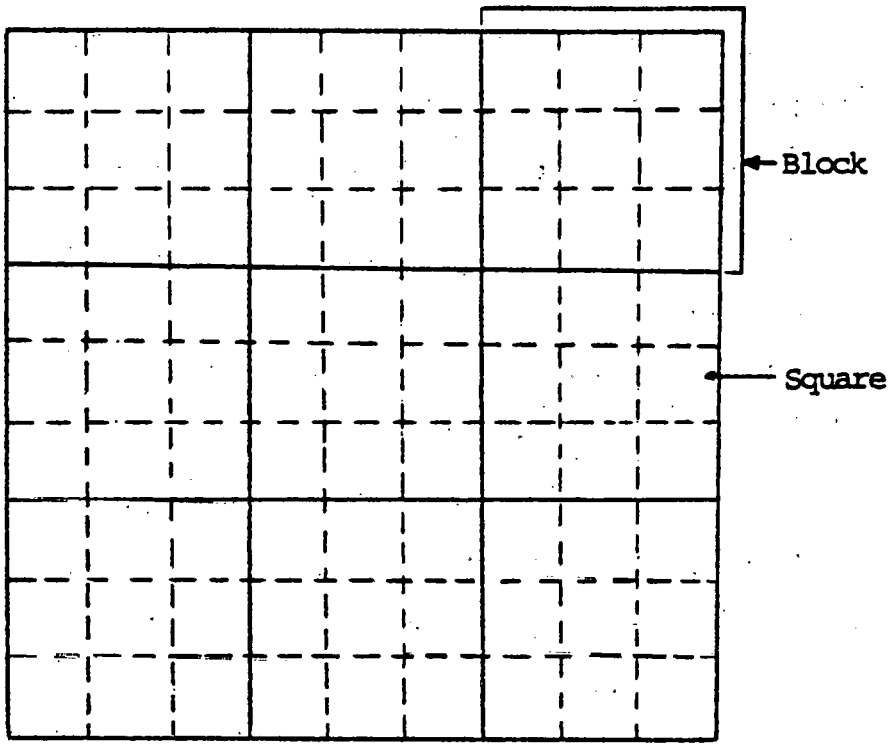

Figure 3G-2 V9A or T9A - Average over Block of 9 Squares

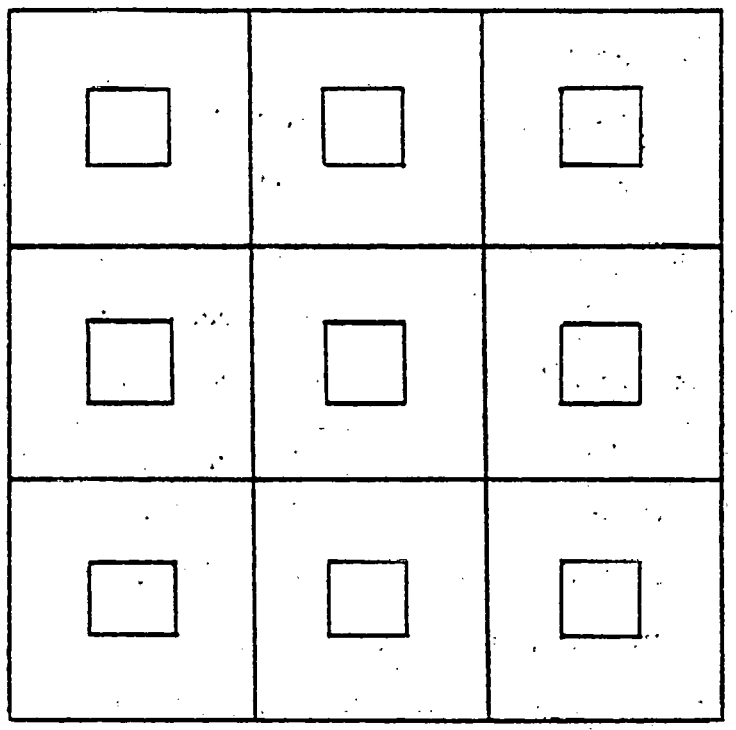

Figure 3G-3 V9 or T9 - Center Square Only

V9 - This will correspond to some measuring procedure where the velocity through the center square only of each block is found. The flow through the entire block is then assumed to have this velocity. These velocities can be used individually or they can be averaged. See Figure 3G-3.

$\overline{\quad}$ - This indicates that the velocities or temperatures have been averaged, e.g. $\overline{T81}=T_{ave}$

A temperature measuring scheme and a velocity measuring scheme can be chosen and the resulting values for velocity and temperature can be substituted into Eq. 3G-3 and the capacity can be computed. Although not all of these measuring scheme combinations are practical, the different combinations will give an indication of differences in capacities resulting from the nonuniformities. For example, V81 together with T81 would be a very time consuming measurement scheme because 81 thermocouples would have to be made and monitored and 81 velocities would have to be measured. Yet this scheme comes the closest to measuring the actual capacity of the unit. As another example, the combination of $\overline{V81}=V_{ave}$ and $\overline{T81}=T_{ave}$ will give results identical with those obtained by the DOE test procedures when "perfect" air mixers are used.

The following numerical example will illustrate how capacity can be affected by nonuniformities in velocity and temperature distributions. Figure 3G-4 shows a sketch of an A-shaped evaporator coil in a duct, with the 81 square

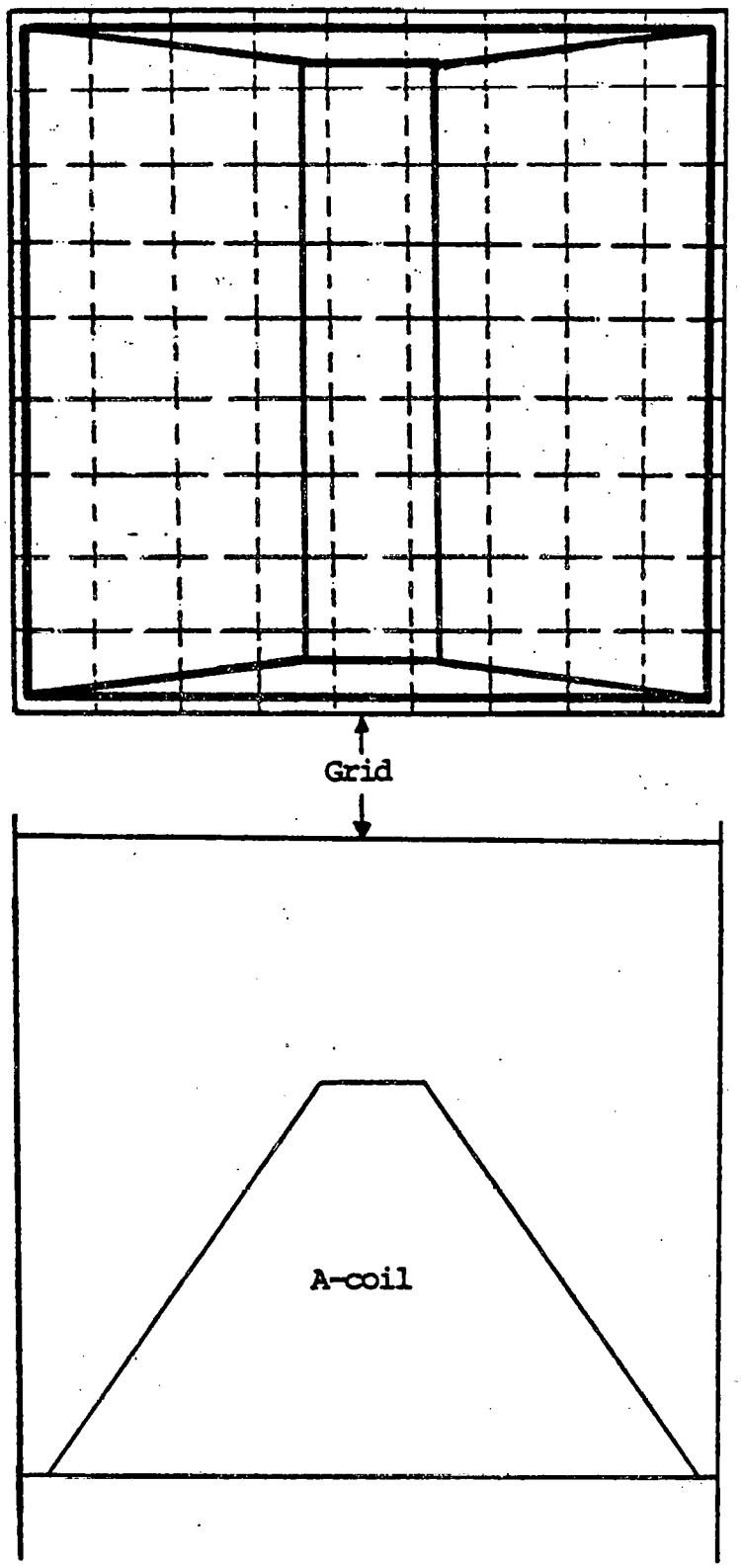

Figure 3G-4 A-coil with 81 Square Grid

grid shown in dotted lines over the top of the A-coil. Figure 3G-5 shows two grids; the squares in the upper grid have been filled in with a selective velocity distribution that might result from air flow through an A-coil. (Though selective, this distribution is based on actual measurements through an A-coil.) The lower grid contains a selective steady state temperature distribution which could result from the air flow through the same coil. (Again, this is based on actual measurements.) The numerical average of the upper grid, V_{ave}, is 15 ft/sec (4.6 m/s). The average of the lower grid, T_{ave}, is 60°F (15.6°C). Figures 3G-6 and 7 show the corresponding grids representing measurements under schemes V9A, V9 and T9A, T9 respectively. Other numerical values for this example are the same as those used for QIDEAL. (See Table 3C-1)

Eq. 3G-3 will be used in two ways in this example. It will be used as written when each thermocouple and individual velocity is to be monitored. When the temperatures or the velocities are to be averaged first, the following form of Eq. 3G-3 will be used:

$$Q_{cyc,dry} = \rho c_p A \bar{V}\{(T_r-\overline{T_{ss}})t_{on} + \tau_h(T_o-\overline{T_{ss}})(e^{-t_{on}/\tau_h}-1)\} \quad (3G-4)$$

Recall that when either the velocity or temperature is uniform and placed in front of the integral sign, the other quantity is mathematically averaged by the integral.

Velocity Distribution - ft/sec

H	H	M	M	L	M	M	H	H
H	H	M	M	L	M	M	H	H
H	H	M	M	L	M	M	H	H
H	H	M	M	L	M	M	H	H
H	H	M	M	L	M	M	H	H
H	H	M	M	L	M	M	H	H
H	H	M	M	L	M	M	H	H
H	H	M	M	L	M	M	H	H
H	H	M	M	L	M	M	H	H

H = 18.5

M = 14.0

L = 5.0

Temperature Distribution - ^{o}F

L	L	M	H	H	H	M	L	L
L	M	M	M	H	M	M	M	L
L	M	M	M	M	M	M	M	L
L	M	M	M	M	M	M	M	L
L	M	M	M	M	M	M	M	L
L	M	M	M	M	M	M	M	L
L	M	M	M	M	M	M	M	L
L	M	M	M	M	M	M	M	L
L	L	M	H	H	H	M	L	L

H = 64.0

M = 61.5

L = 55.0

Figure 3G-5 Selective Velocity and Temperature Distribution

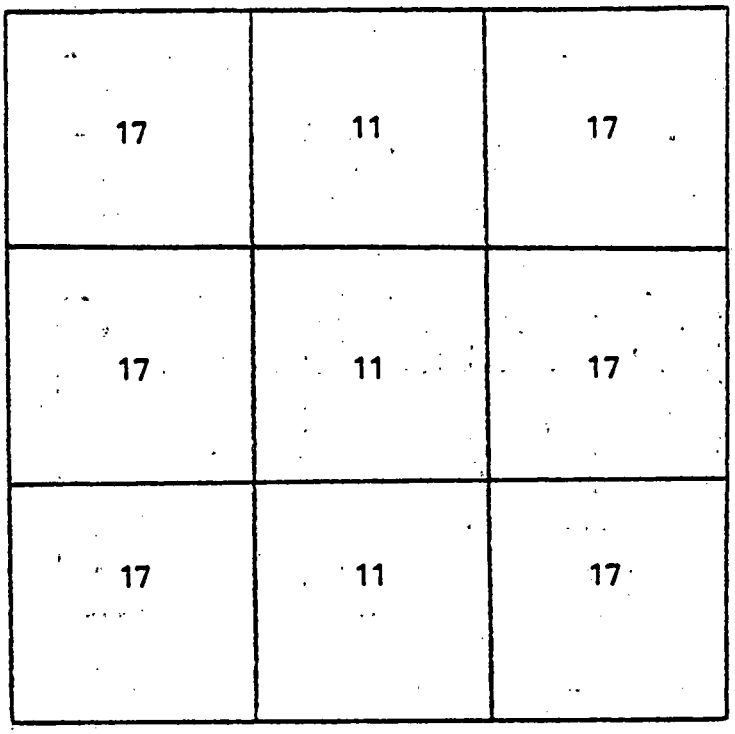

Velocities - ft/sec

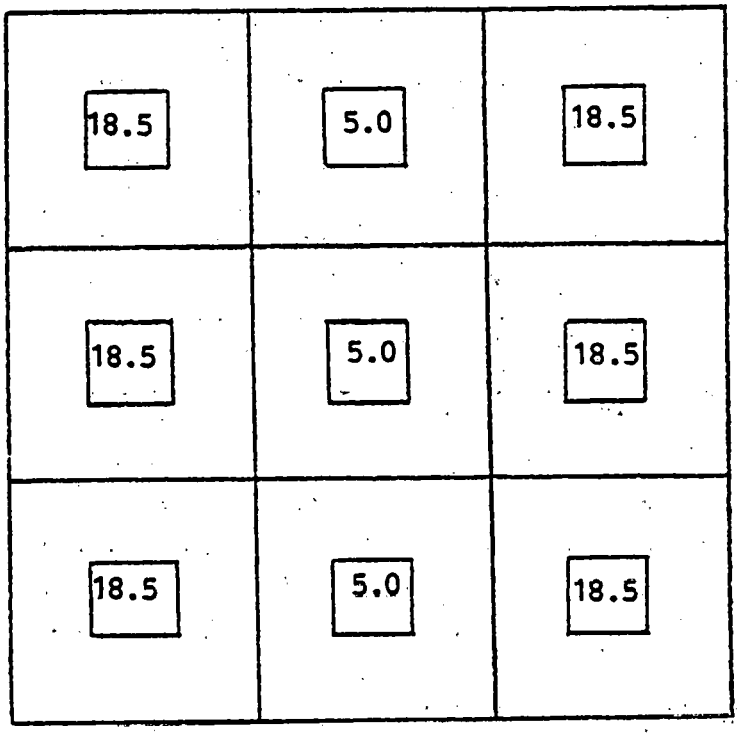

Figure 3G-6 Velocity Distribution for V9A and V9

58.6	62.6	58.6
59.4	61.5	59.4
58.6	62.6	58.6

Temperatures - ^{o}F

61.5	64.0	61.5
61.5	61.5	61.5
61.5	64.0	61.5

Figure 3G-7 Temperature Distribution for T9A and T9

In this example, note that

$\overline{T81} = T_{ave} = 60^{o}F$ (15.6°C

$\overline{V81} = V_{ave} = 15$ ft/sec (4.6 m/s)

$\overline{T9A} = 60^{o}F$ (15.6°C)

$\overline{V9A} = 15$ ft/sec (4.6 m/s)

$\overline{T9} = 62.08^{o}F$ (16.7°C)

$\overline{V9} = 14$ ft/sec (4.3 m/s)

Consider V81 and T81. Substituting the values for V and T_{ss} found in the squares of Figure 3G-5 into Eq. 3G-3, the capacity, Q, is calculated to be

Q = 1729 Btu (507 Whr)

This scheme, among all the other combinations to be examined, provides the most accurate (actual) measure of the unit's capacity because it most closely approximates the integral of Eq. 3G-2. Therefore, this number will be the base to which other combinations will be compared and will be labeled, QACTUAL. The combination of $\overline{T81}$ and $\overline{V81}$ will provide values for Eq. 3G-4. This calculation yields a capacity of 1687 Btu (494 Whr). This value of capacity is recognized as QIDEAL. Recall that "IDEAL" refers to ideal DOE test conditions, including perfect air mixing. Note that QACTUAL and QIDEAL are not necessarily equal. Other combinations of measurement schemes provide values which are substituted into either Eqs. 3G-3 or 3G-4 and the results are tabulated in Table 3G-1. The various combinations are ranked with V81-T81 (QACTUAL) being ranked first and all others are ranked relative to it. Percent error is also listed both relative to QACTUAL and to QIDEAL.

Table 3G-1 Capacities for Various Measurement Schemes

Rank	Combination	Measured Capacity (Btu)	% Error w/ QACTUAL (Btu)	% Error w/ QIDEAL (Btu)
1	V81 - T81	1729	0.0	-2.5
2	V9A - T81	1712	1.0	-1.5
3	V9A - T9A	1712	1.0	-1.5
3	V81 - T9A	1712	1.0	-1.5
4	V_{ave} - T_{ave}	1687	2.5	0.0
4	V_{ave} - T9A	1687	2.5	0.0
5	V9 - T81	1632	5.7	3.3
6	V9 - T9A	1632	5.7	3.3
7	V9 - T_{ave}	1575	9.0	6.7
8	V81 - T9	1524	11.9	9.7
8	V9A - T9	1524	11.9	9.7
9	V_{ave} - T9	1512	12.6	10.4
10	V9 - T9	1439	16.8	14.7
11	$\overline{V9}$ - $\overline{T9}$	1411	18.4	16.4

The results in Table 3G-1 apply strictly only to the above example. However, some trends are observed and will be assumed to apply generally. The results show that the "best" measurements (rankings 1-3) have as many individual velocity and temperature measurements as possible so that Eq. 3G-3 more closely approximates Eq. 3G-2. But this scheme is probably too impractical to implement for general testing. A large thermocouple grid would be time consuming to make, but could be used over again. (However, there might be difficulty in monitoring so many individual signals.) Furthermore, velocity measurements would have to be made for each coil to be tested.

Ranking 4 indicates "good" measurements, which result from good air mixing before measurements are made. This ensures that $\overline{V81}$ and $\overline{T81}$ are as close as possible to the numerical average of measurements made under V81 and T81. Although these measurements yield capacities on the order of 2-3% below QACTUAL (for this example), a good air mixer and flow straightner is all that would be needed to obtain consistent results. Velocity measurements could be made according to the ASHRAE Standard 37-78 and a simple nine point thermocouple could be used.

The "poor" measurements are found in rankings 5-11 and errors as high as 18% (for this example) are observed. The problem with these measurements lies in the fact that extreme values of velocity and/or temperature are measured

which are not representative of the process. For example, ranking 10 gave very poor results. Several thermocouples sensed "higher" temperatures, while, at the same time, a few "lower" velocities were measured. This combination in Eq. 3G-3 resulted in an error on the order of 15%. In other words, if a few measurements are made which include some extreme or unrepresentative values, these might not be "smoothed out" and would tend to dominate the calculation, causing large errors. This applies to both measurements at the same time. Ranking 7, V9-T_{ave}, is an example. T_{ave} could have been made with an 81 point thermocouple grid whose temperatures were then electronically averaged (connected in parallel, for example). But isolated low velocities measured by V9 caused an error on the order of 6%.

In summary, it can be seen that nonuniform velocity and temperature distributions can cause considerable variation in the measured capacity with possible errors as high as 10% or more. The actual capacity can be best measured by monitoring the velocity and temperature over numerous small area elements over the duct cross section and then employing Eq. 3G-3. Poor results will be obtained if too few measurements of velocity and/or temperature are made allowing extreme values to dominate the calculation. Good results with a practical test set-up can be obtained if the air is properly mixed before measurements are taken.

(This section is recommending good air mixing so that representative average values of velocity and/or temperature may be measured. No attempt at detailing how this should be done will be made in this work. However, in light of Section E and thermal storage effects of massive objects, such as an air mixer, it is recommended that "good," "massless" air mixers be further investigated for use in testing.)

Three final points need to be stressed concerning this section. First, the numbers used for the velocity and temperature distributions were arbitrary. But, they were based on experimental measurements taken from an actual test installation and could be representative of many other test set-ups throughout the air conditioning industry.

Secondly, different velocity and temperature distributions could be encountered as the thermocouple grid is moved from one location to another. This, in turn, might affect the measured capacity of the unit. These differences would be attributed to the test set-up, not to the unit being tested. Also, such differences would be in addition to those discussed in Section E.

Lastly, if either the velocity distribution or the temperature distribution can be made uniform, the other quantity is mathematically averaged and the measured capacity would correspond, in principle, to QIDEAL. However, suppose that the temperature distribution is made

uniform by electronic averaging. While the velocity distribution could then be considered uniform mathematically, the velocity effects on thermocouple response time would not be accounted for. As was seen in Section D, significant errors on the order of 4% or more could result if the response times become too long.

Section H - Application

This section will compare the analytical results of the previous sections with actual data taken from the testing facilities of an air conditioning manufacturer. As was mentioned in the introduction to Chapter 3, the air conditioning industry has generally made a sincere effort to comply with the DOE labeling program. They have devoted many hours and spent a considerable amount of money trying to understand and run tests C and D and obtain reliable and consistent results. The data that will be used in this section has come from such a manufacturer. During two separate visits, the author supervised the taking of the data presented in this section (with the exception of the velocity distribution and nine column thermocouple grid data). The author again expresses appreciation to the engineering staff for their time and help. It is hoped that comparisons between this data and predicted results will lead to a better understanding of the DOE test procedures.

The existing test facilities were designed for steady state testing and a considerable amount of ingenuity was needed to convert them so that they could be used for low humidity, transient testing. Figure 3H-1 shows a sketch of the test chambers (the test tunnel was later modified, as will be noted later). As can be seen, room air is drawn through a damper arrangement which is used to control the air flow. The position of these dampers, together with a fan immediately following them (fan motor outside the duct), is matched with the large downstream fan so that a slightly positive pressure exists in the testing tunnel. This is to insure against warmer room air leaking into the cooler air stream. After passing some turning vanes, the air is sampled to determine its wet and dry bulb temperature. Located on top of the sampler fork is a 99 point thermocouple grid, connected in parallel, which also measures the incoming air temperature. This entire inlet section was used as an air trap before an upstream damper was installed. No significant differences in measured capacity were noted between the use of the air trap and an upstream damper.

Following the upstream damper in the test tunnel, the air passes through an A-coil rated at 2½ tons which has a capillary tube for its throttling device. Ten inches above the top of the A-coil is another 99 point thermocouple grid. The air continues through the downstream

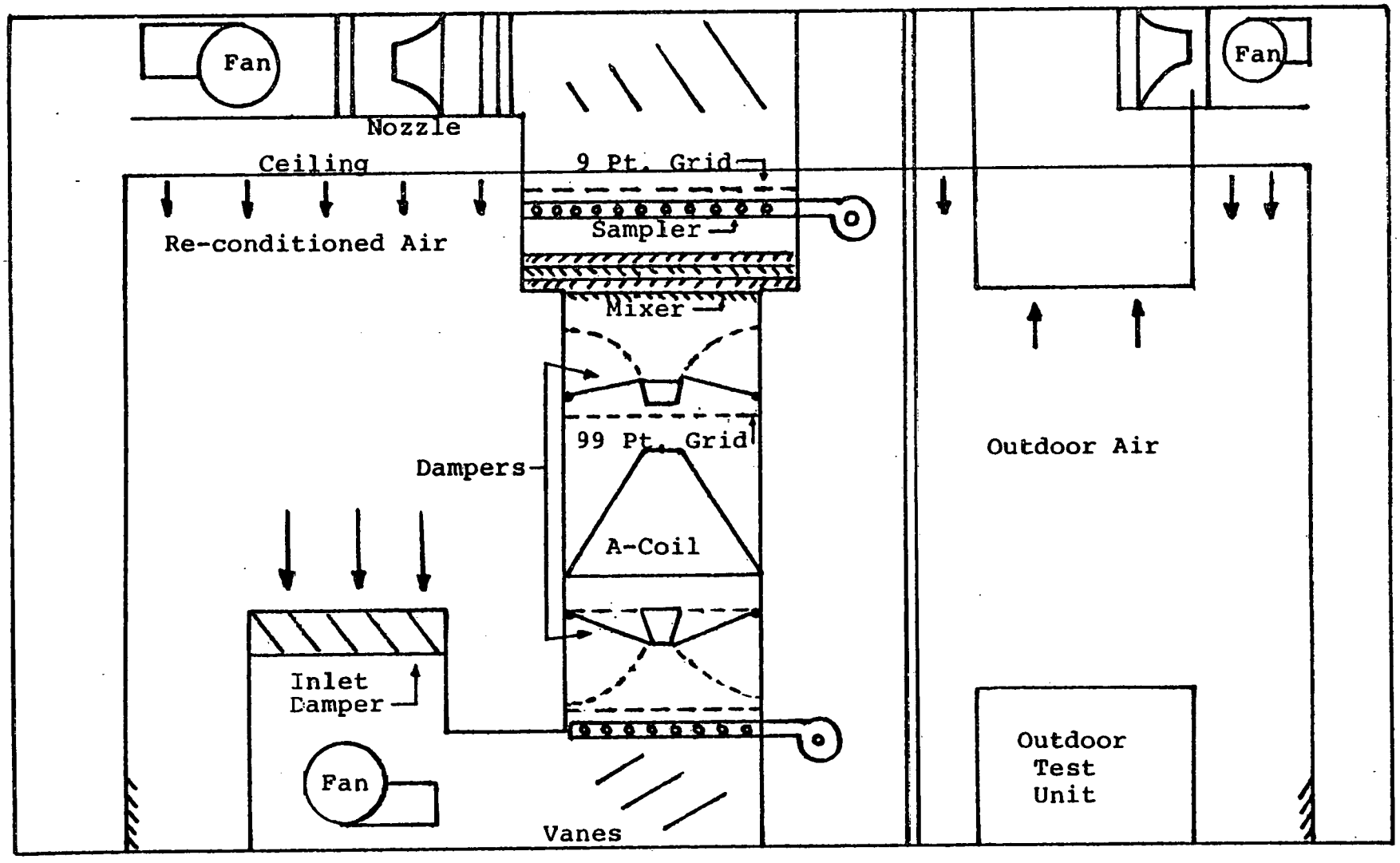

Figure 3 -1 Test Chambers

damper assembly and flows into a four level air mixer. Upon leaving the air mixer, the air is again sampled for wet and dry bulb temperature. Another thermocouple grid consisting of nine thermocouples is placed on the sampler fork for a second reading of leaving air temperature. The air then enters the nozzle and flows into the re-conditioning equipment and returns to the chamber by diffusing through the ceiling.

The downstream damper assembly had to be designed so that off period air would not flow over the coil and so that the room conditioning could continue. Consequently, the two damper doors form two of the four sides of the testing tunnel when they are open. When closed, the room air flows into the tunnel where the damper doors were, bypassing the coil, and continues to the reconditioning equipment. Both damper assemblies are operated by air cylinders. They open and close quickly, in 1-3 seconds, and form an air-tight seal when open or closed.

The data acquisition system consists of a Motorola 6800 microcomputer with an analog to digital converter. Incoming signals from the various sensors, thermocouples, pressure transducers, etc., are processed by in-house software and virtually all information regarding the test that is being conducted can be displayed and printed. This includes continuous monitoring of room temperatures so that the technician can maintain the rooms within their prescribed tolerances.

The testing and data collection for this work occurred during two visits to this installation. On the first visit the data collected included a transient temperature distribution recorded by a 99 point thermocouple grid and time-temperature data for different duct wall-insulation combinations. On the second visit, the testing tunnel was considerably altered from that shown in Figure 3H-1. The ducting was expanded and completely covered with 2 inches of polystyrene insulation. (This was done to accomodate the larger, wider-based coils.) For smaller coils, including the 2½ ton coil for which this data was taken a 2 ft (.6 m) 24 gage sheet metal duct was fitted inside the main tunnel. See Figure 3H-2. With this arrangement, time-temperature data was obtained for test runs with and without the use of dampers and for temperature measurements made downstream of the air mixer. All of this data will be further discussed in this section.

Thermocouple Response

Copper-constantan thermocouples are used in this test facility and are made from 22 AWG wire (.0253 in). The junctions are made by tightly twisting the bare wire leads. The twist is soft soldered and clipped so that it is approximately .25 in (.006 m) long. The junctions are generally cylindrical in shape and due to the solder are slightly thicker than two wire diameters.

Thermocouple response time was discussed in Section D. Figure 3D-2 shows the time constant as a function of

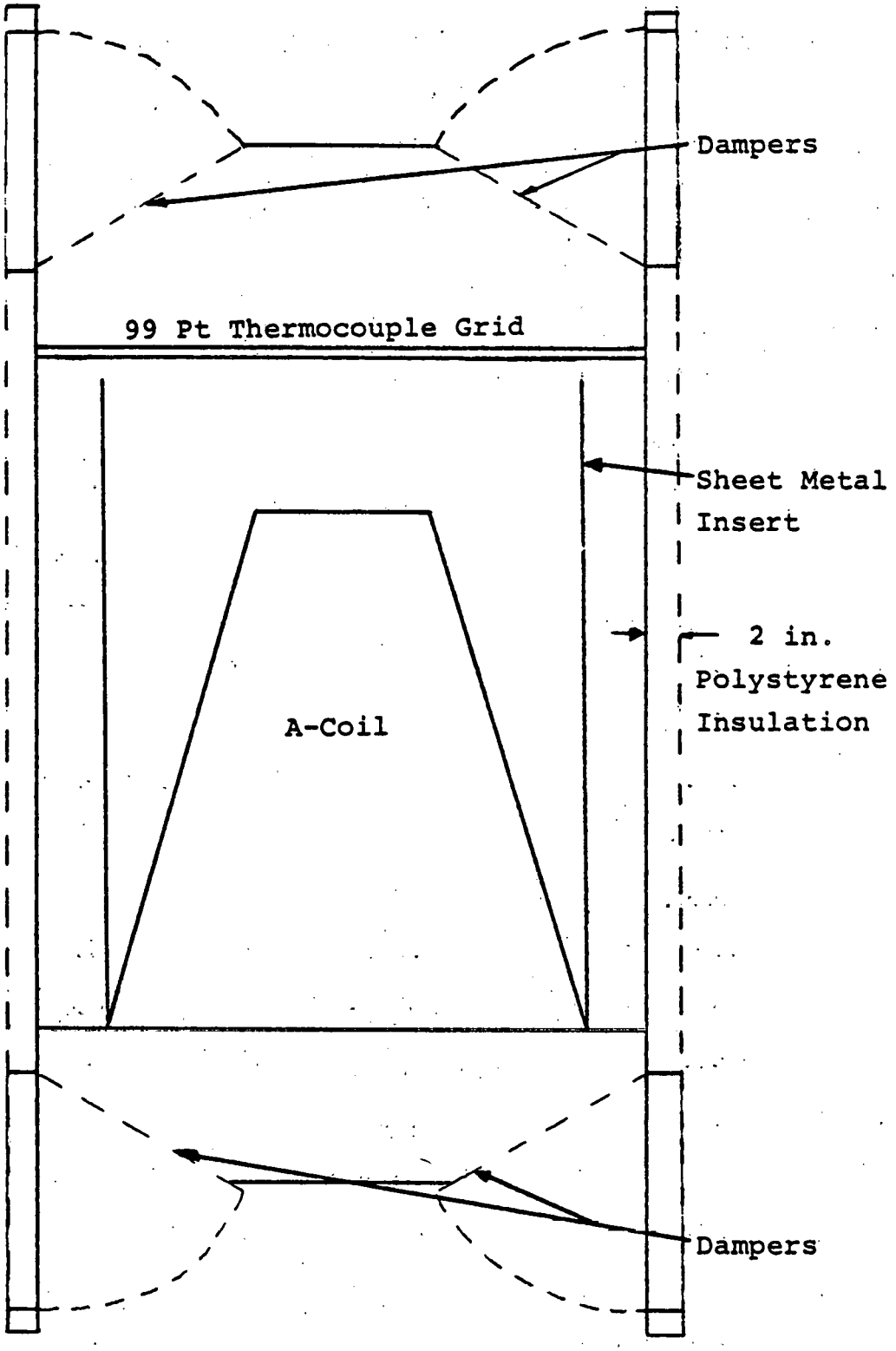

Figure 3H-2 Modified Testing Tunnel

velocity and wire diameter when the junction is considered cylindrical in shape. The velocities encountered in the testing chamber average about 6 ft/sec (1.8 m/sec). The curve for 22 AWG wire in Figure 3D-2 predicts a time constant of about 9 seconds. This is well above the 2.5 second limit set in the test procedures and the effect of such a long time constant should be noticeable on a ΔT vs. TIME curve.

Two 24 minute off-time - 6 minute on-time tests were made and the results for the on-time of the first test are plotted as shown in Figure 3H-3. In this test, the dampers were closed during the off-time. The thermocouple grid was located inside the dampers so that ΔT_o=8.6°F (4.8°C) rather than zero at start-up. The data in Figure 3H-3 show a large initial dip which reaches a minimum value between 15-20 seconds. Then the data points rise until a steady state value of approximately 24. °F (13.7°C) is reached. The fluctuations in the data during the last four minutes are probably due to the variations in room temperature, which, during the first test, varied from 79.5°F to 80.9°F.

The dip in Figure 3H-3 resembles the dips due to thermocouple response in the curves in Figure 3F-3. Several trial-and-error attempts were made to try and "curve-fit" the data in Figure 3H-3 using only a curve generated by Eq. 3F-1. The solid line curve in Figure 3H-3 is the result of these attempts and represents a ΔT vs TIME curve

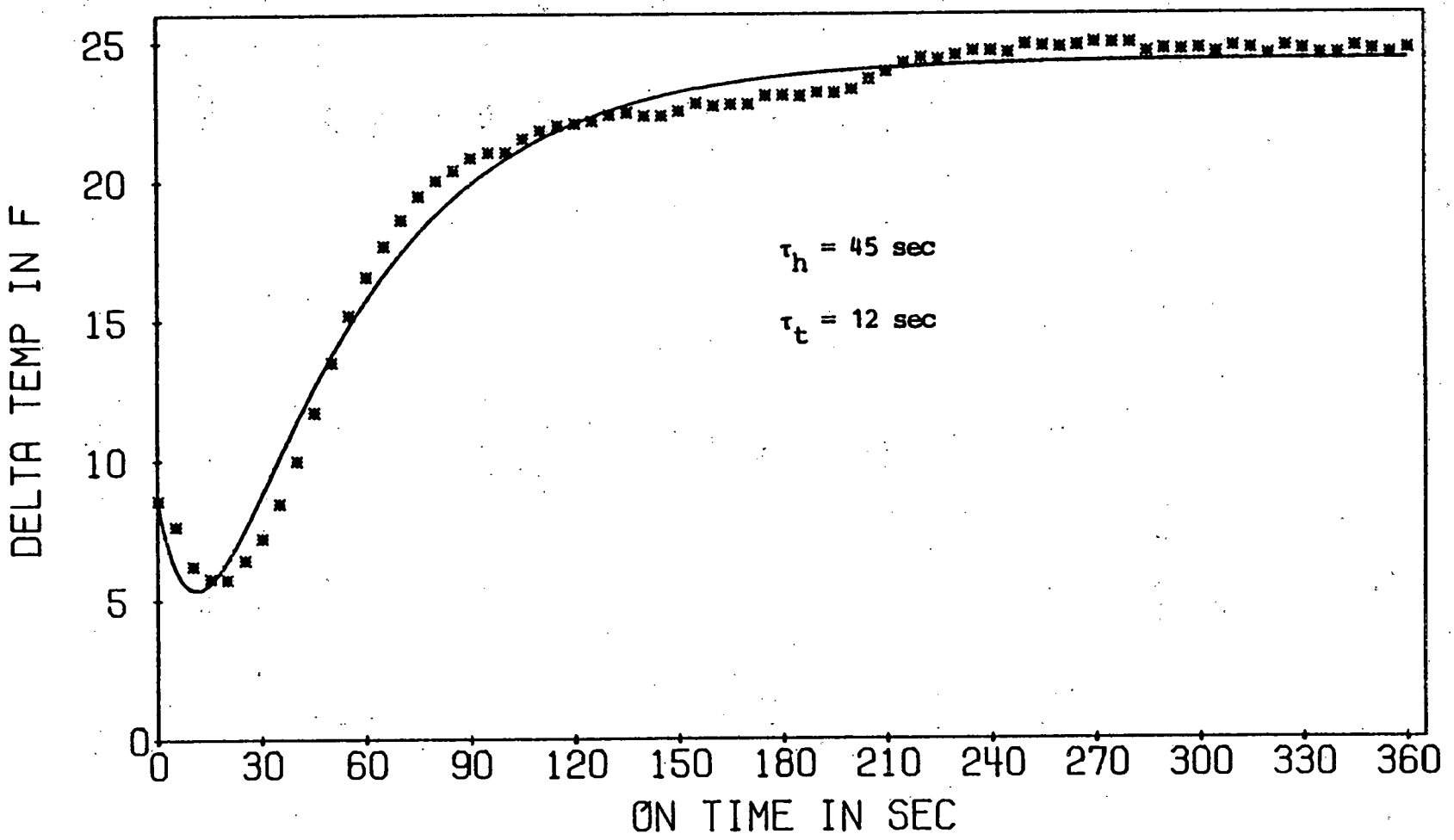

Figure 3H-3 Experimental ΔT vs TIME Curve with Analytical Prediction (Solid Line Curve) - Dampers Used

with a heat exchanger time constant of 45 seconds, a thermocouple response time of 12 seconds, ΔT_o=8.6°F (4.8°C). That this response time is even longer than nine seconds can probably be attributed to the nonuniform velocity distribution over the grid (low velocities increasing the time constant of several thermocouples). This will be discussed in more detail under the sub-heading "Nonuniformity."

In the second test, the dampers were left open during the off-time and the indoor fan ran continuously. Figure 3H-4 is a plot of the on-time data taken during this second test. As can be seen, ΔT_o=0 at t= 0, and the data points rise to a steady state value of approximately 24.5°F (13.6°C). The solid line represents the same analytical curve as in Figure 3H-3 except that T_o=80°F (26.7°C) in Eq. 3F-1. Again, this curve indicates that the grid has a response time of approximately 12 seconds.

Grid Placement

As was seen in Section E, the effect on measured capacity resulting from grid placement occurs because of thermal mass effects and heat transfer through the duct walls. In order to calculate the thermal mass effect, an average initial and an average final temperature of the mass is needed. To calculate an upper bound on heat transfer through the walls, the amount of insulation and composition of the wall are needed.

In order to consider these effects, the original test set-up was slightly modified (recall that this set-up had

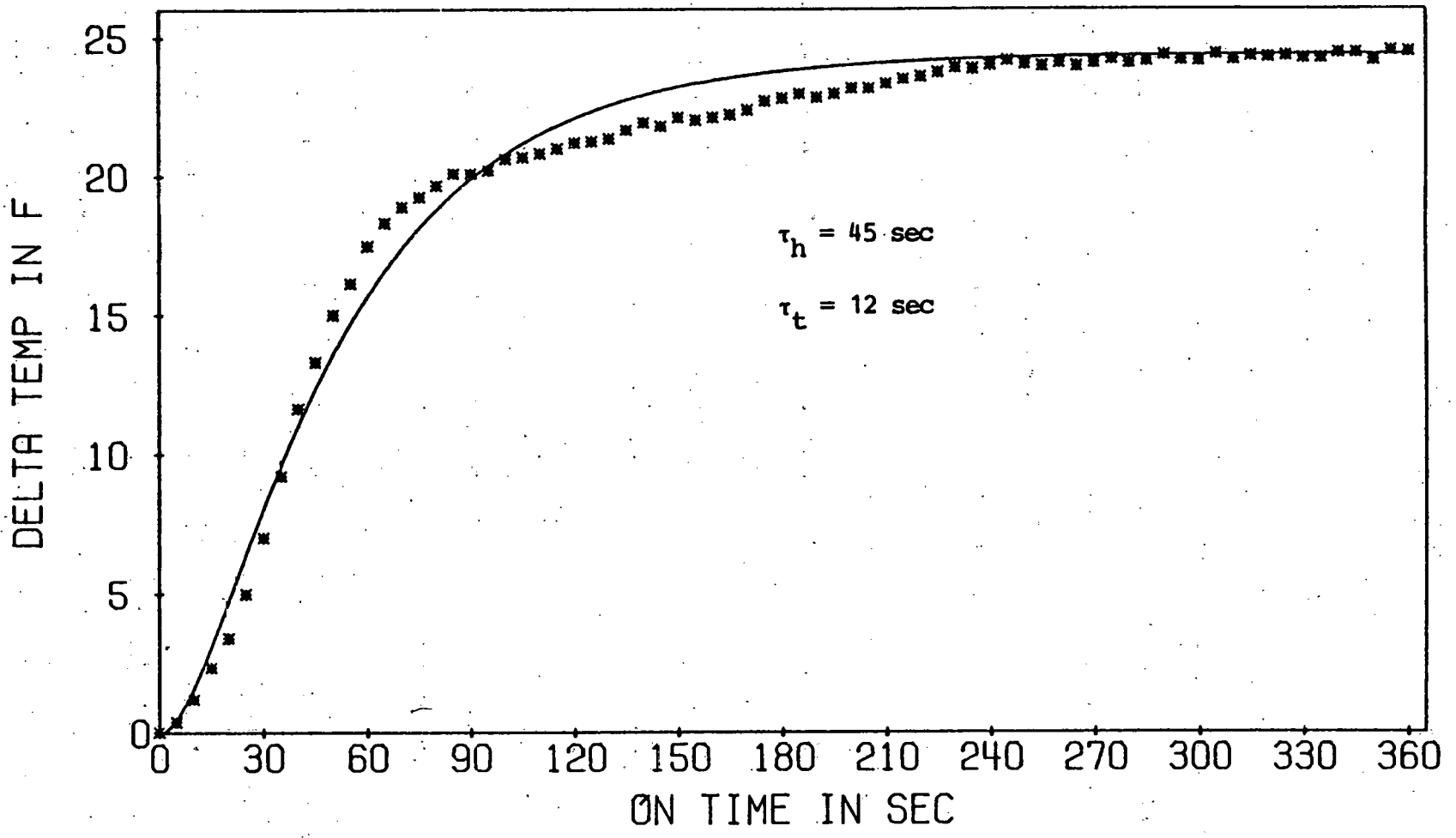

Figure 3H-4 Experimental ΔT vs TIME Curve with Analytical Prediction (Solid Line Curve) - Dampers Not Used

an air trap and little insulation on the dampers). One of the four sheet metal walls that housed the coil was replaced by .25 in. (.006 m) cardboard. This and the two adjacent walls were wrapped with a 1 in. (.025 m) glass wool blanket. The fourth sheet metal wall was insulated with 2 in. (.051 m) of polystyrene insulation. Thermocouples were placed directly on the inside of the walls and on the outside of the insulation, each covered by a 1 $in.^2$ ($6.5 \times 10^{-4} m^2$) of 1 in. thick fiberglass insulation. This set-up, with the thermocouple placement, is shown in Figure 3H-5. These thermocouples were monitored and the results of an approximate 24 minute off - 6 minute on cycle are shown in Figures 3H-6, 7 and 8. The data points are connected by straight lines to help distinguish them.

First, consider Figure 3H-6. These data points represent temperatures on the sheet metal wall covered with 2 in. (.051 m) of polystyrene insulation. The outside thermocouple readings remained fairly constant, varying slightly with room ambient. During the on-time, they dipped about $1^{\circ}F$ ($.6^{\circ}C$). The inside readings stayed about $2\text{-}3^{\circ}F$ ($1.1\text{-}1.7^{\circ}C$) apart while rising during the off-time reaching a maximum value of about $76^{\circ}F$ ($24.4^{\circ}C$). The readings rapidly dropped during the on-time with the lower inside thermocouple reaching a minimum of about $49^{\circ}F$ ($9.4^{\circ}C$). Recall that the average steady state value for this coil is approximately $54^{\circ}F$ ($12.2^{\circ}C$). This indicates a nonuniform temperature distribution over the coil.

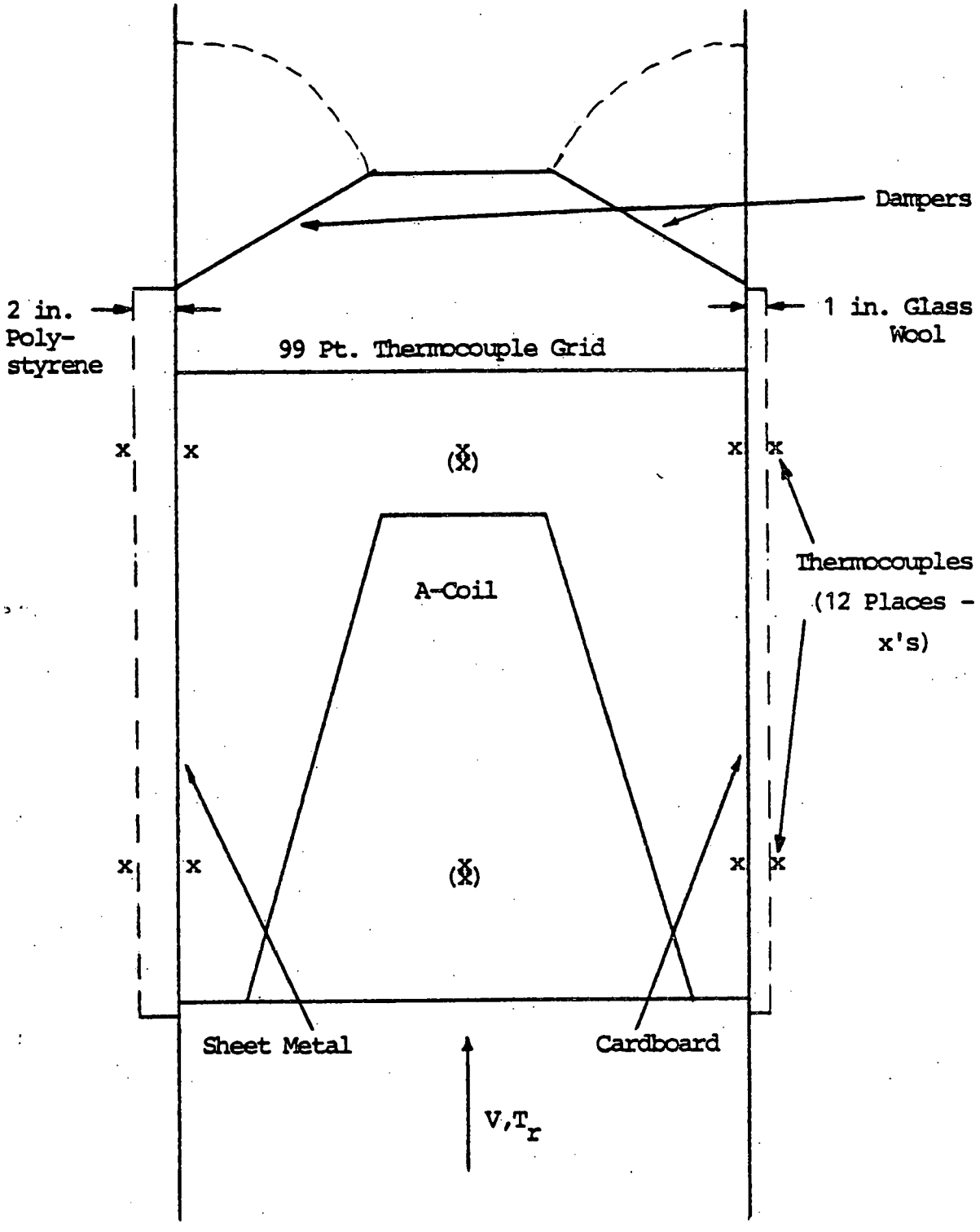

Figure 3H-5 Test Tunnel and Thermocouple Placement

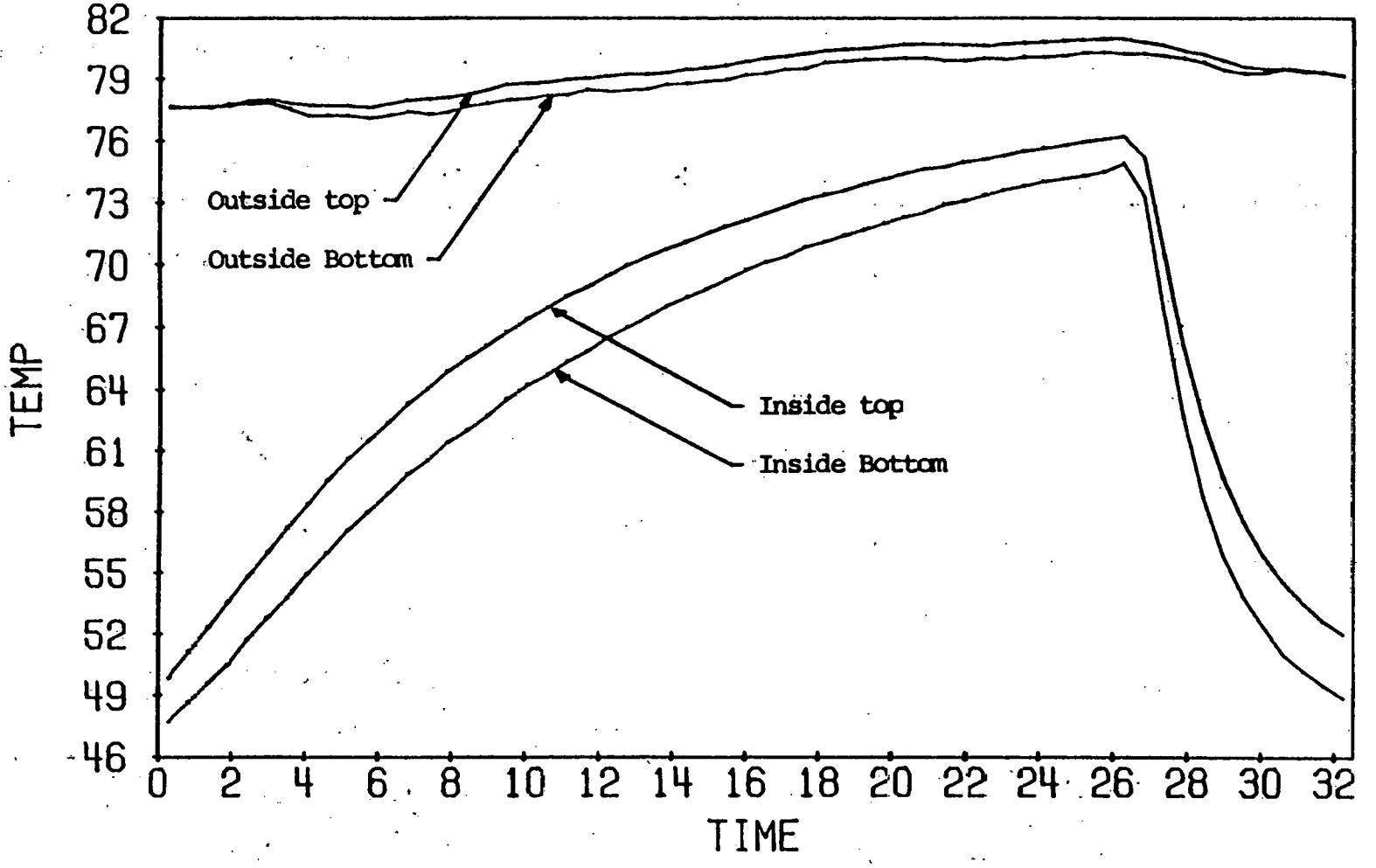

Figure 3H-6 Temperature vs TIME Curves - Metal Wall with Polystyrene Insulation

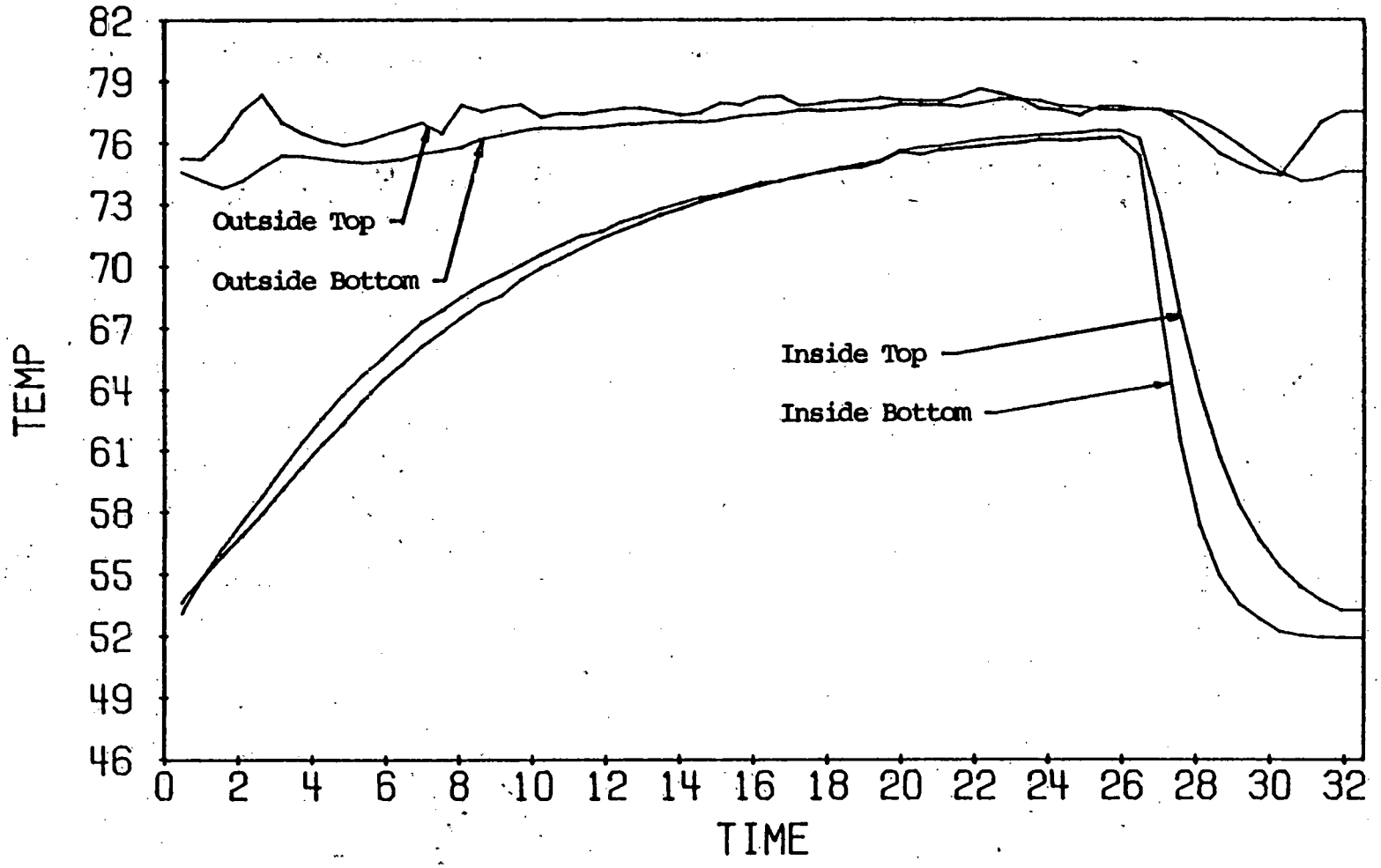

Figure 3H-7 Temperature vs TIME Curves - Cardboard Wall with Glass Wool Insulation

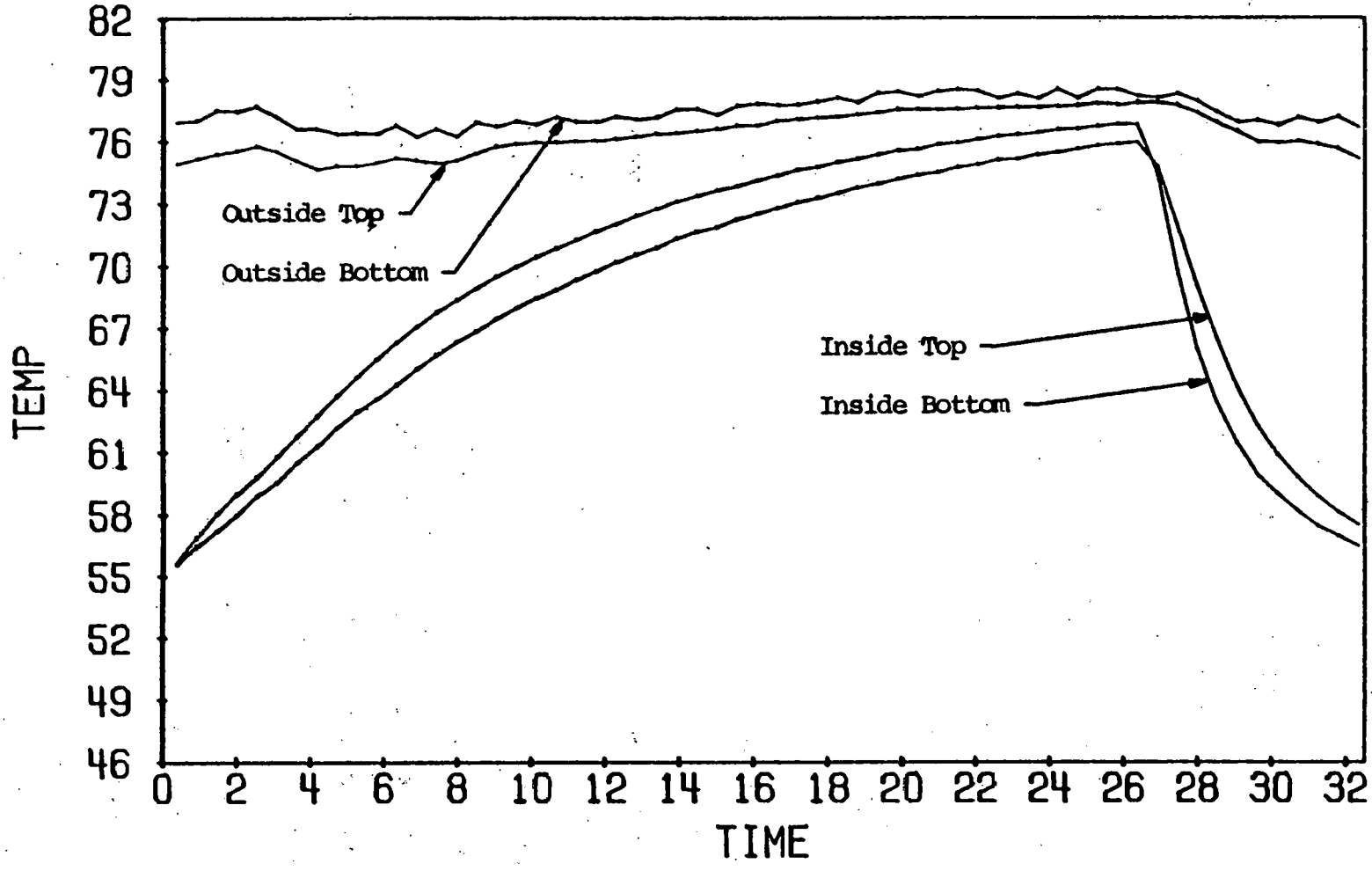

Figure 3H-8 Temperature vs TIME Curves - Metal Wall with Glass Wool Insulation

The fact that the two inside readings remain about 3°F (1.7°C) apart may be due to velocity effects. Finally, the fact that the inside temperatures are so low suggests good insulation since the heat transfer through the wall is effectively stopped. This also means that thermal mass effects are probably maximized.

Figure 3H-7 shows the temperature measurements on the cardboard covered with a 1 in. (.025 m) fiberglass blanket. The top curve represents readings by the top outside thermocouple which was bent .5 in. (.01 m) into the ambient. Its readings are rather erratic due to changing air currents and temperatures around the testing tunnel. The inside readings are similar to those in Figure 3H-6 except that they reach a low value of 52°F (11.1°C).

Figure 3H-8 shows the temperature measurements on the sheet metal wall covered by the glass wool jacket. Recall that the finned sides of the coil do not face this wall, which means that this wall probably does not "feel" the same velocity effects as the other two walls. As can be seen, the readings do not drop as rapidly during the on-time as the other two walls and the low temperature reading is about 57°F (13.9°C). This temperature is also a reflection of higher heat transfer through the wall due to less insulation than the other two walls.

As was seen in Figure 3H-1, this test set-up has a large air mixer which weighs about 40 pounds (18.1 kg).

The mixer was not monitored for temperature but the temperature of the air that had passed through the mixer was. Figure 3H-9 is a ΔT vs TIME plot of this response. The mixer has a large effect in delaying the temperature response. At the end of six minutes of on-time, steady state has not been achieved since the temperature difference is about $21^{\circ}F$ ($11.7^{\circ}C$) instead of $24.5^{\circ}F$ ($13.6^{\circ}C$). It is obvious that if these temperature difference readings were used in the calculation of capacity and the effect of the mixer was not accounted for, a very large error would result. This will be discussed later.

Dampers

The effect of the dampers on the ΔT vs TIME curve was shown in Figure 3H-3. As can be seen, the temperature difference did not start at zero but at $8.6^{\circ}F$ ($4.8^{\circ}C$). The second effect is the initial dip in the data points which is caused by a "cold" thermocouple junction responding to the initial slug of warm room air before the heat exchanger begins to cool the air. These effects will be discussed later.

Nonuniformity

Several measurements were taken to try and determine the extent of the nonuniform temperature and velocity distributions over the cross section where the thermocouple grid was placed. The temperature distribution was examined by constructing a 99 point thermocouple grid.

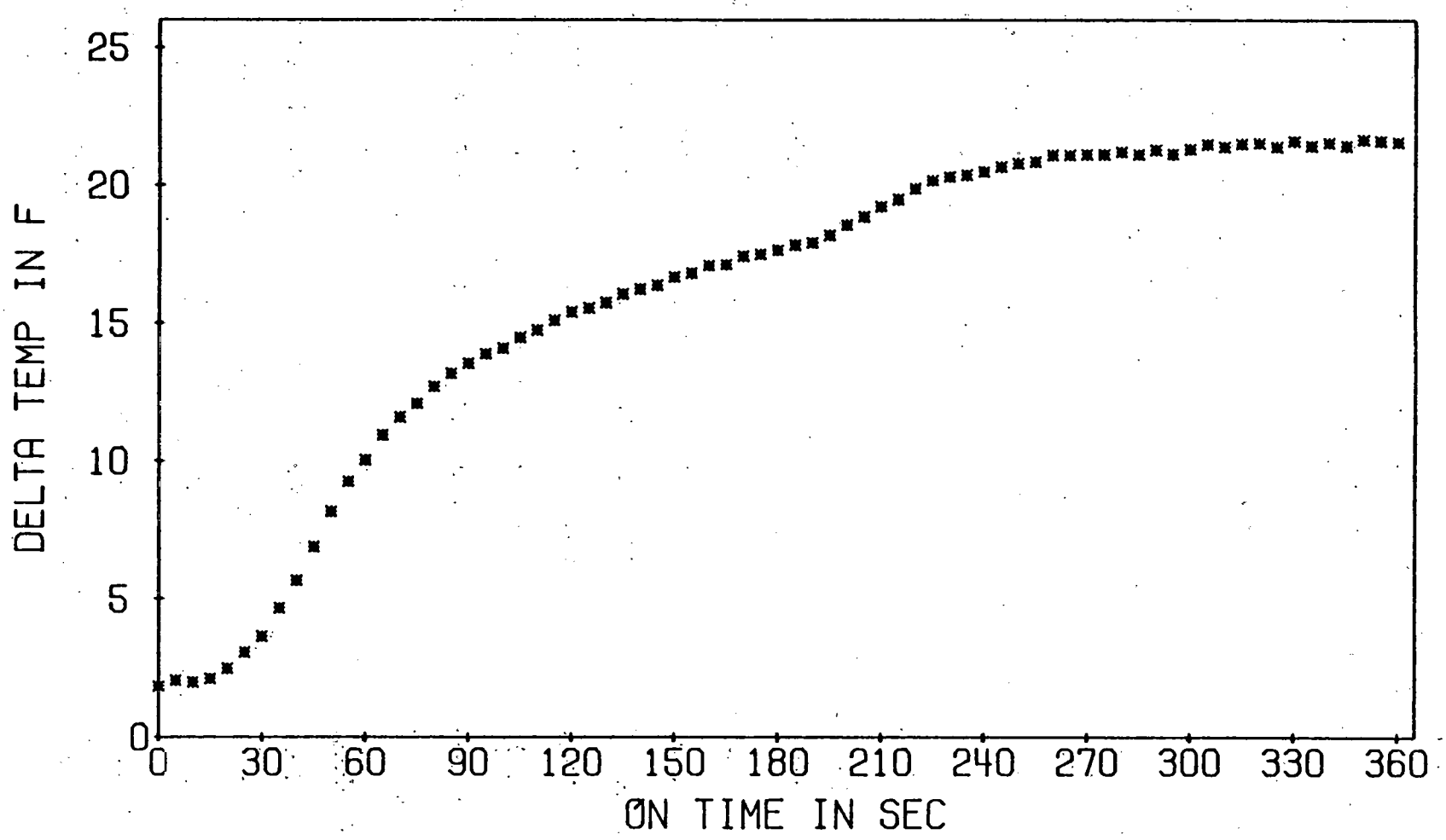

Figure 3H-9 Temperature vs TIME Curve - 9 Point Grid Behind Mixer

Groups of thermocouples were connected in parallel so that four groups could be monitored at the same time. These groups are shown in Figure 3H-10 where the dotted line represents the position of the A-coil. During the subsequent tests, the grid was approximately 6 in. (.15 m) from the top of the coil. Recall that during testing, the average steady state temperature for this coil was about 54°F (12.2°C).

Figure 3H-11 shows the results of an approximate 24 minute off - 6 minute on test. It can be seen that group 1, the outer ring of thermocouples, begins at about 51°F (10.6°C) while the other three groups begin at about 58°F (14.4°C). During the off-time, all four groups reach a maximum temperature of about 77°F (25°C). (This roughly corresponds to ΔT_o=3°F (1.7°C).) At start-up, group 1 rapidly drops to a steady state value of 51°F (10.6°C) while the other groups respond more slowly until reaching a final value of about 58°F (14.4°C). Figure 3H-12 shows a similar set of data in the form of a ΔT vs TIME curve for the six minutes of on-time. These plots clearly show a wide variety of air temperatures coming from the coil.

Another test was made where the 99 point grid was divided into nine columns of eleven thermocouples each. The temperature of each column was measured at the end of a steady state run. After a three minute off-time, the unit was turned on and the temperature was measured after

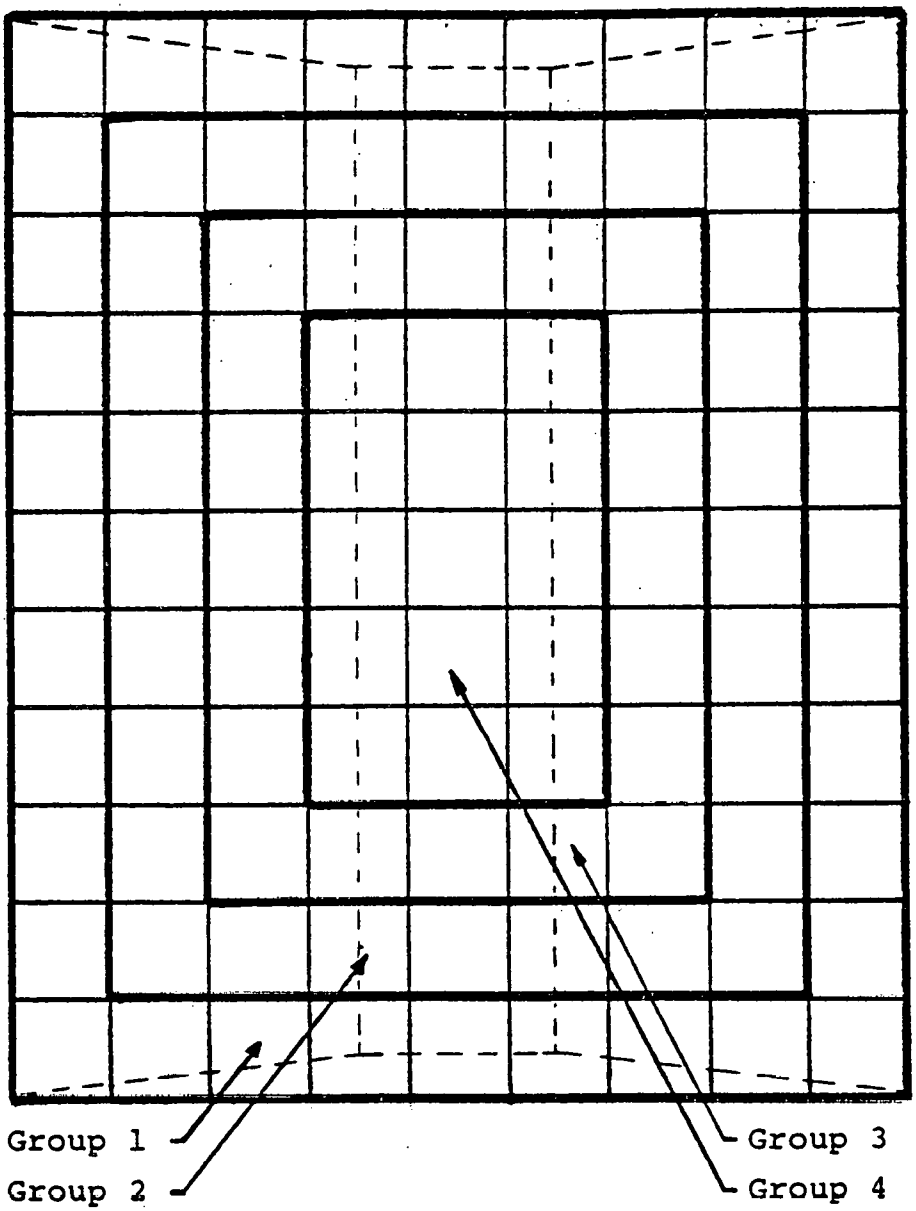

Figure 3H-10 99 Point Thermocouple Grid with 4 Groups

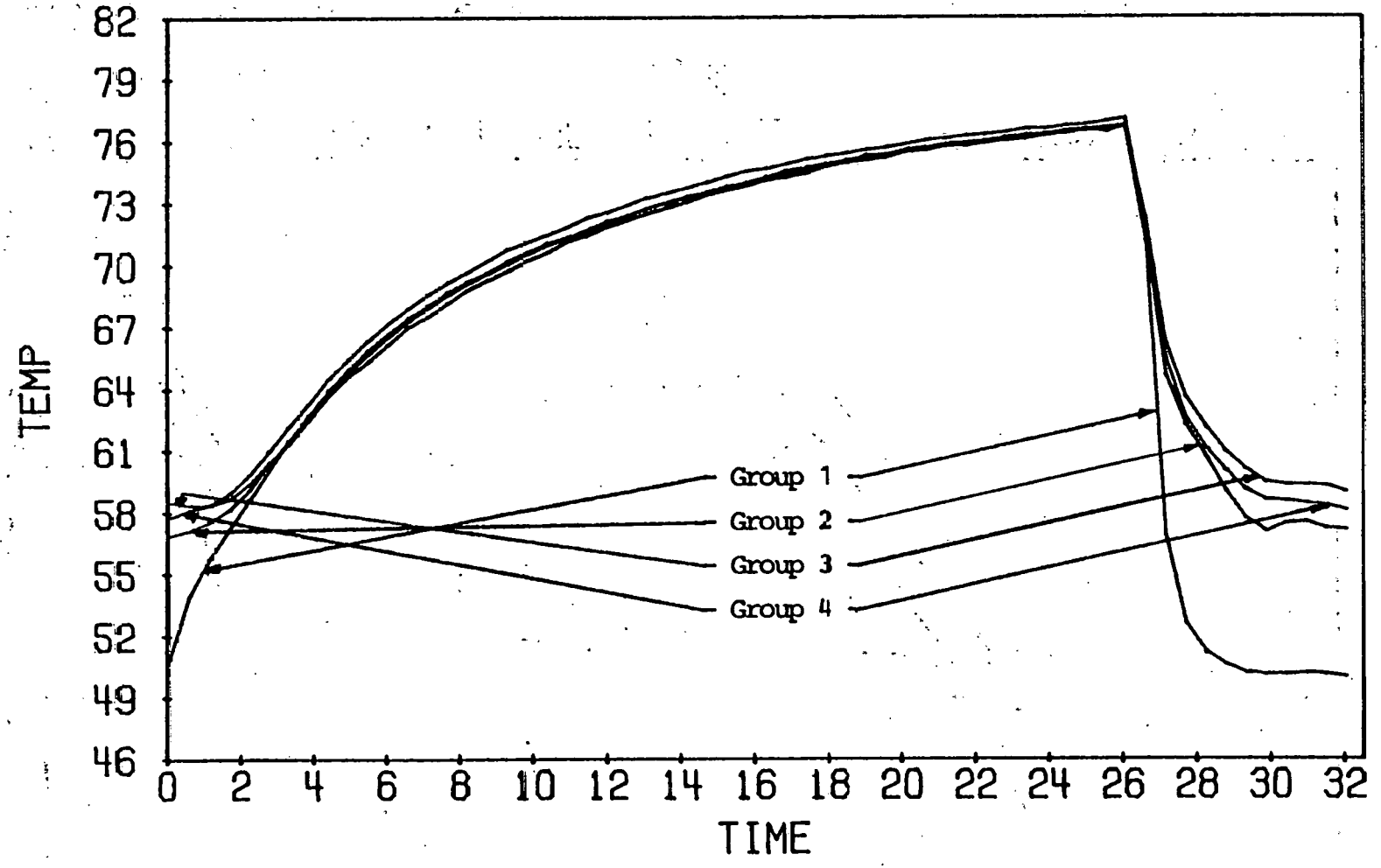

Figure 3H-11 Temperature vs TIME Curves - 4 Groups

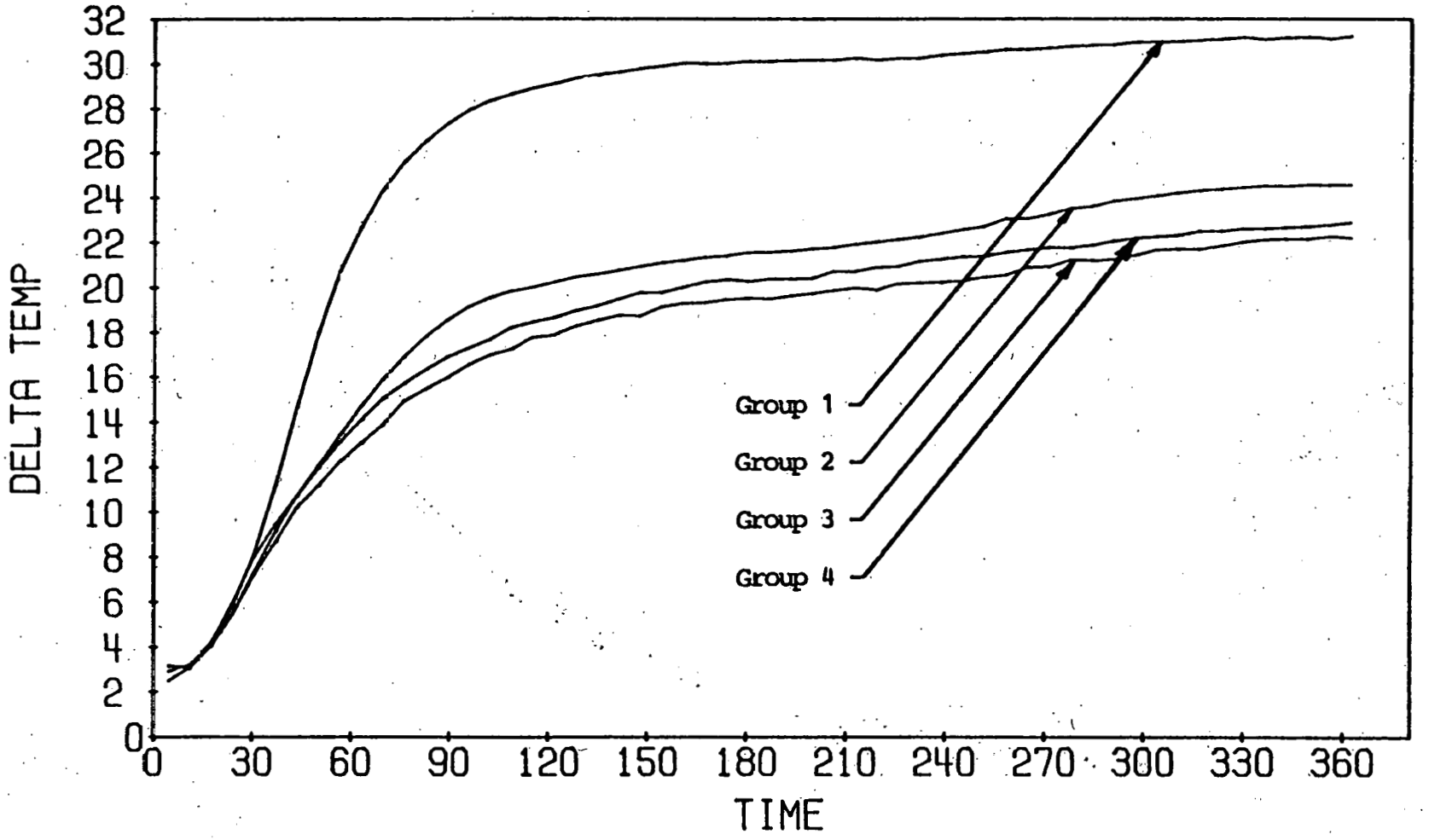

Figure 3H-12 ΔT vs TIME Curves - 4 Groups

about 2½ minutes. These results are shown in Figure 3H-13. Note again the variety of temperatures that exist over the cross section.

The author did not take the velocity measurements; they were supplied to him. They were made apart from the actual test chamber. A cardboard duct was constructed around the A-coil and a large fan was placed several feet behind the coil. A hand-held anemometer was used to measure velocities over the cross-section, at locations approximately 6 in. (.15 m) from the top of the coil. Later, a pitot tube was used to make the same measurements. Three fan speeds were used, 1000, 880 and 650 cfm. This arrangement is sketched in Figure 3H-14. The dotted lines indicate the position of the A-coil in the duct and the solid lines over the cross section indicate the area blocks over which the velocity measurements were made.

Qualitatively, all three fan speeds gave the same distribution. Figure 3H-15 shows the distribution measured with a fan speed of 880 cfm which corresponds to the air flow during actual testing. The number in each block represents the average measured velocity. Note that there are several areas with zero velocity. In these areas, the velocity was so low that the anemometer did not respond and the pitot tube measured negative pressures, indicating possible back flows.

However, this distribution must be considered with caution. Since the velocity measurements were taken

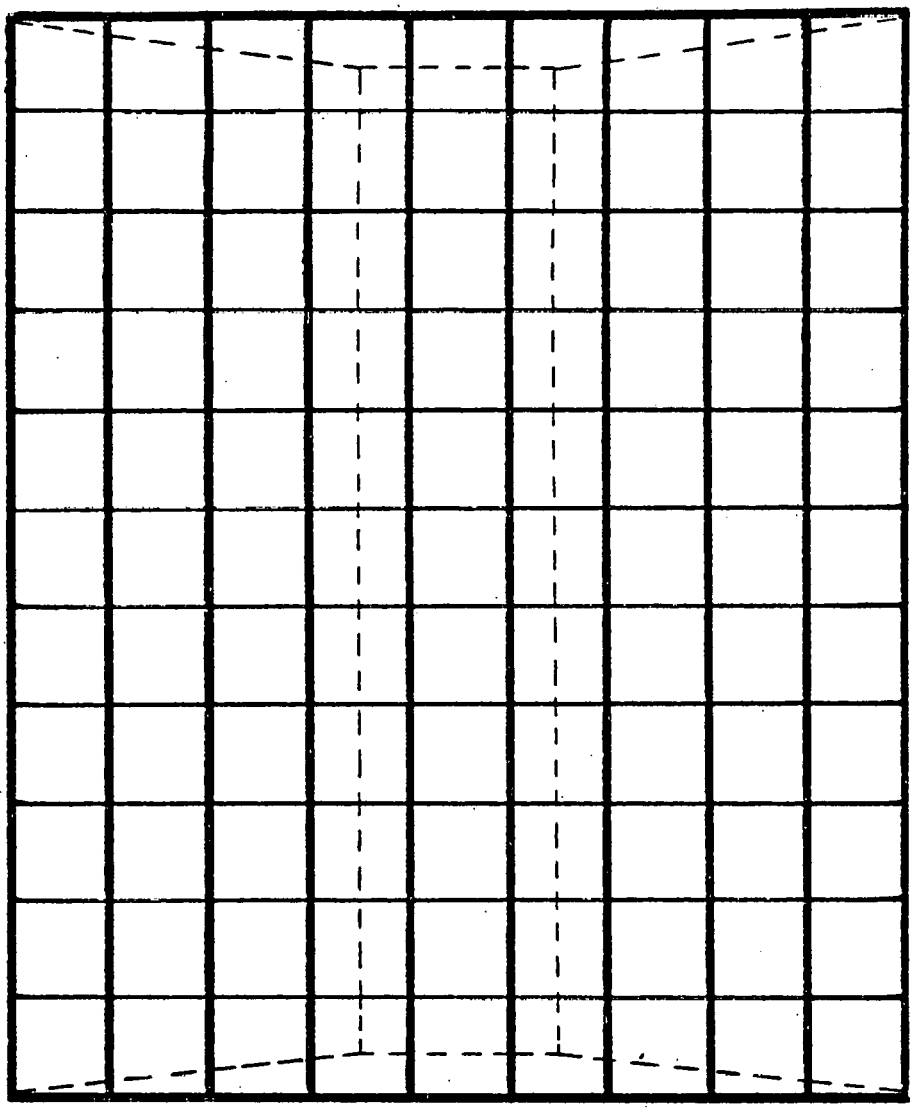

9 Columns of Thermocouples

53.5	51.9	53.7	54.1	54.3	54.0	54.7	53.5	52.2

Temperatures After Steady State

53.9	51.9	57.2	56.3	54.8	54.7	57.5	54.2	51.2

Temperatures After 2.5 Min. of On-Time

Figure 3H-13 9 Column Thermocouple Grid and Results

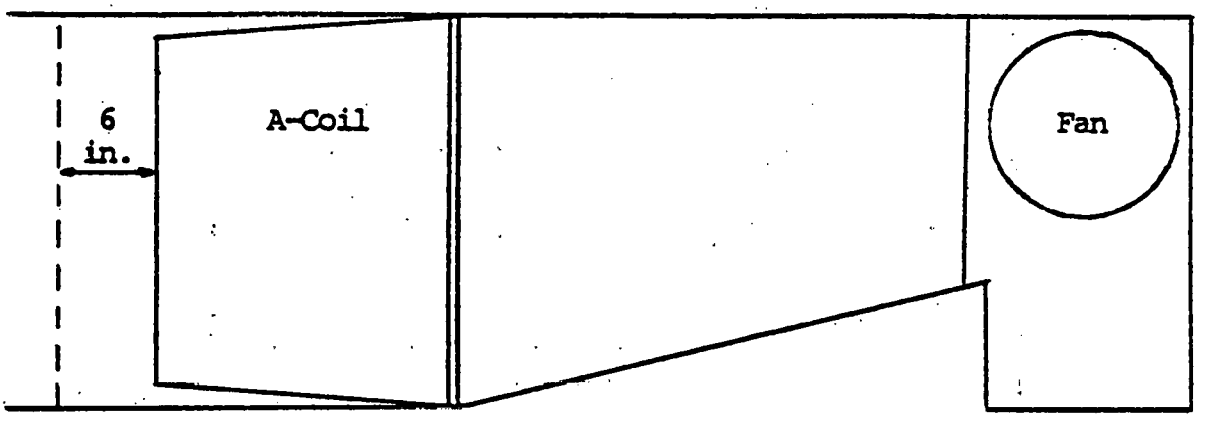

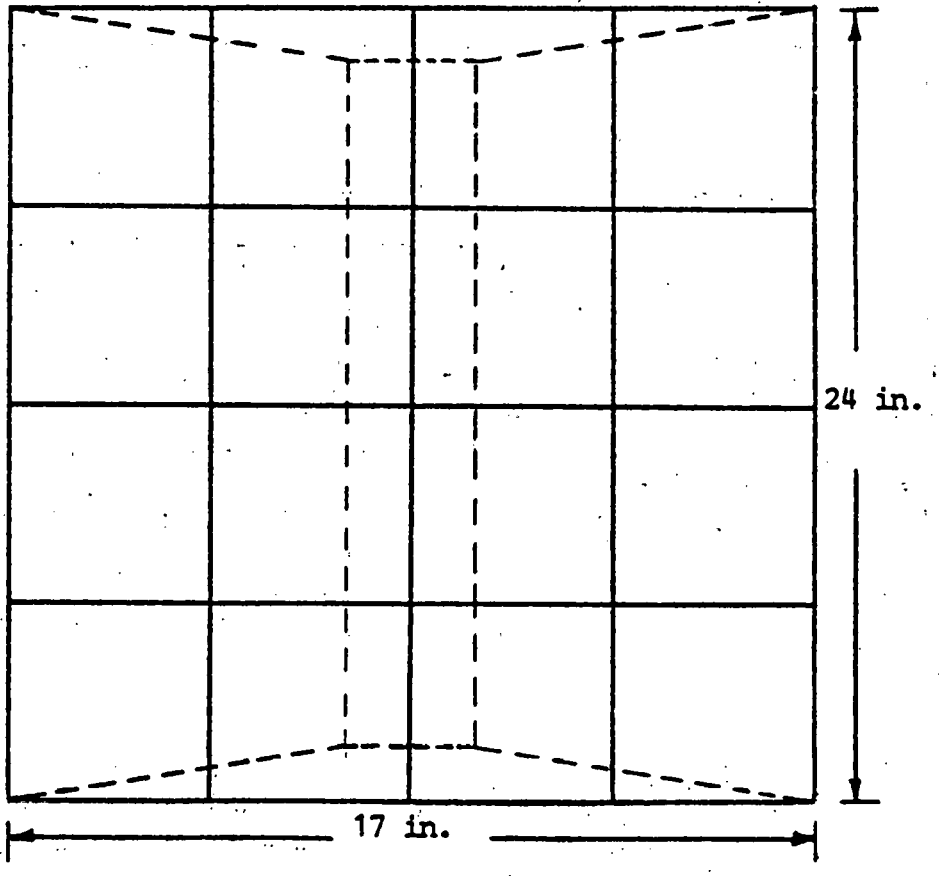

Figure 3H-14 Velocity Measurement Arrangement

9.7	6.7	3.9	11.5
10.8	0.0	0.0	11.0
11.0	0.0	0.0	10.0
8.6	6.3	3.0	5.8

Fan Speed = 880 cfm[2]

Figure 3H-15 Average Velocities over Cross Section (ft/sec)

2- The sum of the product of the average block velocities and the corresponding areas is 1044 cfm, which is greater than 880 cfm. This could be due to undetected back flow.

apart from the actual testing tunnel and with a different fan and duct configuration, this distribution probably will not be the same as that found in the testing tunnel. Nevertheless, this distribution could be representative of some test installation and clearly shows that a nonuniform velocity distribution could be encountered during testing. Furthermore, because of the long thermocouple grid response time discussed earlier, areas of low velocity are suspected. Hence, the distribution in Figure 3H-15 may not be too unrealistic.

Accounting

This last part of Section H will compare four ways of measuring the capacity of the A-coil. If a perfect accounting of all energy involved could be made, a single value for capacity would emerge. However, the time and equipment necessary to obtain sufficient data for such an accounting make the attempt unreasonable. The purpose of the following accounting is to illustrate several of the ideas presented in this work and to emphasize the need to eliminate as many of the errors as possible rather than to try to account for all of them.

Recall Figures 3H-3 and 4. The solid line curve in these plots represents analytically derived curves that fit the measured data reasonably well. These curves have a thermocouple response time of 12 seconds and a heat exchanger time constant of 45 sec. with $\Delta T_o = 8.6^{\circ}F$ ($4.8^{\circ}C$)

and $0^{\circ}F$ ($0^{\circ}C$) respectively. If the thermocouples would have had perfect responses, the solid line curve in Figures 3H-16 and 17 would have resulted and could have been used to calculate the capacity. Finding the area under this solid line curve will be the first approach at calculating capacity.

Both of the curves in Figures 3H-16 and 17 already reflect the effect of the energy added by the compartment walls which raised the air temperature slightly. If this energy is accounted for and added to the predicted capacity (area under curve in Figure 3H-16), the result will be an estimate of the actual capacity.

Capacity (area under predicted curve, τ_t=0 sec)	2058 Btu (603 Whr)
Thermal storage (12.7 ft^2 of wall at 1.2 lbm/ft^2, estimated average $\overline{\Delta T}$=24°F)	40 Btu (12 Whr)
Heat transfer (U=.12 Btu/ft^2 hr °F, $\overline{\Delta T}$=24°F)	4 Btu (1 Whr)
Total	2102 Btu (616 Whr)

For the second method, consider the data points in Figure 3H-16. Using numerical integration to find the area under the curve, these data points represent a measured capacity of 2014 Btu (591 Whr). The effect of the cold coil at start-up is reflected in this number. To account for thermocouple response error, it will be assumed that this error is the same as that between the analytical curves in Figure 3H-3 and 16, τ_t=12 and 0 seconds respectively. This

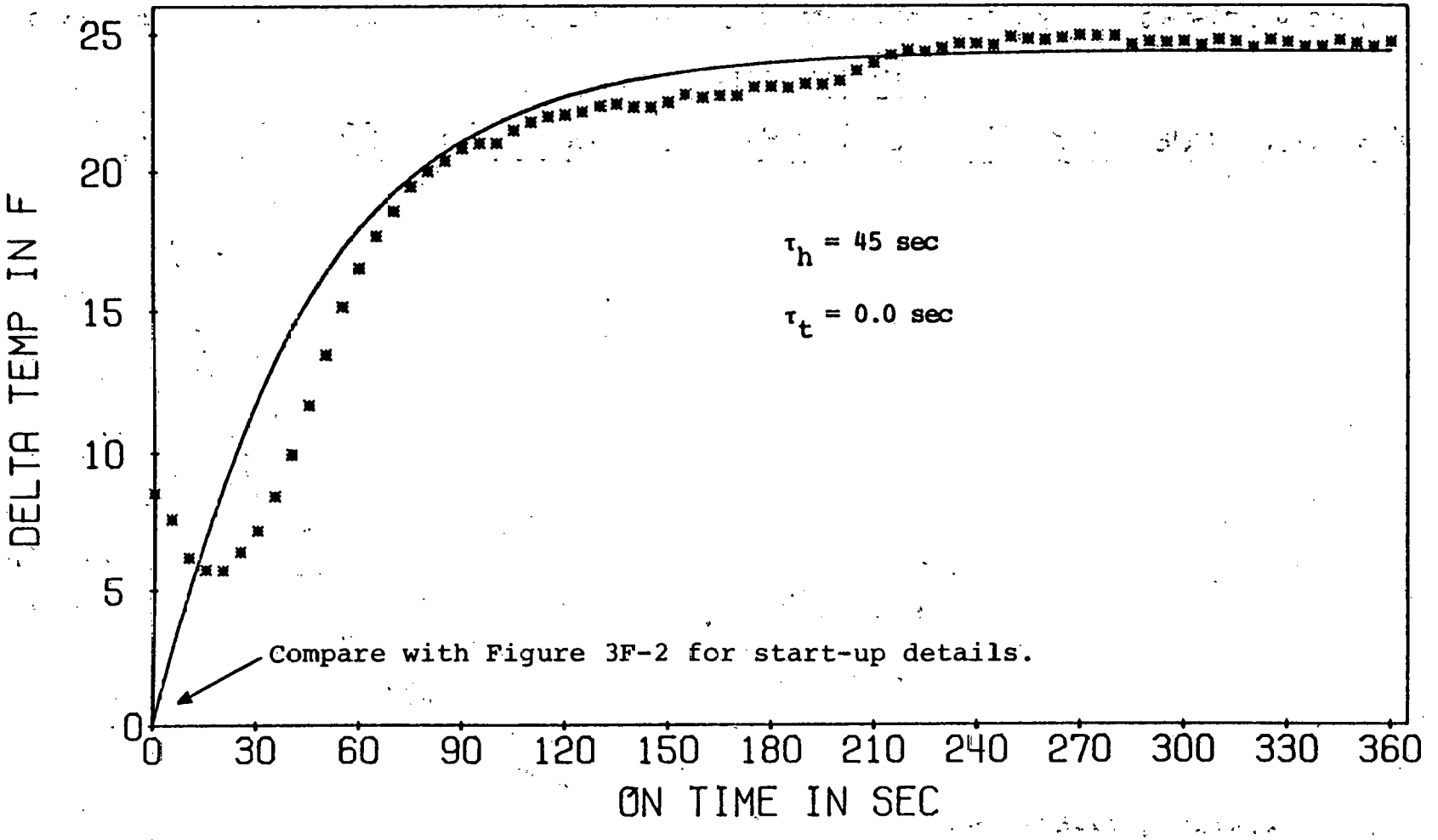

Figure 3H-16 Experimental ΔT vs TIME Curve with Ideal Analytical Prediction - Dampers Used

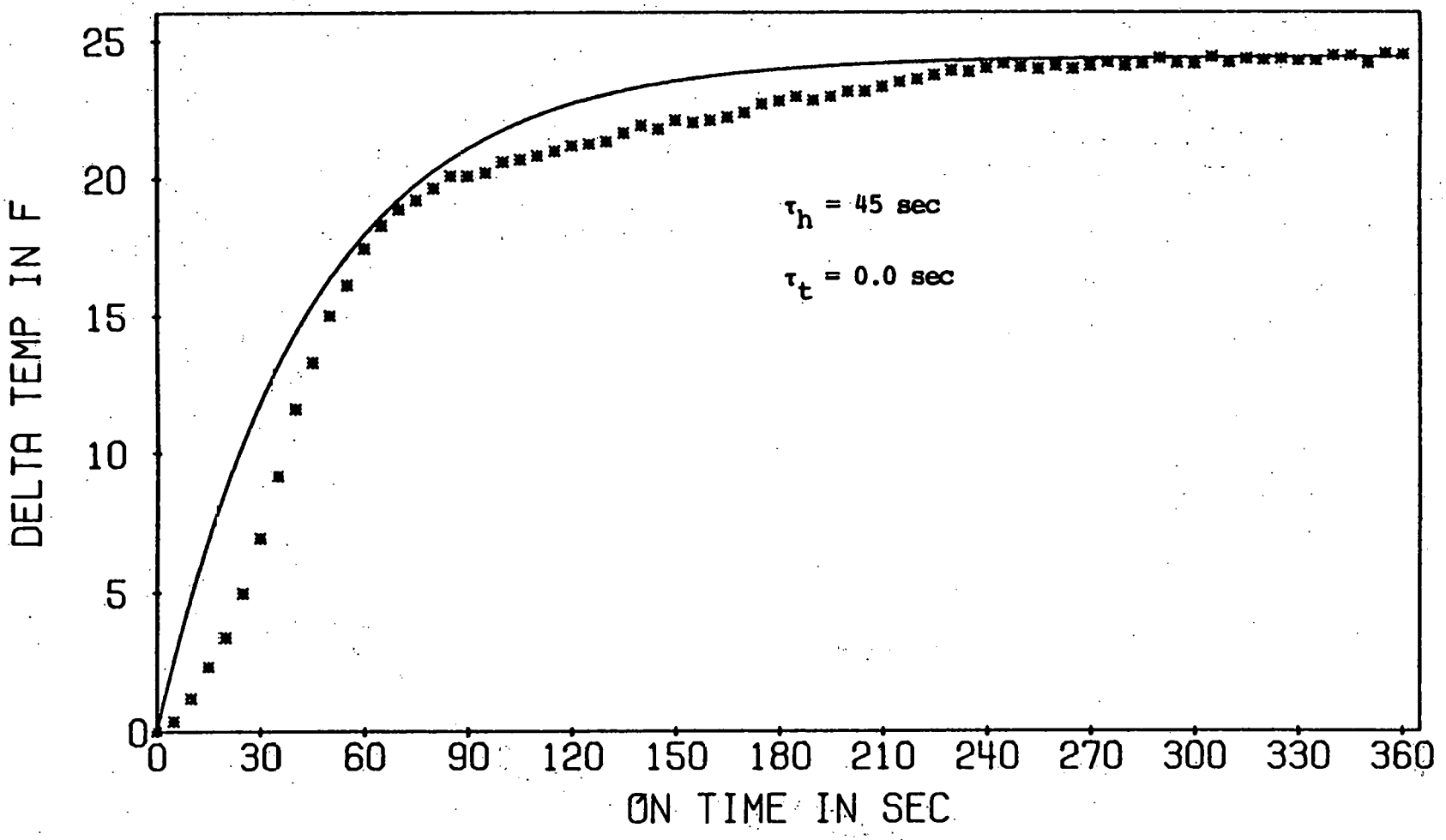

Figure 3H-17 Experimental ΔT vs TIME Curve with Ideal Analytical Prediction - Dampers Not Used

turns out to be about 2.4% ($\frac{2058 - 2008}{2058} \times 100 = 2.4\%$). Since the dampers kept the compartment walls at about 72°F (22.2°C) at start-up, and the assumed average final temperature is 55°F (12.8°C), $\overline{\Delta T}$ = 17°F (9.4°C) exists for calculating thermal storage effects.

Capacity (area under experimental curve)	2014 Btu (591 Whr)
Thermocouple error (2.4% of 2014 Btu)	48 Btu (14 Whr)
Thermal Storage ($\overline{\Delta T}$=17°F)	29 Btu (9 Whr)
Heat transfer (U=.12, $\overline{\Delta T}$=24°F)	4 Btu (1 Whr)
Total	2095 Btu (615 Whr)

For the third method, the test run where the dampers are left open during the entire cycle is used. Using numerical integration with the data points of Figure 3H-17, a measured capacity of 1951 Btu (572 Whr) is found. Thermocouple response error is found in the same way as the second method, using the analytical curves of Figures 3H-4 and 17. The percent error is about 3.8% ($\frac{2058-1979}{2058} \times 100 = 3.8\%$). As in the first method, $\overline{\Delta T}$ = 24°F (13.3°C) will be assumed.

Capacity (area under experimental curve)	1951 Btu (572 Whr)
Thermocouple error (3.8% of 1951 Btu)	74 Btu (22 Whr)
Thermal Storage ($\overline{\Delta T}$ = 24°F)	40 Btu (12 Whr)
Heat transfer (U=.12, $\overline{\Delta T}$=24°F)	4 Btu (1 Whr)
	2069 Btu (607 Whr)

The values found by these first three methods agree within 1.6% of each other.

As the fourth method, consider the test run where the dampers are used but the temperature readings are made downstream of the mixer. By numerical integration using the data points in Figure 3H-9, a measured capacity of 1546 Btu (453 W hr) results. For thermocouple response error, it will be assumed that the response of the grid is about nine sec , because the velocity distribution should be relatively uniform at this location and the thermocouples were predicted to have this response. From Figure 3D-5, a nine second time constant corresponds to about 3% error. Due to the grid placement, there is considerably more thermal mass. From measurements taken on the test set-up, there are about 36 ft^2 (3.3 m^2) of 24 gage sheet metal and about 10 ft^2 (.9 m^2) of 18 gage sheet metal. It will be assumed that $\overline{\Delta T}$ = 24°F (13.3°C) for the 24 gage sheet metal sections. The wall sections made of 18 gage sheet metal are further downstream and are more massive. Hence, a smaller wall average temperature difference will be encountered, $\overline{\Delta T}$=20°F (11.1°C). The 40 lbm. mixer (18.1 kg) is made mostly of 18 gage sheet metal. It will also be assumed that its $\overline{\Delta T}$=20°F (11.1°C). Within the duct, there are several miscellaneous pieces of steel, mostly related to damper operation. It is estimated that they weigh 15 lbm (6.8 kg) and have $\overline{\Delta T}$=10°F (5.6°C).

Capacity (area under experimental curve)	1546 Btu (453 Whr)
Thermocouple error (3% of 1546 Btu)	46 Btu (13 Whr)

Thermal Storage (36 ft^2 of 24 gage at 1.2 lbm/ft^2 and $\overline{\Delta T}=24^oF$; 10 ft^2 of 18 gage at 2.2 lbm/ft^2 and $\overline{\Delta T}=20^oF$)	163 Btu (48 Whr)
Mixer (40 lbm at $\overline{\Delta T}=20^oF$)	88 Btu (26 Whr)
Miscellaneous metal parts (15 lbm, $\overline{\Delta T}=10^oF$)	17 Btu (5 Whr)
Heat transfer ($U=.12$ $\overline{\Delta T}=24^oF$, $A_s=46$ ft^2)	13 Btu (4 Whr)
Total	1873 Btu (549 Whr)

This value is within 11% of the capacity found by the first method. Consideration of mass transfer (leakage) could reduce this disagreement somewhat if it could be adequately measured. Nevertheless, it appears that an accurate energy accounting is more difficult as temperature is measured further downstream because initial and final temperatures of massive objects, leakage, etc., will be increasingly difficult to estimate without more detailed measurements.

In conclusion, the results in this section have been based on data taken from several test runs made on one coil at one test facility and should be used for trends only. However, these trends tend to support and clarify some of the analytical work done in the previous sections.

The thermocouples used in this testing were believed to have a response time of 2.5 seconds or less. Analytically, their time constant was predicted to be about nine seconds. When the data was analyzed, the grid time constant was found to be about 12 seconds. This immediately introduces an error of about 4% in the capacity measurement.

Grid placement had a significant effect. If the capacity had been computed using the data from the nine point grid behind the mixer, there would have been an error of over 20% compared to a measured capacity based on data from the 99 point grid (2014 Btu vs 1546 Btu). It was also found that 2 in. of polystyrene insulation was quite effective, permitting only about 3 Btu/6 minutes per 10 square feet of surface area to enter the cooler air stream (about .2% of measured capacity).

The dampers had a noticeable effect on the ΔT vs. TIME curve, causing a large dip at the beginning of the on-time. Nevertheless, capacity based on this data was more than 3% higher than the capacity calculated from the data when the dampers were left open.[3]

Finally, very nonuniform velocity and temperature profiles were inferred from measurements. The "dead" spots in the velocity profile probably caused several thermocouples to respond very slowly, lengthening the response time of the entire grid to about 12 seconds. The nonuniform temperature distribution emphasized the possibility of a nine point grid reading individual "hot" and "cold" spots over the cross section and producing unrepresentative temperature measurements.

3- Different refrigerant control could give different results.

CHAPTER IV - CONCLUSIONS AND RECOMMENDATIONS

Section A - The Thermostat

Conclusions

The closed-loop feedback model of a thermostat, proposed by Didion, was studied in Chapter 2. The intent of this study was to examine some of the parameters in the model to determine their influence on the cycling of the system.

It was found that the thermostat is the dominant factor in determining the cycle rate of the system. In particular, it was found that the switch differential and the anticipator temperature rise are the two most important parameters in controlling the cycle rate. The anticipator time constant, the heating plant steady state output and the heating plant time constant are the least important parameters. The time constant of the bimetal element can exert a strong influence on the cycle rate if it ranges to its extreme values. In a typical thermostat, its influence is fixed and it is not a dominant factor.

It was further noted that the on-time of the system tended to be a finite value as percent on-time tended to zero. This indicates that the thermostat is responding to the anticipator and the switch differential, which causes

the equipment to run for a finite amount of time even though the load on the system is tending to zero. This again supports the dominant role of the thermostat in cycling.

As far as the DOE test procedures are concerned, the cycling scheme of test D appears to conform to normal thermostat dynamics and adequately represents field operation.

Recommendations

There are two recommendations to be made. First, a more detailed thermostat model is needed to quantitatively study the effects of thermal mass in the conditioned space, particularly its effect on cycling.

Second, with the advent of solid state thermostats, and even programmable thermostats, various effects such as fixed on-time, no switch differential, perfect anticipation, night set-back, etc. should be studied. It is possible that such thermostats could play an important role in energy conservation and thermal comfort.

Section B - Measurement Errors

Conclusions

The overall conclusion of Chapter 3 is that differences in test set-ups can, indeed, have a significant effect on the measured capacity of a unit. This conclusion is based on the analysis of four areas which are directly affected by the test set-up. The effect of these four areas on measured capacity will be summarized and briefly discussed. It should be remembered that percent errors are found by comparing QMEAS with QIDEAL, and that the numbers and assumptions used in the calculation of

and that the numbers and assumptions used in the calculation of these quantities are not typical of all air conditioners and heat pumps and testing facilities. Nevertheless, they are representative of many test set-ups and do provide a way of examining the effects of these test set-ups on the measured capacity.

Table 4B-1 provides a summary of possible errors in measured capacity. The first column lists the causes of the error while the second column lists a possible range of error due to that cause. The extreme value in each range is an error that could result from some test set-up and , in fact, could be greater under some circumstances. Typically, though, it is expected that the percent error will lie somewhere within the range of values listed. As an example, the third column gives a percent error for each cause that might be encountered in some testing situation.

It was seen in Section D that if a thermocouple has a response time of 2.5 seconds or less, less than 1% error will occur in the measurement of capacity. It was also seen that response time is very dependent on wire diameter and velocity. Therefore, while an individual thermocouple may respond quickly in a known air stream, it is possible that several thermocouples in a grid could respond very slowly due to low velocity areas over a cross section. This could have the effect of slowing the overall response of the grid and could lead to larger errors on the order of 2 - 4%.

As was seen in Section E, grid placement does matter

Table 4B-1 Summary of Possible Errors in Measured Capacity

Cause of Error	Possible Range	Example
Thermocouple Response	<1% - 4%	2%
Lag Time	<1%	0%
Leakage	-1% - 10%	-2%
Heat Transfer	1% - 10%	2%
Thermal Storage	1% - 15%	4%
Dampers	-3% - 1%	0%
Nonuniform Velocity and Temperature Distribution	1% - 15%	5%
Total error for example is about 11% (1)		

1- These errors are related to each other, but are generally additive.

because of the effects of leakage, heat transfer through walls and thermal storage. Under certain circumstances (long, leaky ducts, no insulation and a large air mixer,for example) each of these effects could be quite large. However, by sealing obvious cracks, holes, etc., and by providing some insulation (R-3), leakage and heat transfer effects could be made smaller. Thermal storage effects would still be present and could be accounted for, but an average initial and final temperature would be needed for each massive object and this could be quite impractical. Therefore, errors due to grid placement on the order of 5 - 10% could be typical.

Section F discussed the role of the dampers. It was seen that dampers could magnify the effect of thermocouple response time causing measured temperature to lag actual temperature. This adversely affects the measured capacity. Nevertheless, depending on ΔT_o, measured capacity will generally be enhanced by using dampers. The sum total of the effects of dampers can be quite high (significant insulation and refrigerant control, for example), but it will usually not improve measured capacity by more than 3% nor decrease it by more than 1%.

Section G discussed the effects of nonuniform velocity and temperature distributions. It was seen that if too few measurements are made, the chances of measuring an extreme value of temperature or velocity are high. This could distort the measured capacity as much as 15% or more. By

mixing the air before it is sensed, more reliable results will be obtained, with errors of 5 - 10% or less, depending on the quality of the mixing.

Recommendations

The overall recommendation of Chapter 3 is to make changes in the governing standards to reflect the special needs of transient testing and to make changes in the test procedures so that testing might go more smoothly. More specific recommendations will follow. It is hoped that the end result of these recommendations will be a revised test procedure that will allow the air conditioning industry to obtain more meaningful and reproducible results with a minimum of confusion and cost.

Thermocouple Response Recommendations

1. Thermocouple response time should be found in air that has a velocity representative of the air flow it will be sensing. 30 AWG wire is recommended for thermocouples and the junction should be soft soldered with as small a bead as possible.

2. The entire thermocouple grid should be tested to insure that its response time is 2.5 seconds or less.

Grid Placement Recommendations

1. The test set-up should be insulated and sealed to eliminate heat transfer and leakage. Insulation of R-7 or more is recommended.

2. Thermal mass problems should be eliminated. Duct walls could be made of a low mass, poor thermal conducting

material such as cardboard, rigid foam, fiberglass, etc. In fact, sheet metal could be used with the insulation on the inside.

3. Massive objects such as mixers could be made of plastic, fiberglass,etc., to reduce thermal mass problems.

4. Grid placement should be as close to the coil as possible, allowing for a mixer.

Damper Recommendations

1. If dampers are retained in the test procedures, their intent, installation and operation should be more clearly defined so that their function may be uniform throughout the industry. The above recommendations regarding grid placement should be followed, i.e., insulation, low thermal mass, etc.

2. If dampers are retained, it is recommended that more study be made on refrigerant dynamics, both during the on-time and the off-time. It is important that the relationship between dampers and refrigerant control be understood.

3. It is recommended that dampers be eliminated, and that the indoor fan run continuously during the off-time to insure that all tests begin with $\Delta T_o = 0$. Credit for off-time cooling should be given by continuing to monitor the ΔT vs TIME curve until $\Delta T = 0$ (or some increment close to 0). Subtract the power consumed by the fan during the off-time.

If dampers are eliminated and ΔT is monitored for the complete cycle, the problems of thermal storage are also eliminated, greatly simplifying the test set-up.

Nonuniformity Recommendations

1. A good air mixer should be used to avoid thermocouple response problems.

2. A large thermocouple grid could be used to electronically mix the nonuniform temperature distribution and yield a more accurate average temperature. But, as mentioned before, overall response problems need to be remembered.

General Recommendations

1. The monitoring of the ΔT vs TIME curve and its integration should begin when the unit is turned on and not 10-15 seconds later. If all tests begin at $\Delta T_o=0$, the same starting point will be guaranteed.

2. The effects of a fluctuating indoor and outdoor ambient on the measured capacity should be studied. It would be worthwhile to know how close to specification the indoor and outdoor temperatures need to be held in order to maintain an accurate measurement of capacity.

3. Additional work is recommended to find practical ways to account for differences in test installations as discussed in this work. This would allow a unit to be tested in two different test set-ups and the results be corrected to yield a single measure of capacity.

LIST OF REFERENCES

Air Conditioning and Refrigeration Institute (ARI), "Standard for Unitary Air Conditioning Equipment," Standard 210, 1979.

American Society of Heating, Refrigeration and Air Conditioning Engineers (ASHRAE), "Method of Testing for Rating Unitary Air Conditioning and Heat Pump Equipment," Standard 37-78, 1978.

Personal communication with R. Anderson and S. McGill, Heil Quaker Co., September 9, 1980.

Anderson, V. R. and Tobias, J. R., "Comfort Control for Central Electric Heating Systems," IEEE Transactions on Industry Applications, Vol. IA-10, No. 6, November/December, 1974.

Arpaci, V. S., Conduction Heat Transfer, Reading, Mass., Addison-Wesley Publishing Co., 1966.

ASHRAE Fundamentals 1977, ASHRAE, New York, New York, 1977.

Beckwith, T. G. and Buck,N. L., Mechanical Mesurements, Reading, Mass.,1961.

Cape, R. C. and Tull, R. H., "Test-room Performance of Low-voltage Thermostats," IEEE Transactions on Industry and General Applications, Vol. IGA-5, No. 3, May/June 1969.

Colborne, W. G., "Performance of Intermittently-fired Oil Furnaces," ASHRAE Transactions, Vol. 63, No. 1613, 1957.

Department of Energy Workshops, Purdue University, August 15, 16, 1980.

Personal communication with David Didion, National Bureau of Standards, Sept. 5, 1980 - A.

Personal communication with David Didion, National Bureau of Standards, Aug. 16, 1980 - B.

Didion, D., "Low Voltage Room Thermostat Evaluations," (an unpublished draft), National Bureau of Standards, September, 1978.

Doebelin, E. O., Measurement Systems - Application and Design, McGraw-Hill Book Company, New York, New York, 1975.

Federal Register, Thursday, December 27, 1979, pp. 76700-76723.

Gable, G. K. and Koenig, K., "Seasonal Operating Performance of a Gas Heating System with Certain Energy Saving Features," ASHRAE Transactions, Vol. 83, Part 1, 1977.

Goldschmidt, V. W. and Murphy, W. E., "Transient Performance of Air Conditioners," ASHRAE Transactions, 1979.

Hart, G. H., "The Performance of the Air Distribution System and of an Air-to-Air Heat Pump, in the Heating Mode," Master's Thesis, Purdue University, West Lafayette, Indiana, 1978. (Also published as Herrick Laboratories Report HL 78-58)

Hise, E. C. and Holman, A.S., "Heat Balance and Efficieny Measurements of Central, Forced Air, Residential Gas Furnaces," ASHRAE Transactions, Vol. 83, Part 1, 1977.

Holman, J. P., Experimental Methods for Engineers, McGraw-Hill Book Company, New York, New York, 1966.

Johnson, N. R., Weinstein, A. S. and Osterle, F., "The Influence of Gradient Temperature Fields on Thermocouple Measurements," ASME Paper No. 57-HT-18, 1957.

Kelly, G. E. and Parken, W. H., "Method of Testing, Rating and Estimating the Seasonal Performance of Central Air Conditioners and Heat Pumps Operating in the Cooling Mode," National Bureau Standards, NBSIR 77-1271, April, 1978.

Kreith, F., Principles of Heat Transfer, Third Edition, New York, New York, Intext Press, Inc., 1973.

Kuelhert, H. F., "Development of Performance Testing Procedures for Evaluation of Room-size Electrically Heated Thermal Energy Storage Units," Master's Thesis, Purdue University, West Lafayette, Indiana, 1980.

McAdams, W. H., Heat Transmission, New York, New York, McGraw-Hill Co., 1954.

McBride, M. F., Dynamic Modeling of System Transients by Computer Simulation for Prediction of Residential Energy Consumption," Ph.D. Thesis, The Ohio State University, Columbus, Ohio, 1979.

McPherson, H. L., Badger, K. L. and Zawada, W. S., "Furnace Thermal Efficiency Determined from Flue and Jacket Losses," ASHRAE Transactions, Vol. 57, No. 1432, 1951.

Moffat, R. J., "How to Specify Thermocouple Response," ISA Journal, Vol. 4, 1957.

Murphy, W. E., "Mobile Home Air Conditioning: An Analysis of Seasonal Performance," Master's Thesis, Purdue University, West Lafayette, Indiana, 1977. (Also published as Herrick Laboratories Report HL 77-30)

Murphy, W. E. and Goldschmidt, V. W., "Qualitative Interpretation of Transient Performance," Ray W. Herrick Laboratories, HL 79-3, Feb. 1979.

Murphy, W. E., and Goldschmidt, V. W., "Analysis of Measurement Procedure," Ray W. Herrick Laboratories, HL 78-4, Feb., 1978.

National Electric Manufacturers Association (NEMA), "Residential Controls - Low Voltage Room Thermostats," Pub. No. DC 3 - 1972.

Nelson, L. W., "Predicting Control Performance of Residential Heating Systems with an Analog Computer," IEEE Transactions, Vol. IA-10, No. 6, November/December, 1974.

Nelson, L. W. and Magnussen, J. L., "Analytical Predictions of Residential Electric Heating System Performance," IEEE Transactions on Industrial Applications, Vol. IA-10, No. 6, November/December. 1974.

Nguyen,N., Master's thesis to be published, Ray W. Herrick Laboratories, Purdue University, Indiana, 1981.

Thomas, S. B., Tree, D. R. and Goldschmidt, V. W., "Compilation of Data and Analysis of Test Procedure for SEER," Ray W. Herrick Laboratories Report No. HL 79-2, Purdue University, West Lafayette, Indiana,1979.

Thomas, S. B., "A Study of the Prediction and Measurement of Air Conditioning System Seasonal Performance Characteristics," Master's Thesis, Purdue University, West Lafayette, Indiana, 1980.

APPENDIX

The thermostat model of Didion, with the transfer equations, was seen in Figure 2B-2. This section will take these transfer equations and derive the equation for T_e. This equation was solved by iteration to yield on/off times of the cycling of the system.

In operator notation (D = d/dt), these equations can be written as follows:

$$T_e = \frac{1}{\tau_e D+1} (T_a + T_s) \tag{A-1}$$

$$T_a = \frac{K_a}{\tau_a D+1} (E) \tag{A-2}$$

$$X_p = \frac{K_p}{\tau_p D+1} (E) \tag{A-3}$$

$$T_s = \frac{1}{D} (X_p - L) \tag{A-4}$$

These can also be written in differential equation form:

$$\frac{dT_e}{dt} + \frac{1}{\tau_e} T_e = \frac{1}{\tau_e} (T_a + T_s) \tag{A-5}$$

$$\frac{dT_a}{dt} + \frac{1}{\tau_a} T_a = \frac{1}{\tau_a} (K_a E) \tag{A-6}$$

$$\frac{dX_p}{dt} + \frac{1}{\tau_p} X_p = \frac{1}{\tau_p} (K_p E) \tag{A-7}$$

$$\frac{dT_s}{dt} = X_p - L \tag{A-8}$$

Equations A-6 and A-7 are easily solved and yield:

$$T_a = K_a E + (T_{a1} - K_a E)\, e^{-t/\tau_a} \tag{A-9}$$

$$X_p = K_p E + (X_{p1} - K_p E)\, e^{-t/\tau_p} \tag{A-10}$$

where T_{a1} and X_{p1} are the initial conditions of T_a and X_p (at $t = 0$). Substituting Eq. A-10 into Eq. A-8, a solution can be found for T_s as follows:

$$\frac{dT_s}{dt} = K_p E + (X_{p1} - K_p E)\, e^{-t/\tau_p} - L \tag{A-11}$$

$$T_s - T_{s1} = K_p E\, t + (X_{p1} - K_p E)\, [-\tau_p\, (e^{-t/\tau_p} - 1)] - L\, t \tag{A-12}$$

$$T_s = T_{s1} + (K_p E - L)\, t + \tau_p\, (X_{p1} - K_p E) - \tau_p\, (X_{p1} - K_p E)\, e^{-t/\tau_p} \tag{A-13}$$

where T_{s1} is the initial condition of T_s.

Finally, the expressions for T_a and T_s, Eqs. A-9 and 13, are substituted into Eq. A-5 and a solution for T_e is found:

$$\frac{dT_e}{dt} + \frac{1}{\tau_e} T_e = \frac{1}{\tau_e} K_a E + \frac{1}{\tau_e} T_{s1} + \frac{\tau_p}{\tau_e} (X_{p1} - K_p E) -$$

$$\frac{\tau_p}{\tau_e} (X_{p1} - K_p E)\, e^{-t/\tau_p} + \frac{1}{\tau_e} (T_{a1} - K_a E)\, e^{-t/\tau_a} +$$

$$\frac{1}{\tau_e} (K_p E - L)\, t \tag{A-14}$$

$$(T_e - T_{e1})\, e^{t/\tau_e} = (K_a E + T_{s1} + \tau_p\,(X_{p1} - K_p E))\,[e^{t/\tau_e} - 1] -$$

$$\frac{\tau_p^2}{\tau_p - \tau_e}\,(X_{p1} - K_p E)\,[e^{-t/\tau_p + t/\tau_e} - 1] +$$

$$\frac{\tau_a}{\tau_a - \tau_e}\,(T_{a1} - K_a E)\,[e^{-t/\tau_a + t/\tau_e} - 1] +$$

$$(K_p - L)\, t\, e^{t/\tau_e} - \tau_e\,(K_p E - L)\,[e^{t/\tau_e} - 1] \qquad \text{(A-15)}$$

$$T_e = T_{e1}\, e^{-t/\tau_e} + (K_a E + T_{s1} + \tau_p\,(X_{p1} - K_p e))\,[1 - e^{-t/\tau_e}] -$$

$$\frac{\tau_p^2}{\tau_p - \tau_e}\,(X_{p1} - K_p E)\,[e^{-t/\tau_p} - e^{-t/\tau_e}] +$$

$$\frac{\tau_a}{\tau_a - \tau_e}\,(T_{a1} - K_a E)\,[e^{-t/\tau_a} - e^{-t/\tau_e}] +$$

$$(K_p - L)\, t - \tau_e\,(K_p E - L)\,[1 - e^{-t/\tau_e}] \qquad \text{(A-16)}$$

where T_{e1} is the initial condition for T_e.

For special cases where a time constant equals zero or two time constants are equal, a similar derivation is followed. It will not b repeated here.

By substituting appropriate values for T_e, T_{e1}, T_{s1}, T_{a1}, X_{p1}, E, etc., Eq. A-16 can be solved by iteration to yield the on/off times. For example, to find the on-time, let E = 1, T_{s1} = TSET (the thermostat set point), T_{e1} = TSET, T_{a1} = 0, X_{p1} = 0 and T_e = TSET + SD.

Once the on and off-times are found, cycle time, cycle rate and percent on-time can be calculated, and the analysis continues.

☆U.S. GOVERNMENT PRINTING OFFICE: 1981-740-145/2172